澳門大學
UNIVERSIDADE DE MACAU
UNIVERSITY OF MACAU

Outstanding Academic Papers by Students
學 生 優 秀 作 品

Adaptive Control of Autonomous Vehicles

by

ZHU Xuanzhi

Final Year Project Report submitted in partial fulfillment

of the requirements for the Degree of

Bachelor of Science in Electrical and Computer Engineering

2017

Faculty of Science and Technology
University of Macau

Bachelor's Thesis (or Final Report of ECEB420 Design Project II)

In presenting this Final Report of Design Project II (ECEB420) in partial fulfillment of the requirements for a Bachelor's Degree at the University of Macau, I agree that the **UM Library** and **Faculty of Science and Technology (FST)** shall make its copies available strictly for internal circulation or inspection. No part of this thesis can be reproduced by any means (electronic, mechanical, visual, and etc.) before the valid date (usually less than 3 years) limit listed below. Copying of this thesis before the valid date from other parties is allowable **only** under the prior written permission of the author(s).

Printed name: ZHU Xuanzhi

Signature: 朱轩志)

Student number: D-B3-2700-2

Date: May 10, 2017

Reliable Contact information (address, tel. no., email, etc.) of author:

Address: 359 Sub mailbox, 5142 Mailbox, Court No.104, YouYi Road, Beijing, China

Telephone Number: (+86)15010992001

Email: xzbdfz@sina.com

Valid date until June 30, 2017

DECLARATION

I declare that the project report here submitted is original except for the source materials explicitly acknowledged and that this report as a whole, or any part of this report has not been previously and concurrently submitted for any other degree or award at the University of Macau or other institutions.

I also acknowledge that I am aware of the Rules on Handling Student Academic Dishonesty and the Regulations of the Student Discipline of the University of Macau.

Signature   :

Name   : ZHU Xuanzhi

Student ID   : D-B3-2700-2

Date   : May 10, 2017

APPROVAL FOR SUBMISSION

This project report entitled "**Adaptive Control of Autonomous Vehicles**" was prepared by ZHU Xuanzhi (D-B3-2700-2) in partial fulfillment of the requirements for the degree of Bachelor of Science in Electrical and Computer Engineering at the University of Macau.
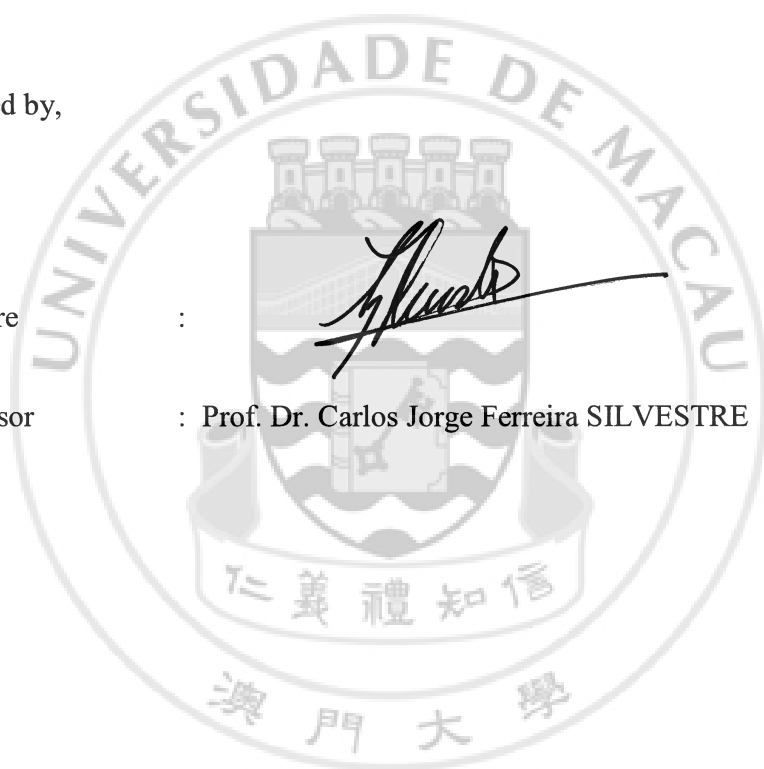

Endorsed by,

Signature   :

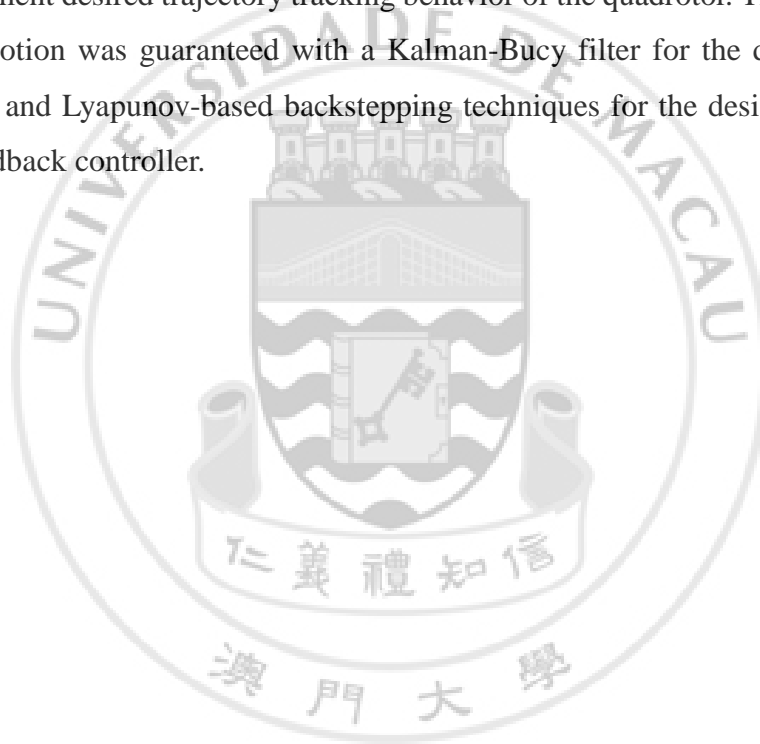Supervisor   : Prof. Dr. Carlos Jorge Ferreira SILVESTRE

ACKNOWLEDGEMENTS

ABSTRACT

Autonomous vehicles belong to a class of systems whose dynamic characteristics are independent of time. Due to their nonlinear dynamics, classical theories that deal with linear systems are no longer applicable in the analysis or design The specific autonomous vehicle considered in this work was an underactuated quadrotor with more degrees of freedom than the number of actuations. At the same time, the quadrotor was assumed to have an unknown mass and experience constant force disturbances. A model-reference adaptive control strategy was designed with an observer and controller to implement desired trajectory tracking behavior of the quadrotor. The overall stability of the motion was guaranteed with a Kalman-Bucy filter for the design of the state observer and Lyapunov-based backstepping techniques for the design of the adaptive state feedback controller.

TABLE OF CONTENTS

LIST OF FIGURES

Chapter 1 INTRODUCTION

Motion control of autonomous vehicles always leads to the control of a non-autonomous system that interprets the corresponding error dynamics. Therefore, the study of the stability of a motion is equivalent to the study of the stability around an equilibrium point defined in the state space as explained in [1]. In some cases, the control of a nonlinear system can be performed on its LTI (linear time-invariant) model which guarantees local exponential stability, as indicated in results of linear system theory. Such control law is easy to design. However, the performance of such a method can be deteriorated when the system undergoes large deviations from the nominal point and when system parameters suffer from changes with respect to time. Linear methods have been applied in [2] and [3] but the vehicle system only represented closed loop stability for small regions near the equilibrium point. Generally, direct method of Lyapunov analysis works well on the stability of a nonlinear system but the difficulty is to find a Lyapunov function with specific properties. Backstepping techniques are adopted to guarantee the tracking error dynamics uniformly globally asymptotically stable. However, the specific autonomous vehicle in this work is a quadrotor with four propellers actuated in thrust and angular velocities. As a result, the number of actuations are less than the total degrees of freedom, which is six for a quadrotor. Generally, backstepping techniques are not applicable to this kind of underactuated systems. However, as indicated in [4], a simplified model of a quadrotor is feedback linearizable, and hence backstepping techniques can be used. For example, it has been adopted to quadrotor trajectory tracking problem in [5].

Typically, a system is influenced by its surroundings and its internal changes in the dynamic parameters, and hence should be observed either by external or internal sensors for control purpose. However, full state observations are not always available. This posed the necessity of state estimation from available states. Algorithms for state estimation can be found in [6] with estimation law derived in the backstepping procedures for constant external forces, and in [7] with estimation of multiple states with extended Kalman-Bucy filter.

In practical cases, the control law designed should not contain unbounded terms or singularities and hence bounds should be exerted on the control quantities either automatically by the working limitations of a system or manually.

In this work, the specific autonomous vehicle is a quadrotor with four propellers actuated in thrust and angular velocities with six degrees of freedoms. Its mass is assumed to be a constant but is unknown. And a constant term accounts for the constant force disturbance like constant wind and uncertainties in the model like uneven mass distribution of the quadrotor. It is interesting to notice that the estimated quantities, both the mass and the force disturbance can be suited in a linear time-varying system that mimics exactly the behaviors of the nonlinear system through proper state transformation. And Kalman-Bucy filter provides an easy and tunable solution for the state estimation problem. The inputs of controller are expected to include the desired trajectory, the estimation of mass and constant force disturbance, and other states from a VICON Bonita motion capture system [8]. Bounds on the desired trajectory position vector that is time-parameterized and its time derivatives should be exerted when selecting the appropriate trajectory. And working limits of the quadrotor should be put into consideration because there are cases when the vehicle is not able to achieve calculated thrust and angular velocities. These constraints should be analyzed in terms of stability of the controller. Generally, interconnection of two stable systems may not lead to an overall stable system and hence the stability of the interconnection of the stabilized Kalman-Bucy filter and the controller is of great importance for the overall performance of the adaptive control system.

The structure of this paper is as followed: chapter 2 presents the required theorems and mathematics background used in this work; chapter 3 deals with the modelling of the dynamics of the vehicle and simulation of an open loop model; chapter 4 focuses on the modeling of a state observer and corresponding simulations; chapter 5 presents the modeling of a backstepping controller and corresponding simulations; chapter 6 studies with the derivation of the interconnected system of the proposed observer and controller, and corresponding simulations; chapter 7 deals with experimental results and comparison with simulation results ;chapter 8 presents problems encountered and possible solutions; chapter 9 is the conclusion; chapter 10 gives some recommendations for future work.

Chapter 2 MATHEMATICAL PRELIMINARIES

2.1 NONLINEAR SYSTEMS AND EQUILIBRIUM POINTS

As explained in [9], a nonlinear dynamic system can usually be represented by nonlinear differential equations as

$$\dot{\mathbf{x}} = \boldsymbol{f}(\mathbf{x}, t) \tag{2.1}$$

where $\boldsymbol{f}$ is an $n \times 1$ nonlinear vector function, and $\mathbf{x}$ is an $n \times 1$ state vector. $\mathbf{x}(t)$ is the system trajectory. Equilibrium points $\mathbf{x}^*$ of such a system are defined to be

$$\boldsymbol{f}(\mathbf{x}^*, t) \equiv 0 \qquad \forall t \geq t_0 \tag{2.2}$$

In the special case of a linear time-varying system,

$$\dot{\mathbf{x}} = \mathbf{A}(t)\mathbf{x} \tag{2.3}$$

a unique equilibrium point is at the origin $\mathbf{0}$ unless $\mathbf{A}(t)$ is always singular.

Autonomous systems are systems that $\boldsymbol{f}$ does not depend explicitly on time such that

$$\dot{\mathbf{x}} = \boldsymbol{f}(\mathbf{x}) \tag{2.4}$$

is satisfied. Non-autonomous systems are hence those that are in the form of Eq. (2.1). In the field of control, the above definitions have not included the controlling vector $\mathbf{u}$, which is an $m \times 1$ input vector.

For an autonomous system described in Eq. (2.4), when control variables are included, the closed-loop dynamics becomes

$$\dot{\mathbf{x}} = \boldsymbol{f}(\mathbf{x}, \mathbf{u}) \tag{2.5}$$

and the overall dynamics may be either autonomous if $\mathbf{u} = \mathbf{u}(\mathbf{x})$ or non-autonomous if $\mathbf{u} = \mathbf{u}(\mathbf{x}, t)$.

In practical problems, we are more concerned with stability of a motion rather than an equilibrium point. The ability to follow the original motion trajectory if slightly perturbed away from it. Let $\mathbf{x}^*(t)$ be the solution of Eq. (2.4) corresponding to initial condition $\mathbf{x}^*(0) = \mathbf{x}_0$ and the perturbation $\mathbf{x}(0) = \mathbf{x}_0 + \delta\mathbf{x}_0$. Then the variation of the motion error is

$$\mathbf{e}(t) = \mathbf{x}(t) - \mathbf{x}^*(t) \tag{2.6}$$

$$\dot{\mathbf{e}} = \boldsymbol{f}(\mathbf{x}^* + \mathbf{e}, t) - \boldsymbol{f}(\mathbf{x}^*, t) = \boldsymbol{g}(\mathbf{e}, t) \tag{2.7}$$

and the corresponding motion error dynamic system is a non-autonomous system.

2.2 STABILITY OF DYNAMIC SYSTEMS

2.2.1 Local Stability and Local Uniform Stability

As explained in [9], the equilibrium point $\mathbf{0}$ is stable at t_0 if $\forall R > 0,\ \exists\, r(R, t_0) > 0$ such that

$$\|\mathbf{x}(t_0)\| < r(R, t_0) \implies \|\mathbf{x}(t)\| < R \qquad \forall\, t \geq t_0 \qquad (2.8)$$

Otherwise, the equilibrium point $\mathbf{0}$ is unstable.

The equilibrium point $\mathbf{0}$ is locally uniformly stable if the scalar r in Eq. (2.8) can be chosen independently of t_0.

2.2.2 Local Asymptotic Stability and Local Uniform Asymptotic Stability

As explained in [9], the equilibrium point $\mathbf{0}$ is locally asymptotically stable at t_0 if it is stable, and $\exists\, r(t_0) > 0$ such that

$$\|\mathbf{x}(t_0)\| < r(t_0) \implies \|\mathbf{x}(t)\| \to 0 \quad \text{as} \quad t \to \infty \qquad (2.9)$$

The equilibrium point $\mathbf{0}$ is locally uniformly asymptotically stable if it is uniformly stable, and $\exists\, \mathbf{B}_{R_o}$, a ball of attraction whose radius is independent of t_0, such that $\forall$ system trajectory with initial states in $\mathbf{B}_{R_0}$ converges to $\mathbf{0}$ uniformly in t_0.

2.2.3 Exponential Stability

As explained in [9], the equilibrium point $\mathbf{0}$ is exponentially stable if $\exists\, \alpha, \lambda > 0$, such that for some ball $\mathbf{B}_{r_o}$,

$$\|\mathbf{x}(t)\| \leq \alpha \|\mathbf{x}(t_0)\| e^{-\lambda(t - t_0)} \qquad \forall\, t \geq 0 \qquad (2.10)$$

2.2.4 Local Stability and Global Stability

As explained in [9], local stability implies that values of r in Eq. (2.8) and (2.9) is not arbitrarily chosen, global stability implies that values of r in Eq. (2.8) and (2.9) can be arbitrarily chosen in the set of positive real number.

2.2.5 Input-to-state Stability

From [10], a nonlinear system in Eq. (2.5) is said to be locally input-to-state stable if there exist a class $\mathcal{KL}$ function β, a class $\mathcal{K}$ function γ, and positive constants k_1 and k_2 such that for any initial state $\mathbf{x}(t_0)$ with $\|\mathbf{x}(t_0)\| < k_1$ and any input $\mathbf{u}(t)$ with $\sup_{t \geq t_0} \|\mathbf{u}(t)\| < k_2$, the solution exists and satisfies

$$\|\mathbf{x}(t)\| \leq \beta(\|\mathbf{x}(t_0)\|, t - t_0) + \gamma\left(\sup_{t_0 \leq \tau \leq t} \|\mathbf{u}(\tau)\|\right) \tag{2.11}$$

for all $t \geq t_0 \geq 0$. Let $D = \{\mathbf{x} \in \mathbf{R}^n | \|\mathbf{x}\| < r\}$, $D_u = \{\mathbf{u} \in \mathbf{R}^m | \|\mathbf{u}\| < r_u\}$. It is said to be input-to-state stable if $D = \mathbf{R}^n$, $D_u = \mathbf{R}^m$, and inequality is satisfied for any initial state $\mathbf{x}(t_0)$ and any bounded input $\mathbf{u}(t)$.

Stability of perturbed systems can be proved under certain constraints. Let $D = \{\mathbf{x} \in \mathbf{R}^n | \|\mathbf{x}\| < r\}$, $D_u = \{\mathbf{u} \in \mathbf{R}^m | \|\mathbf{u}\| < r_u\}$, and $\boldsymbol{f}: [0, \infty) \times D \times D_u \to \mathbf{R}^n$ be piecewise continuous in t and locally Lipschitz in u and. Let $V: [0, \infty) \times D \to \mathbf{R}$ be a continuously differentiable function such that

$$\alpha_1(\|\mathbf{x}\|) \leq V(t, \mathbf{x}) \leq \alpha_2(\|\mathbf{x}\|) \tag{2.12}$$

$$\frac{\partial V}{\partial t} + \frac{\partial V}{\partial \mathbf{x}} \boldsymbol{f}(t, \mathbf{x}, \mathbf{u}) \leq -\alpha_3(\|\mathbf{x}\|) \quad \forall \|\mathbf{x}\| \geq \rho(\|\mathbf{u}\|) \geq 0 \tag{2.13}$$

$\forall (t, \mathbf{x}, \mathbf{u}) \in [0, \infty) \times D \times D_u$ where α_1, α_2 and α_3 are class $\mathcal{K}$ functions. Then, the system described in Eq. (2.5) is locally input-to-state stable with $\gamma = \alpha_1^{-1} \circ \alpha_2 \circ \rho$, $k_1 = \alpha_2^{-1}(\alpha_1(r))$, and $k_2 = \rho(\min\{k_1, \rho(r_u)\})$. Moreover, if $D = \mathbf{R}^n$, $D_u = \mathbf{R}^m$, and α_1 is a class $\mathcal{K}_\infty$ function, then the system in Eq. (2.5) is input-to-state stable with $\gamma = \alpha_1^{-1} \circ \alpha_2 \circ \rho$.

2.3 LYAPUNOV'S DIRECT METHOD FOR NON-AUTONOMOUS SYSTEMS

2.3.1 Locally Positive Definite Lyapunov Function

As explained in [9], a scalar time-varying function $V(\mathbf{x}, t)$ is locally positive definite if $V(\mathbf{0}, t) = 0$ and $\exists$ a time-invariant positive definite function $V_o(\mathbf{x})$ in a ball $\mathbf{B}_{R_o}$ such that

$$V(\mathbf{x}, t) \geq V_o(\mathbf{x}) \qquad \forall\, t \geq 0 \tag{2.14}$$

Globally positive definite functions can be defined similarly for $\mathbf{x}$ to be arbitrarily chosen in $\mathbf{R}^{n \times 1}$ other than $\mathbf{0}$.

2.3.2 Decrescent Function

As explained in [9], a scalar time-varying function $V(\mathbf{x}, t)$ is decrescent if $V(\mathbf{0}, t) = 0$ and $\exists$ a time-invariant positive definite function $V_l(\mathbf{x})$ in a ball $\mathbf{B}_{R_o}$ such that

$$V(\mathbf{x}, t) \leq V_l(\mathbf{x}) \qquad \forall\, t \geq 0 \tag{2.15}$$

2.3.3 Lyapunov Theorem for Non-Autonomous Systems

2.3.3.1 Lyapunov Local Stability

As explained in [9], if, in a ball $\mathbf{B}_{R_o}$ around the equilibrium point $\mathbf{0}$, $\exists$ a scalar function $V(\mathbf{x}, t)$ with continuous partial derivatives with respect to $\mathbf{x}$ such that $V(\mathbf{x}, t)$ is positive definite, and $\dot{V}(\mathbf{x}, t)$ is negative semi-definite, then the equilibrium point $\mathbf{0}$ is locally stable in the sense of Lyapunov.

2.3.3.2 Lyapunov Local Uniform Stability and Local Uniformly Asymptotic Stability

As explained in [9], if the equilibrium point $\mathbf{0}$ is locally stable in the sense of Lyapunov, and $V(\mathbf{x}, t)$ is decrescent, then the equilibrium point $\mathbf{0}$ is locally uniformly stable.

If, in a ball $\mathbf{B}_{R_o}$ around the equilibrium point $\mathbf{0}$, $\exists$ a scalar function $V(\mathbf{x}, t)$ with continuous partial derivatives with respect to $\mathbf{x}$ such that $V(\mathbf{x}, t)$ is positive definite and decrescent, and $\dot{V}(\mathbf{x}, t)$ is negative definite, then the equilibrium point $\mathbf{0}$ is locally uniformly asymptotically stable.

2.3.3.3 Lyapunov Global Uniform Asymptotic Stability

As explained in [9], if $\exists$ a scalar function $V(\mathbf{x}, t)$ with continuous partial derivatives with respect to $\mathbf{x}$ such that $V(\mathbf{x}, t)$ is positive definite and decrescent, and $\dot{V}(\mathbf{x}, t)$ is negative definite, and $V(\mathbf{x}, t)$ is radially unbounded, then the equilibrium point $\mathbf{0}$ is globally uniformly asymptotically stable.

2.4 OBSERVABILITY AND OBSERVER DESIGN THROUGH STATE AND OUTPUT TRANSFORMATION

2.4.1 Observability for Nonlinear Systems

As discussed in [11], given a nonlinear, non-autonomous dynamic system

$$\begin{cases} \dot{\mathbf{x}}(t) = \boldsymbol{f}(t, \mathbf{x}(t), \mathbf{u}(t)) \\ \mathbf{y}(t) = \boldsymbol{h}(t, \mathbf{x}(t), \mathbf{u}(t)) \end{cases}, \qquad \mathbf{x}(t_0) = \mathbf{x}_0 \qquad (2.16)$$

where $\mathbf{x}(t) \in \mathbf{R}^{n \times 1}$, $\mathbf{u}(t) \in \mathbf{R}^{m \times 1}$, $\mathbf{y}(t) \in \mathbf{R}^{o \times 1}$. The system is observable on $[t_0, t_f]$ for a given $\mathbf{u} : [t_0, t_f] \to \mathbf{R}^{m \times 1}$ if and only if for that input $\mathbf{u}(t)$ the initial state $\mathbf{x}(t_0) = \mathbf{x}_0$ is uniquely determined by the response $\mathbf{y}(t)$ of the system for $t \in [t_0, t_f]$.

The nonlinear system is observable if and only if it is observable for $\forall\, \mathbf{u}(t): [t_0, t_f] \to \mathbf{R}^{n \times 1}$.

2.4.2 Linear Mimicking Systems

If $\exists\, \mathbf{T}_x: \mathbf{R}^{n \times 1} \to \mathbf{R}^{p \times 1}\ \mathbf{v}(t)$ and $\mathbf{T}_y: \mathbf{R}^{o \times 1} \to \mathbf{R}^{q \times 1}$ with $\mathbf{T}_x(\mathbf{x}_0) = \mathbf{w}_0$ and $\mathbf{v}(t) = \mathbf{u}(t)$ for $\forall\, t \in [t_0, t_f]$ such that

$$\begin{cases} \mathbf{w}(t) = \mathbf{T}_x(\mathbf{x}(t)) \\ \mathbf{z}(t) = \mathbf{T}_y(\mathbf{y}(t)) \end{cases} \tag{2.17}$$

holds for $\forall\, t \in [t_0, t_f]$, then the system

$$\begin{cases} \dot{\mathbf{w}}(t) = \mathbf{A}(t, \mathbf{u}(t), \mathbf{y}(t))\mathbf{w}(t) + \mathbf{B}(t, \mathbf{u}(t), \mathbf{y}(t))\mathbf{v}(t) \\ \quad\quad \mathbf{z}(t) = \mathbf{C}(t, \mathbf{u}(t), \mathbf{y}(t))\mathbf{w}(t) \\ \quad\quad\quad \mathbf{w}(t_0) = \mathbf{w}_0 \end{cases} \tag{2.18}$$

is mimicking the dynamics of the nonlinear system described in Eq. (2.13).

2.4.3 Observability Equivalence

If the nonlinear system described in Eq. (2.13) with a given input $\mathbf{u}(t): [t_0, t_f] \to \mathbf{R}^{m \times 1}$, and

(1) $\exists\, \mathbf{T}_x: \mathbf{R}^{n \times 1} \to \mathbf{R}^{p \times 1}$ and $\mathbf{T}_y: \mathbf{R}^{o \times 1} \to \mathbf{R}^{q \times 1}$ such that the linear time-varying system described in Eq. (2.15) mimics the dynamics of the nonlinear system;

(2) For $\forall\, \mathbf{y}(t): [t_0, t_f] \to \mathbf{R}^{o \times 1}$, the resulting linear time-varying system is observable on $[t_0, t_f]$;

(3) The state transformation $\mathbf{T}_x$ is injective.

Then, the nonlinear system is observable on $[t_0, t_f]$ for the given $\mathbf{u}(t)$.

2.4.4 Stability Equivalence

Define $\mathbf{T}'_x: \mathbf{R}^{p \times 1} \to \mathbf{R}^{n \times 1}$ that satisfies $\mathbf{T}'_x(\mathbf{T}_x(\mathbf{x})) = \mathbf{x}$ for $\forall\, \mathbf{x} \in \mathbf{R}^{n \times 1}$. The above equivalence of the observability between the nonlinear system and the linear time-varying mimicking system can guarantee the observability that initial state $\mathbf{w}(t_0) = \mathbf{w}_0$ is uniquely determined by the response $\mathbf{z}(t)$ of the system for $t \in [t_0, t_f]$ but cannot guarantee the observation convergence of the state $\mathbf{x}(t)$ through the inverse transformation $\mathbf{T}'_x(\mathbf{w}(t))$. However, if $\exists\, \alpha > 0$ such that

$$\|\mathbf{T}'_x(\mathbf{w}_a) - \mathbf{T}'_x(\mathbf{w}_b)\| \leq \alpha \|\mathbf{w}_a - \mathbf{w}_b\| \tag{2.19}$$

holds for $\forall\ \mathbf{w}_a, \mathbf{w}_b \in \mathbf{R}^{p \times 1}$, and assume there $\exists$ a state observer with globally exponential stable error dynamics, then the estimated state $\hat{\mathbf{x}}(t)$ converges exponentially fast to the state $\mathbf{x}(t)$.

A special situation is when the state transformation is selected as

$$\mathbf{T}_x\big(\mathbf{x}(t)\big) = \begin{bmatrix} \mathbf{x} \\ \mathbf{T}_a\big(\mathbf{x}(t)\big) \end{bmatrix} \tag{2.20}$$

where $\mathbf{T}_a : \mathbf{R}^{n \times 1} \to \mathbf{R}^{(p-n) \times 1}$, and this state transformation is injective and satisfied the inequality specified in Eq. (2.16).

2.4.5 Observability of Linear Systems

Linear dynamic systems are special cases of nonlinear dynamic systems in the form of

$$\begin{cases} \dot{\mathbf{w}}(t) = \mathbf{A}(t)\mathbf{w}(t) + \mathbf{B}(t)\mathbf{v}(t) \\ \mathbf{z}(t) = \mathbf{C}(t)\mathbf{w}(t) \\ \mathbf{w}(t_0) = \mathbf{w}_0 \end{cases} \tag{2.21}$$

$\mathbf{w}(t) \in \mathbf{R}^{p \times 1}$, $\mathbf{v}(t) \in \mathbf{R}^{m \times 1}$, $\mathbf{z}(t) \in \mathbf{R}^{q \times 1}$, then the linear state Eq. (2.18) is observable on $[t_0, t_f]$ if and only if the $n \times n$ matrix

$$\mathbf{M}(t_0, t_f) = \int_{t_0}^{t_f} \mathbf{\Phi}^T(t, t_0)\mathbf{C}^T(t)\mathbf{C}(t)\mathbf{\Phi}(t, t_0)dt \tag{2.22}$$

is invertible, as proved in [12].

2.4.6 Stability of State Observer

If the linear time-varying system specified in Eq. (2.18) is uniformly complete observable, then the Kalman-Bucy filter used in the design of a state observer is globally exponentially stable [13] and [14], which requires that given t_0, for $\forall\ \Delta T > 0$,

$$\mathbf{M}(t_0, t_0 + \Delta T) = \int_{t_0}^{t_0+\Delta T} \mathbf{\Phi}^T(t, t_0)\mathbf{C}^T(t)\mathbf{C}(t)\mathbf{\Phi}(t, t_0)dt \tag{2.23}$$

is invertible.

2.5 IMPORTANT INEQUALITIES

2.5.1 Young's inequality

As explained in [9], a special case of Young's inequality is:

$$ab \leq \frac{a^2}{2\varepsilon} + \frac{\varepsilon b^2}{2} \tag{2.24}$$

where $a, b \geq 0$, and ε is any positive constant.

2.5.2 Gronwall-Bellman inequality

As explained in [9], suppose that $\phi(t)$ and $v(t)$ are continuous functions defined for $t \geq t_0$ with $v(t) \geq 0$ for $t \geq t_0$, and suppose Ψ is a constant. Then the implicit inequality

$$\phi(t) \leq \Psi + \int_{t_0}^{t} v(\sigma)\,\phi(\sigma)d\sigma, \qquad t \geq t_0 \tag{2.25}$$

implies the explicit inequality

$$\phi(t) \leq \Psi e^{\int_{t_0}^{t} v(\sigma)d\sigma}, \qquad t \geq t_0 \tag{2.26}$$

Chapter 3 VEHICLE MODEL

3.1 PHYSICAL MODEL

Figure 1. Quadrotor platform

The mini quadrotor is shown in figure 1. The quadrotor has four propellers located at each end of the four extended arms and they are driven by four motors that provides different rotating speeds. Results in fluid dynamics suggest that the air undergoes pressure change from above the propellers to the beneath of them and hence the propellers are acted with air dynamic forces that maintain the overall stable motion of the quadrotor. The central controlling unit is located at the center of the quadrotor along with batteries. The mass of the total system is usually known by measurement in advance. It is also observed that the quadrotor represents geometric symmetry with respect to its center. Hence, inertia quantities of it can be simplified and measured.

However, uneven mass distribution of the quadrotor, like the one in figure 1 caused by the asymmetric part of an undercarriage, can be observed. And the thrust produced by the propellers is not ideally perpendicular with respect to the surface of the propellers due to the complicated air dynamics in the surroundings of the quadrotor. These imperfections lead to the following problems:

(1) the inertia matrix is not diagonal;

(2) the thrust force can have different orientations during a motion.

3.2 SIMPLIFICATION OF THE PHYSICAL MODEL

The two problems addressed above show imperfections of the physical model when mathematical model is desired for calculations. The following assumptions are based on empirical observations:

(1) The center of mass is located on the center of the quadrotor;

(2) The inertia matrix is diagonal with respect to the center of mass;

(3) The force produced by propellers are perpendicular to the surface of the propellers and thus the total thrust can be seen acting on the center of mass.
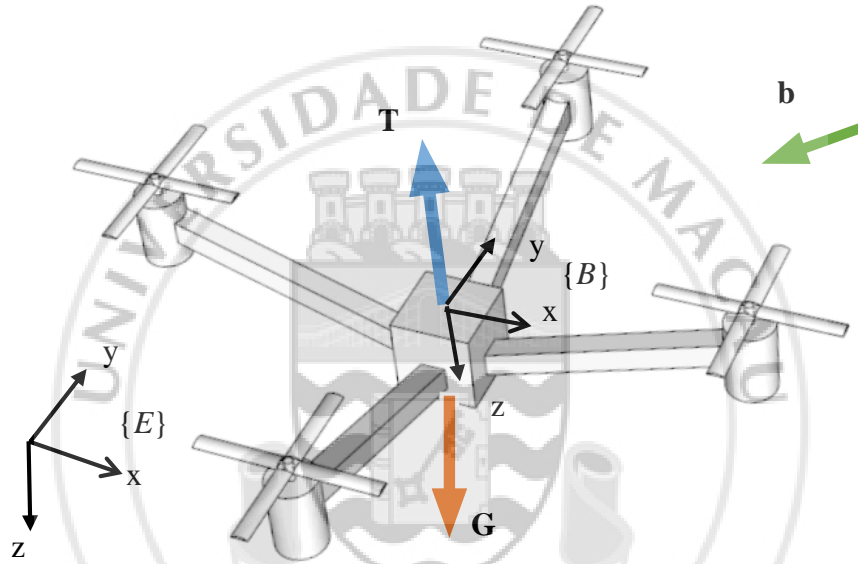
Figure 2. Quadrotor setup

3.3 MATHEMATICAL MODEL

The quadrotor was modeled as a rigid body with a body frame $\{B\}$ attached to the center of the quadrotor with its z-axis perpendicular the surface of the four propellers. Forces produced by the four propellers were equivalent to a single thrust acting on the center of mass along the z-axis in the body frame. The gravity vector was along the negative z-axis in the Earth frame $\{E\}$, which is a fixed inertia frame.

Denote the linear position of the center of mass as $^E\mathbf{P} \in \mathbf{R}^{3\times1}$ with respect to $\{E\}$, and $^B\mathbf{P} \in \mathbf{R}^{3\times1}$ with respect to $\{B\}$, the rotational matrix $^E_B\mathbf{R} \in \mathrm{SO}(3)$ that satisfied

$$^E\mathbf{P} = {}^E\mathbf{P}_{BORG} + {}^E_B\mathbf{R}\,{}^B\mathbf{P} \tag{3.1}$$

Then the linear velocity of the center of mass $^B\mathbf{V} \in \mathbf{R}^{3\times1}$ with respect to $\{B\}$ can be defined as:

$$^B\mathbf{V} = \,^B\!\left(\frac{^E d}{dt}\,^E\mathbf{P}_{BORG}\right) = \,^B\!\left(\frac{^E d}{dt}\,^E\mathbf{P}\right) = \,^B_E\mathbf{R}\,^E\dot{\mathbf{P}} \tag{3.2}$$

Denote the angular velocity in $\{B\}$ as $^B\boldsymbol{\omega} \in \mathbf{R}^{3\times1}$. The rotational matrix $^E_B\mathbf{R}$ was an orthonormal one which had the property

$$^E_B\dot{\mathbf{R}} = \,^E_B\mathbf{R}\mathbf{S}(^B\boldsymbol{\omega}) \tag{3.3}$$

where $\mathbf{S}(\cdot)$ yielded a skew symmetric matrix that verifies

$$\mathbf{S}(\mathbf{x})\mathbf{y} = \mathbf{x} \times \mathbf{y} \qquad \mathbf{x}, \mathbf{y} \in \mathbf{R}^{3\times1} \tag{3.4}$$

Denote the thrust as $^B\mathbf{T} = \,^B T\mathbf{e}_3 \in \mathbf{R}^{3\times1}$, $^E\mathbf{b} \in \mathbf{R}^{3\times1}$, $^E\mathbf{G} = mg\mathbf{e}_3 \in \mathbf{R}^{3\times1}$ with $\mathbf{e}_3 = \begin{bmatrix} 0 \\ 0 \\ 1 \end{bmatrix}$. The net force acting on the quadrotor was

$$^E\mathbf{F} = -\,^E_B\mathbf{R}\,^B\mathbf{T} + mg\mathbf{e}_3 + \,^E\mathbf{b} \tag{3.5}$$

$$^B\mathbf{F} = -\,^B\mathbf{T} + mg\,^B_E\mathbf{R}\mathbf{e}_3 + \,^B_E\mathbf{R}\,^E\mathbf{b} \tag{3.6}$$

According to Newton's Law of motion:

$$^E\mathbf{F} = m\,^E\ddot{\mathbf{P}} \tag{3.7}$$

$$^E\mathbf{F} = m\frac{d}{dt}(^E_B\mathbf{R}\,^B\mathbf{V}) \tag{3.8}$$

$$^E\mathbf{F} = m(^E_B\dot{\mathbf{R}}\,^B\mathbf{V} + \,^E_B\mathbf{R}\,^B\dot{\mathbf{V}}) \tag{3.9}$$

$$^E\mathbf{F} = m[^E_B\mathbf{R}\mathbf{S}(^B\boldsymbol{\omega})\,^B\mathbf{V} + \,^E_B\mathbf{R}\,^B\dot{\mathbf{V}}] \tag{3.10}$$

$$^B_E\mathbf{R}\,^E\mathbf{F} = m(^B\boldsymbol{\omega} \times \,^B\mathbf{V} + \,^B\dot{\mathbf{V}}) \tag{3.11}$$

$$^B\mathbf{F} = m(^B\boldsymbol{\omega} \times \,^B\mathbf{V} + \,^B\dot{\mathbf{V}}) \tag{3.12}$$

$$m\,^B\dot{\mathbf{V}} = -m\,^B\boldsymbol{\omega} \times \,^B\mathbf{V} + \,^B\mathbf{F} \tag{3.13}$$

$$^B\dot{\mathbf{V}} = -\mathbf{S}(^B\boldsymbol{\omega})\,^B\mathbf{V} + \frac{1}{m}\,^B\mathbf{F} \tag{3.14}$$

replacing by $^B\mathbf{F}$ by specific forces in Eq. (3.5)

$$^B\dot{\mathbf{V}} = -\mathbf{S}(^B\boldsymbol{\omega})\,^B\mathbf{V} + \frac{1}{m}(-\,^B\mathbf{T} + mg\,^B_E\mathbf{R}\mathbf{e}_3 + \,^B_E\mathbf{R}\,^E\mathbf{b}) \tag{3.15}$$

$$^B\dot{\mathbf{V}} = -\mathbf{S}(^B\boldsymbol{\omega})\,^B\mathbf{V} - \frac{1}{m}\,^B\mathbf{T} + g\,^B_E\mathbf{R}\mathbf{e}_3 + \frac{1}{m}\,^B_E\mathbf{R}\,^E\mathbf{b} \tag{3.16}$$

Denote $^B\mathbf{I} \in \mathbf{R}^{3\times3}$ to be the inertia matrix, and Euler's equation related angular velocity $^B\boldsymbol{\omega}$ with $^B\mathbf{I}$ and the torque $^B\mathbf{n} \in \mathbf{R}^{3\times1}$ as followed

$$^B\boldsymbol{\tau} = \,^B\dot{\boldsymbol{\omega}} + \,^B\boldsymbol{\omega} \times (^B\mathbf{I}\,^B\times\boldsymbol{\omega}) \tag{3.17}$$

$$^B\dot{\boldsymbol{\omega}} = -\,^B\mathbf{I}^{-1}\mathbf{S}(^B\boldsymbol{\omega})\,^B\mathbf{I}\,^B\boldsymbol{\omega} + \,^B\mathbf{I}^{-1}\,^B\mathbf{n} \tag{3.18}$$

Summing up equations through (3.1) to (3.17)

$$\begin{cases} {}^E_B\dot{\mathbf{R}} = {}^E_B\mathbf{R}\mathbf{S}({}^B\boldsymbol{\omega}) \\ {}^E\dot{\mathbf{P}} = {}^E_B\mathbf{R}\,{}^B\mathbf{V} \\ {}^B\dot{\mathbf{V}} = -\mathbf{S}({}^B\boldsymbol{\omega})\,{}^B\mathbf{V} - \frac{1}{m}\,{}^B\mathbf{T} + g^B_E\mathbf{R}\mathbf{e}_3 + \frac{1}{m}\,{}^B_E\mathbf{R}\,{}^E\mathbf{b} \\ {}^B\dot{\boldsymbol{\omega}} = -\,{}^B\mathbf{I}^{-1}\mathbf{S}({}^B\boldsymbol{\omega})\,{}^B\mathbf{I}\,{}^B\boldsymbol{\omega} + {}^B\mathbf{I}^{-1}\,{}^B\mathbf{n} \end{cases} \tag{3.19}$$

In this work, the specific quadrotor was actuated in thrust ${}^B\mathbf{T}$ and angular velocity ${}^B\boldsymbol{\omega}$. Meanwhile, Eq. (3.19) could be simplified by the input transform ${}^B\mathbf{n} = {}^B\mathbf{I}\,{}^B\boldsymbol{\tau} + \mathbf{S}({}^B\boldsymbol{\omega})\,{}^B\mathbf{I}\,{}^B\boldsymbol{\omega}$, given that the control in angular velocity ${}^B\boldsymbol{\omega}$ was available.

$$\begin{cases} {}^E_B\dot{\mathbf{R}} = {}^E_B\mathbf{R}\mathbf{S}({}^B\boldsymbol{\omega}) \\ {}^E\dot{\mathbf{P}} = {}^E_B\mathbf{R}\,{}^B\mathbf{V} \\ {}^B\dot{\mathbf{V}} = -\mathbf{S}({}^B\boldsymbol{\omega})\,{}^B\mathbf{V} - \frac{1}{m}\,{}^B\mathbf{T} + g^B_E\mathbf{R}\mathbf{e}_3 + \frac{1}{m}\,{}^B_E\mathbf{R}\,{}^E\mathbf{b} \\ {}^B\dot{\boldsymbol{\omega}} = {}^B\boldsymbol{\tau} \end{cases} \tag{3.20}$$

Then, transforming the Eq. (3.20) into the form of Eq. (2.13), one can get

$$\begin{cases} \dot{\mathbf{x}}(t) = \boldsymbol{f}(\mathbf{x}(t), \mathbf{u}(t)) \\ \mathbf{y}(t) = \boldsymbol{h}(\mathbf{x}(t), \mathbf{u}(t)) \end{cases}, \quad \mathbf{x}(t_0) = \mathbf{x}_0 \tag{3.21}$$

where $\mathbf{x}(t) = {}^E\mathbf{P} \in \mathbf{R}^{3\times1}$, $\mathbf{u}(t) = \begin{bmatrix} {}^B\mathbf{T} \\ {}^B\boldsymbol{\omega} \end{bmatrix} \in \mathbf{R}^{6\times1}$ or $\mathbf{u}(t) = \begin{bmatrix} {}^B\mathbf{T} \\ {}^B\boldsymbol{\tau} \end{bmatrix} \in \mathbf{R}^{6\times1}$, $\mathbf{y}(t) = \mathbf{x}(t) \in \mathbf{R}^{6\times1}$, $\mathbf{x}_0 = {}^E\mathbf{P}(t_0) \in \mathbf{R}^{3\times1}$.

3.4 MODEL WITH OPEN LOOP DESIGN AND FULL STATE OBSERVATION

The model in Matlab/Simulink environment was built as shown in the following figure:
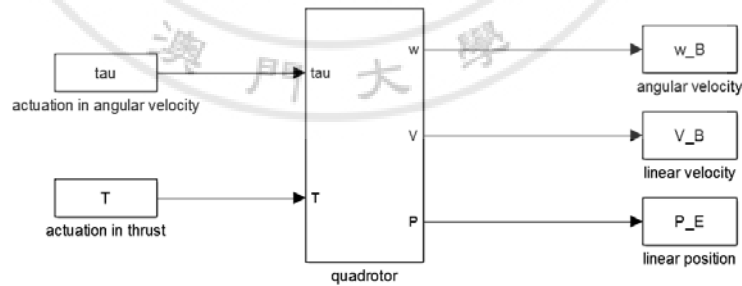
Figure 3. Open loop model

The open loop model was constructed with the Eq. (3.20) that described the overall dynamics of the quadrotor. The nonlinear behavior of the dynamics triggered the use of function block in Simulink, which allowed convenient coding and better visualization of the model.

The mass of the quadrotor was assumed to be known at this stage, with $m = 0.206$ kg. And the gravity was set to the local gravity near the ground of $g = 9.7877$ m/s^2 [15]. The actuation quantities were set to $^B\mathbf{T} = \begin{bmatrix} 0 \\ 0 \\ 1 \end{bmatrix}$ Newton, $^B\boldsymbol{\tau} = \begin{bmatrix} 0.1 \\ 0.1 \\ 0.1 \end{bmatrix}$ rad/s^2, $^B_E\mathbf{R}(t_0) = \begin{bmatrix} 1 & 0 & 0 \\ 0 & 1 & 0 \\ 0 & 0 & 1 \end{bmatrix}$, and $^E\mathbf{b} = \begin{bmatrix} 0.3 \\ 0.2 \\ 0.1 \end{bmatrix}$ Newton. And the initial conditions were $^B\mathbf{V}(t_0) = \begin{bmatrix} 0 \\ 0 \\ 0 \end{bmatrix}$ m/s, $^E\mathbf{P}(t_0) = \begin{bmatrix} 0 \\ 0 \\ -1 \end{bmatrix}$ m. The simulation result was shown in the following figure:
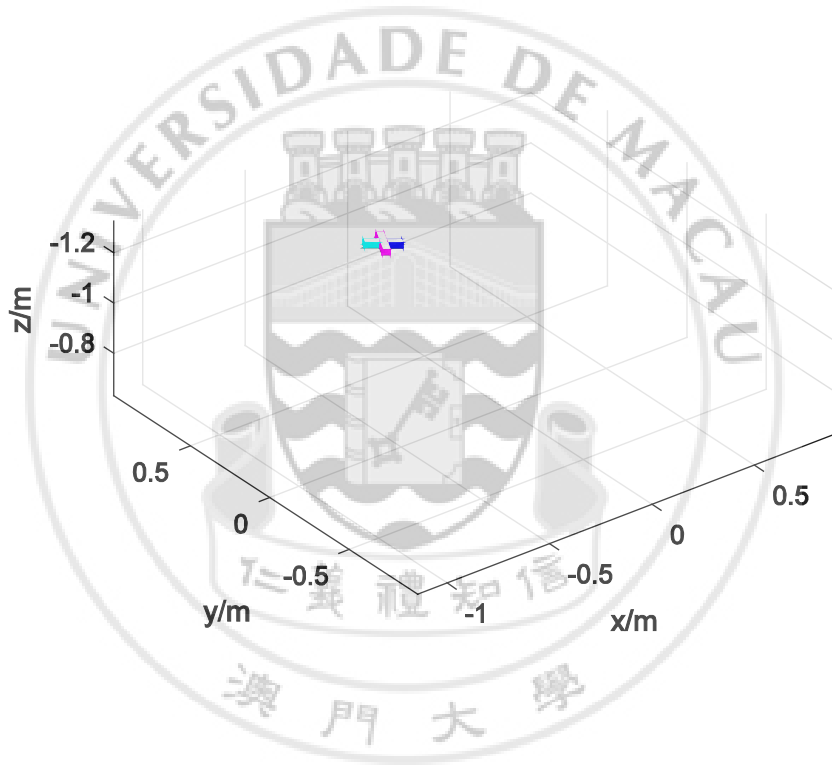
Figure 4. Simulation of open loop model

The visualization of quadrotor in figure 4 specified the top surface of the quadrotor with white color, the bottom surface as black (not visible in the figure 4), and four propellers were simplified with four outstretched arms colored with light blue and light pink. The simulation result met the expectation with the given input, where the quadrotor was gradually lifted at the beginning of the motion due to a bigger thrust than gravitational force. And it was rotated clockwise around each axes of the body frame.

Chapter 4 OBSERVER DESIGN

This section dealt with the situation when full state observation was not available and thus should be observed through the use of an observer. As stated in the Chapter 2, the observer used in the work was one with Kalman-Bucy filter. This required a corresponding LTV (linear time-varying) dynamic system to be observed. The first part of this section simplified the observation problem by ignoring the external force disturbances. The second part of the section checked and transformed the nonlinear dynamic system described in Eq. (3.20) into a linear time varying system that mimicked exacted the behavior of the nonlinear dynamic system.

4.1 OBSERVER DESIGN WITH UNKNOWN MASS BUT NO EXTERNAL FORCE DISTURBANCE

As a trial, the mass of the quadrotor m was unknown and the external force disturbance $^E\mathbf{b}$ was assumed to be zero. Then the Eq. (3.20) became

$$\begin{cases} {}_B^E\dot{\mathbf{R}} = {}_B^E\mathbf{R}\mathbf{S}(^B\boldsymbol{\omega}) \\ {}^E\dot{\mathbf{P}} = {}_B^E\mathbf{R}\,{}^B\mathbf{V} \\ {}^B\dot{\mathbf{V}} = -\mathbf{S}(^B\boldsymbol{\omega})\,{}^B\mathbf{V} - \frac{1}{m}\,{}^B\mathbf{T} + g_E^B\mathbf{R}\mathbf{e}_3 \\ {}^B\dot{\boldsymbol{\omega}} = {}^B\boldsymbol{\tau} \end{cases} \tag{4.1}$$

Naturally, an additional state m should be added in the above equation but the resulting system was nonlinear in state variables. Notice that $\frac{1}{m}$ was linear with state variables, one can get

$$\begin{bmatrix} {}^B\dot{\mathbf{V}} \\ {}^B\dot{\boldsymbol{\omega}} \\ \frac{d}{dt}\left(\frac{1}{m}\right) \end{bmatrix} = \begin{bmatrix} \mathbf{0}_{3\times6} & -{}^B\mathbf{T} \\ \mathbf{0}_{4\times6} & \mathbf{0}_{4\times1} \end{bmatrix} \begin{bmatrix} {}^B\mathbf{V} \\ {}^B\boldsymbol{\omega} \\ \left(\frac{1}{m}\right) \end{bmatrix} + \begin{bmatrix} -\mathbf{S}(^B\boldsymbol{\omega})\,{}^B\mathbf{V} + g_B^E\mathbf{R}^T\mathbf{e}_3 \\ {}^B\boldsymbol{\tau} \\ 0 \end{bmatrix} \tag{4.2}$$

Define a state variable $\mathbf{x}(t) = \begin{bmatrix} {}^B\mathbf{V} \\ {}^B\boldsymbol{\omega} \end{bmatrix} \in \mathbf{R}^{6\times1}$. Assume that the linear velocity and the angular velocity can be observed (angular velocity equaled to the controlling variable $^B\boldsymbol{\tau}$), then an output variable $\mathbf{y}(t) = \begin{bmatrix} {}^B\mathbf{V} \\ {}^B\boldsymbol{\omega} \end{bmatrix} \in \mathbf{R}^{6\times1}$ can be defined. Hence the Eq. (4.2) became

$$\begin{cases} \begin{bmatrix} \dot{\mathbf{x}} \\ \frac{d}{dt}(\frac{1}{m}) \end{bmatrix} = \begin{bmatrix} \mathbf{0}_{3\times6} & -{}^{B}\mathbf{T} \\ \mathbf{0}_{4\times6} & \mathbf{0}_{4\times1} \end{bmatrix} \begin{bmatrix} \mathbf{x} \\ (\frac{1}{m}) \end{bmatrix} + \begin{bmatrix} -\mathbf{S}({}^{B}\boldsymbol{\omega})\,{}^{B}\mathbf{V} + g_{B}^{E}\mathbf{R}^{T}\mathbf{e}_3 \\ {}^{B}\boldsymbol{\tau} \\ 0 \end{bmatrix} \\ \mathbf{y}(t) = \mathbf{I}_6\mathbf{x}(t) \end{cases} \tag{4.3}$$

Consider the state and output transformation described in Eq. (2.17) and (2.14), define the two transformations as

$$\begin{cases} \mathbf{T}_x\big(\mathbf{x}(t)\big) = \begin{bmatrix} \mathbf{x}(t) \\ (\frac{1}{m}) \end{bmatrix} \\ \mathbf{T}_y\big(\mathbf{y}(t)\big) = \mathbf{I}_6\mathbf{y}(t) \end{cases} \tag{4.4}$$

and let new state variables $\mathbf{w}(t) = \mathbf{T}_x\big(\mathbf{x}(t)\big)$ and $\mathbf{z}(t) = \mathbf{T}_y\big(\mathbf{y}(t)\big)$. The overall system now has the dynamics in the form like that of Eq. (2.18).

$$\begin{cases} \dot{\mathbf{w}} = \begin{bmatrix} \mathbf{0}_{6\times6} & \begin{bmatrix} -{}^{B}\mathbf{T} \\ \mathbf{0}_{3\times1} \end{bmatrix} \\ \mathbf{0}_{1\times6} & 0 \end{bmatrix} \mathbf{w} + \begin{bmatrix} -\mathbf{S}({}^{B}\boldsymbol{\omega})\,{}^{B}\mathbf{V} + g_{B}^{E}\mathbf{R}^{T}\mathbf{e}_3 \\ {}^{B}\boldsymbol{\tau} \\ 0 \end{bmatrix} \\ \mathbf{z} = [\mathbf{I}_6 \quad \mathbf{0}_{6\times1}]\mathbf{w} \\ \mathbf{w}(t_0) = \begin{bmatrix} {}^{B}\mathbf{V}(t_0) \\ {}^{B}\boldsymbol{\omega}(t_0) \\ 0 \end{bmatrix} \end{cases} \tag{4.5}$$

Define $\mathbf{A}(t) = \begin{bmatrix} \mathbf{0}_{6\times6} & \begin{bmatrix} -{}^{B}\mathbf{T} \\ \mathbf{0}_{3\times1} \end{bmatrix} \\ \mathbf{0}_{1\times6} & 0 \end{bmatrix}$, $\mathbf{C}(t) = [\mathbf{I}_6 \quad \mathbf{0}_{6\times1}]$. To guarantee the nonlinear system described in Eq. (4.1) was observable, one should check the observability of the resulting linear time-varying system described in Eq. (4.5) on time interval $[t_0, t_f]$ by calculating the observability matrix defined in Eq. (2.19). Note that the transition matrix

$$\boldsymbol{\Phi}(t, t_0) = \mathbf{I} + \int_{t_0}^{t_f} \mathbf{A}(\sigma_1)\, d\sigma_1 + \int_{t_0}^{t_f} \mathbf{A}(\sigma_1) \int_{\sigma_2}^{\sigma_1} \mathbf{A}(\sigma_2)\, d\sigma_2 d\sigma_1 +$$

$$\int_{t_0}^{t_f} \mathbf{A}(\sigma_1) \int_{\sigma_2}^{\sigma_1} \mathbf{A}(\sigma_2) \int_{\sigma_3}^{\sigma_2} \mathbf{A}(\sigma_3)\, d\sigma_3 d\sigma_2 d\sigma_1 + \cdots,\ \text{Then}$$

$$\boldsymbol{\Phi}(t, t_0) = \mathbf{I} + \int_{t_0}^{t_f} \mathbf{A}(\sigma)\, d\sigma = \begin{bmatrix} \mathbf{I}_6 & \begin{bmatrix} -\int_{t_0}^{t_f} {}^{B}\mathbf{T}\, d\sigma \\ \mathbf{0}_{3\times1} \end{bmatrix} \\ \mathbf{0}_{1\times6} & 1 \end{bmatrix} \tag{4.6}$$

$$\mathbf{M}(t_0, t_f) = \int_{t_0}^{t_f} \boldsymbol{\Phi}^{T}(t, t_0)\mathbf{C}^{T}(t)\mathbf{C}(t)\boldsymbol{\Phi}(t, t_0)dt \tag{4.7}$$

$$\mathbf{M}(t_0, t_f) = \int_{t_0}^{t_f} \begin{bmatrix} \mathbf{I}_6 \\ \left[-\int_{t_0}^{t_f} {}^{B}\mathbf{T}^{T}\, d\sigma \quad \mathbf{0}_{1\times3}\right] \end{bmatrix} \begin{bmatrix} \mathbf{I}_6 & \begin{bmatrix} -\int_{t_0}^{t_f} {}^{B}\mathbf{T}\, d\sigma \\ \mathbf{0}_{3\times1} \end{bmatrix} \end{bmatrix} dt \tag{4.8}$$

Denote $\mathbf{K}_{6\times1} = \begin{bmatrix} -\int_{t_0}^{t_f} {}^{B}\mathbf{T}\, d\sigma \\ \mathbf{0}_{3\times1} \end{bmatrix}$, one can get

$$\mathbf{M}(t_0, t_f) = \int_{t_0}^{t_f} \begin{bmatrix} \mathbf{I_6} & \mathbf{K_{6\times1}} \\ \mathbf{K^T}_{1\times6} & \mathbf{K^T}_{1\times6}\mathbf{K_{6\times1}} \end{bmatrix} dt \tag{4.9}$$

which satisfied $\mathbf{M}^T(t_0, t_f) = \mathbf{M}(t_0, t_f)$, now introduce a unit vector $\mathbf{\hat{q}} \in \mathbf{R}^{7\times1}$, and consider the quadratic form

$$\mathbf{Q} = \mathbf{\hat{q}}^T\mathbf{M}(t_0, t_f)\mathbf{\hat{q}} \tag{4.9}$$

$\mathbf{Q}$ was positive definite if and only if all the principal minors were non-singular. Thus, if $\mathbf{Q}$ was positive definite, then $\mathbf{M}(t_0, t_f)$ was invertible. Expand the expression (4.9)

$$\mathbf{Q} = \mathbf{\hat{q}}^T \int_{t_0}^{t_f} \begin{bmatrix} \mathbf{I_6} \\ \mathbf{K^T}_{1\times6} \end{bmatrix} [\mathbf{I_6}\ \mathbf{K_{6\times1}}]dt\ \mathbf{\hat{q}} \tag{4.10}$$

$$\mathbf{Q} = \int_{t_0}^{t_f} \mathbf{\hat{q}}^T \begin{bmatrix} \mathbf{I_6} \\ \mathbf{K^T}_{1\times6} \end{bmatrix} [\mathbf{I_6}\ \mathbf{K_{6\times1}}]\mathbf{\hat{q}}dt \tag{4.11}$$

The induced norm of the matrix $\mathbf{K} \in \mathbf{R}^{m\times n}$ was defined as

$$\|\mathbf{K}\| \triangleq max\|\mathbf{Kq}\| \quad \exists \mathbf{q} \in \mathbf{R}^{n\times1}, \|\mathbf{q}\| = 1 \tag{4.12}$$

Hence, let the $\mathbf{\hat{q}}$ be such that the induced norm of a matrix is defined. Then the quadratic form can be written as

$$\mathbf{Q} = \int_{t_0}^{t_f}\|[\mathbf{I_6}\ \mathbf{K_{6\times1}}]\|^2 dt \tag{4.13}$$

$$\mathbf{Q} = \int_{t_0}^{t_f}\|[\mathbf{I_6}\ \mathbf{K_{6\times1}}]\mathbf{\hat{q}}\|^2 dt \tag{4.14}$$

If $\mathbf{M}(t_0, t_f)$ was not invertible, then $\mathbf{Q} = 0$, and

$$\int_{t_0}^{t_f}\|[\mathbf{I_6}\ \mathbf{K_{6\times1}}]\mathbf{\hat{q}}\|^2 dt = 0 \tag{4.15}$$

$$\|[\mathbf{I_6}\ \mathbf{K_{6\times1}}]\mathbf{\hat{q}}\| = 0 \tag{4.16}$$

Let $\mathbf{\hat{q}} = \begin{bmatrix} \mathbf{q_1} \\ q_2 \end{bmatrix}$, then

$$\mathbf{q_1} + \mathbf{K_{6\times1}}q_2 = \mathbf{0} \tag{4.17}$$

$$\mathbf{q_1} + \begin{bmatrix} -\int_{t_0}^{t_f} {}^B\mathbf{T}\, d\sigma \\ \mathbf{0_{3\times1}} \end{bmatrix} q_2 = \mathbf{0} \tag{4.18}$$

Setting $t_f = t_0$, then $\mathbf{q_1} = \mathbf{0}$. Hence

$$\begin{bmatrix} \int_{t_0}^{t_f} {}^B\mathbf{T}\, d\sigma \\ \mathbf{0_{3\times1}} \end{bmatrix} q_2 = \mathbf{0} \tag{4.19}$$

$$\int_{t_0}^{t_f} {}^B\mathbf{T}\, d\sigma q_2 = \mathbf{0} \tag{4.20}$$

$$\int_{t_0}^{t_f} {}^BT\, d\sigma q_2 = 0 \tag{4.21}$$

Thus, if no $q_2 \in \mathbf{R}\backslash\{0\}$ can be found that satisfies the condition in Eq. (4.21), the observability matrix $\mathbf{M}(t_0, t_f)$ was invertible. This implied that The $\mathbf{M}(t_0, t_f)$ was

invertible if and only if $^B\mathbf{T}$ did not always equal to $\mathbf{0}$ on $[t_0, t_f]$. Also, if $^B\mathbf{T}$ did not always equal to $\mathbf{0}$, then given t_0, for $\forall \Delta T > 0$, $\mathbf{M}(t_0, t_0 + \Delta T)$ was invertible. The physical meaning of the argument was that the thrust cannot be zero during the whole time interval.

In all, the linear time-varying mimicking system was observable and the nonlinear system was observable with global stability with Kalman-Bucy filter under the condition that $^B\mathbf{T}$ was not always $\mathbf{0}$ on $[t_0, t_f]$. Observation noise and state noise were assumed to be white noises.

The linear time-varying model and the observer were constructed in Simulink environment. The same input quantities were applied to the linear time-varying model with $^B\mathbf{T} = \begin{bmatrix} 0 \\ 0 \\ 2 \end{bmatrix}$ Newton and $^B\boldsymbol{\tau} = \begin{bmatrix} 0.1 \\ 0.1 \\ 0.1 \end{bmatrix}$ rad/s^2, $^B_E\mathbf{R}(t_0) = \begin{bmatrix} 1 & 0 & 0 \\ 0 & 1 & 0 \\ 0 & 0 & 1 \end{bmatrix}$. And the initial conditions that served as guesses to the unknown states in the observer were $^B\widehat{\mathbf{V}}(t_0) = \begin{bmatrix} 2 \\ 2 \\ 2 \end{bmatrix}$ m/s, $\widehat{m}(t_0) = 0.22$ kg, and $^B\widehat{\boldsymbol{\omega}}(t_0) = \begin{bmatrix} 2 \\ 2 \\ 2 \end{bmatrix}$ rad/s.
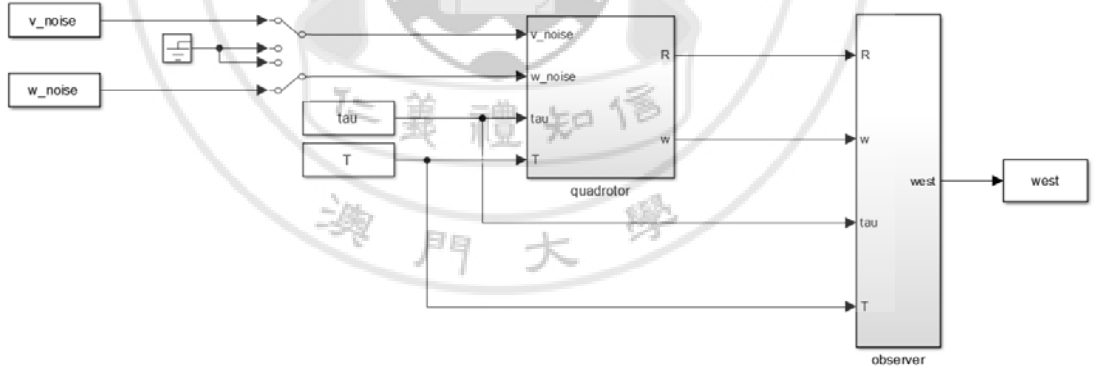
Figure 5. LTV model and observer model

The observer received signal from the available measurements of the state, which were $^B\mathbf{V}$ and $^B\boldsymbol{\omega}$, as well as the control input $^B\mathbf{T}$ and $^B\boldsymbol{\tau}$. Then, the observer outputted the estimated states that involved not only $^B\mathbf{V}$ and $^B\boldsymbol{\omega}$, but also the mass m.
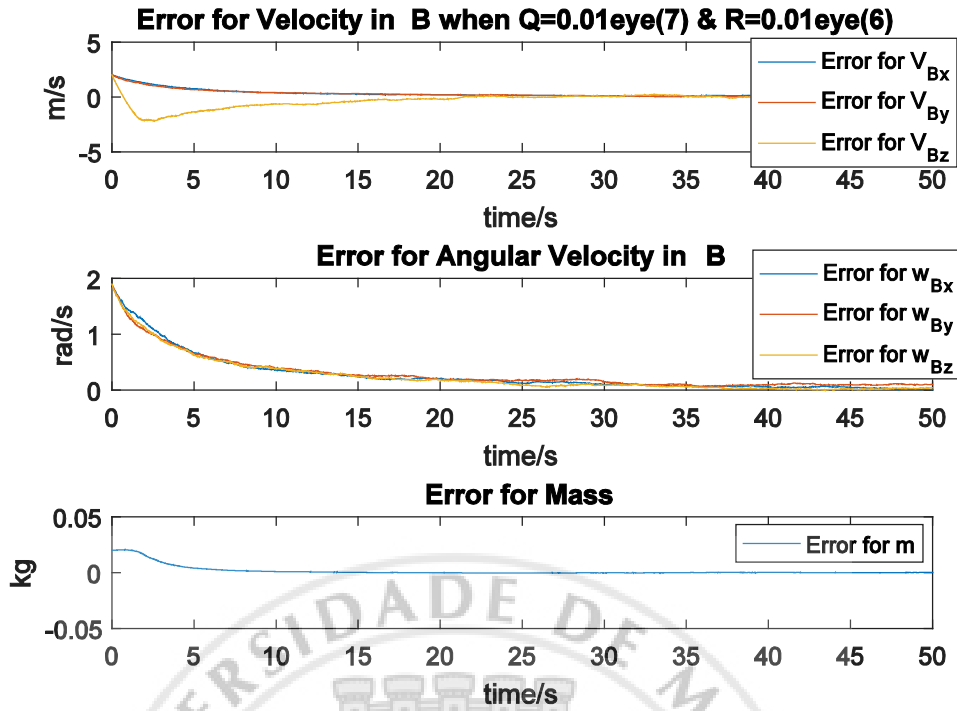
Figure 6. Simulation result of open loop system with observer

As shown in figure 6, all of the error for the estimated states converged to zero in less than seconds. For the Kalman-Bucy filter that returned the optimal feedback gain, two covariance matrices were defined in advance that reflected the system behavior of whether more noise existed in the dynamics of the system or in the observation. Effects were shown in the following figures.
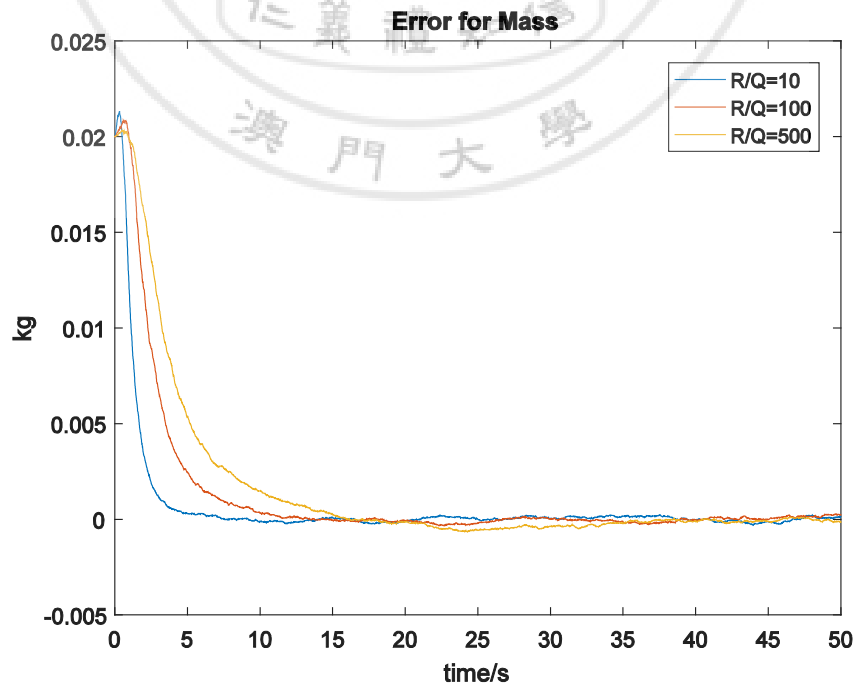
Figure 7. Simulation result of different relative noises level

The above figure showed that relative higher noise level in the observation than that in the state led to slower convergence rate of the error dynamics, which can be explained with the implementation of the Kalman-Bucy filter. With the LTV model

$$\begin{cases} \dot{\mathbf{w}} = \mathbf{A}\mathbf{w} + \mathbf{B}\mathbf{u} + \mathbf{p} \\ \mathbf{z} = \mathbf{C}\mathbf{w} + \mathbf{q} \\ \mathbf{w}(t_0) = \begin{bmatrix} {}^B\mathbf{V}(t_0) \\ {}^B\boldsymbol{\omega}(t_0) \\ 0 \end{bmatrix} \end{cases} \tag{4.22}$$

where $\mathbf{A}(t) = \begin{bmatrix} \mathbf{0}_{6\times6} & \begin{bmatrix} -{}^B\mathbf{T} \\ \mathbf{0}_{3\times1} \end{bmatrix} \\ \mathbf{0}_{1\times6} & 0 \end{bmatrix}$, $\mathbf{B}(t)\mathbf{u}(t) = \begin{bmatrix} -\mathbf{S}({}^B\boldsymbol{\omega}){}^B\mathbf{V} + g{}^E_B\mathbf{R}^T\mathbf{e}_3 \\ {}^B\boldsymbol{\tau} \\ 0 \end{bmatrix}$, $\mathbf{C}(t) =$

$[\mathbf{I}_6 \quad \mathbf{0}_{6\times1}]$, $\mathbf{w}(t_0)\sim\mathcal{N}(\mathbf{w}_0, \mathbf{P}(t_0) > 0)$, $\mathbf{p}(t)\sim\mathcal{N}(\mathbf{0}, \mathbf{Q}(t) \geqslant 0)$, $\mathbf{q}(t)\sim\mathcal{N}(\mathbf{0}, \mathbf{R}(t) > 0)$.

Time dependence (t) was omitted for convenience. Then the Kalman-Bucy filter was

$$\begin{cases} \dot{\hat{\mathbf{w}}} = \mathbf{A}\hat{\mathbf{w}} + \mathbf{B}\mathbf{u} + \mathbf{K}(\mathbf{z} - \mathbf{C}\mathbf{w}) \\ \hat{\mathbf{w}}(t_0)\sim\mathcal{N}(\mathbf{w}_0, \mathbf{P}(t_0)) \\ \dot{\mathbf{P}} = \mathbf{A}\mathbf{P} + \mathbf{P}\mathbf{A}^T + \mathbf{Q} - \mathbf{P}\mathbf{C}^T\mathbf{R}^{-1}\mathbf{C}\mathbf{P} \\ \mathbf{K} = \mathbf{P}\mathbf{C}^T\mathbf{R}^{-1} \end{cases} \tag{4.23}$$

As can be inferred from the above equation, a bigger value of $\mathbf{R}$ would result in a smaller inverse $\mathbf{R}^{-1}$ and the optimal Kalman-Bucy gain $\mathbf{K}(t)$ would be smaller in the sense that the convergence rate would be slower. Hence, the characteristics of the Kalman-Bucy filter provided a convenient way of tuning the convergence rate.

4.2 OBSERVER DESIGN WITH BOTH UNKNOWN MASS AND EXTERNAL FORCE DISTURBANCE

In previous part, observation of the full state variables was proved and simulated to be successful. However, the angular velocity was just the integral of the input torque signal. Thus, estimation of the angular velocity was unnecessary and should be eliminated from the observer. Then the Eq. (3.20) became

$$\begin{cases} {}^E_B\dot{\mathbf{R}} = {}^E_B\mathbf{R}\mathbf{S}({}^B\boldsymbol{\omega}) \\ {}^E\dot{\mathbf{P}} = {}^E_B\mathbf{R}\,{}^B\mathbf{V} \\ {}^B\dot{\mathbf{V}} = -\mathbf{S}({}^B\boldsymbol{\omega})\,{}^B\mathbf{V} - \frac{1}{m}\,{}^B\mathbf{T} + g{}^B_E\mathbf{R}\mathbf{e}_3 + \frac{1}{m}\,{}^B_E\mathbf{R}\,{}^E\mathbf{b} \\ {}^B\dot{\boldsymbol{\omega}} = {}^B\boldsymbol{\tau} \end{cases} \tag{4.24}$$

Notice that $\frac{1}{m}$ and $\frac{{}^E\mathbf{b}}{m}$ was linear with state variables, one can get

$$\begin{bmatrix} {}^B\dot{\mathbf{V}} \\ \frac{d}{dt}\left(\frac{1}{m}\right) \\ \frac{d}{dt}\left(\frac{{}^E\mathbf{b}}{m}\right) \end{bmatrix} = \begin{bmatrix} \mathbf{0}_{3\times3} & -{}^B\mathbf{T} & {}^E_B\mathbf{R}^T \\ \mathbf{0}_{1\times3} & 0 & \mathbf{0}_{1\times3} \\ \mathbf{0}_{3\times3} & \mathbf{0}_{3\times1} & \mathbf{0}_{3\times3} \end{bmatrix} \begin{bmatrix} {}^B\mathbf{V} \\ \left(\frac{1}{m}\right) \\ \left(\frac{{}^E\mathbf{b}}{m}\right) \end{bmatrix} + \begin{bmatrix} -\mathbf{S}\left({}^B\boldsymbol{\omega}\right){}^B\mathbf{V} + g{}^E_B\mathbf{R}^T\mathbf{e}_3 \\ 0 \\ \mathbf{0}_{3\times1} \end{bmatrix} \quad (4.25)$$

Define a state variable $\mathbf{x}(t) = {}^B\mathbf{V} \in \mathbf{R}^{3\times1}$ and an output variable $\mathbf{y}(t) = {}^B\mathbf{V} \in \mathbf{R}^{3\times1}$ can be defined. Hence the Eq. (4.25) became

$$\begin{cases} \begin{bmatrix} \dot{\mathbf{x}} \\ \frac{d}{dt}\left(\frac{1}{m}\right) \\ \frac{d}{dt}\left(\frac{{}^E\mathbf{b}}{m}\right) \end{bmatrix} = \begin{bmatrix} \mathbf{0}_{3\times3} & -{}^B\mathbf{T} & {}^E_B\mathbf{R}^T \\ \mathbf{0}_{1\times3} & 0 & \mathbf{0}_{1\times3} \\ \mathbf{0}_{3\times3} & \mathbf{0}_{3\times1} & \mathbf{0}_{3\times3} \end{bmatrix} \begin{bmatrix} \mathbf{x} \\ \left(\frac{1}{m}\right) \\ \left(\frac{{}^E\mathbf{b}}{m}\right) \end{bmatrix} + \begin{bmatrix} -\mathbf{S}\left({}^B\boldsymbol{\omega}\right){}^B\mathbf{V} + g{}^E_B\mathbf{R}^T\mathbf{e}_3 \\ 0 \\ \mathbf{0}_{3\times1} \end{bmatrix} \\ \mathbf{y}(t) = \mathbf{I}_3\mathbf{x}(t) \end{cases} \quad (4.26)$$

Consider the state and output transformation described in Eq. (2.17) and (2.14), define the two transformations as

$$\begin{cases} \mathbf{T}_x\big(\mathbf{x}(t)\big) = \begin{bmatrix} \mathbf{x}(t) \\ \left(\frac{1}{m}\right) \\ \left(\frac{{}^E\mathbf{b}}{m}\right) \end{bmatrix} \\ \mathbf{T}_y\big(\mathbf{y}(t)\big) = \mathbf{I}_3\mathbf{y}(t) \end{cases} \quad (4.27)$$

and let new state variables $\mathbf{w}(t) = \mathbf{T}_x\big(\mathbf{x}(t)\big)$ and $\mathbf{z}(t) = \mathbf{T}_y\big(\mathbf{y}(t)\big)$. The overall system now has the dynamics in the form like that of Eq. (2.18).

$$\begin{cases} \dot{\mathbf{w}} = \begin{bmatrix} \mathbf{0}_{3\times3} & -{}^B\mathbf{T} & {}^E_B\mathbf{R}^T \\ \mathbf{0}_{1\times3} & 0 & \mathbf{0}_{1\times3} \\ \mathbf{0}_{3\times3} & \mathbf{0}_{3\times1} & \mathbf{0}_{3\times3} \end{bmatrix} \mathbf{w} + \begin{bmatrix} -\mathbf{S}\left({}^B\boldsymbol{\omega}\right){}^B\mathbf{V} + g{}^E_B\mathbf{R}^T\mathbf{e}_3 \\ 0 \\ \mathbf{0}_{3\times1} \end{bmatrix} \\ \mathbf{z} = [\mathbf{I}_3 \quad \mathbf{0}_{3\times1} \quad \mathbf{0}_{3\times3}]\mathbf{w} \\ \mathbf{w}(t_0) = \begin{bmatrix} {}^B\mathbf{V}(t_0) \\ 0 \\ 0 \end{bmatrix} \end{cases} \quad (4.28)$$

Define $\mathbf{A}(t) = \begin{bmatrix} \mathbf{0}_{3\times3} & -{}^B\mathbf{T} & {}^E_B\mathbf{R}^T \\ \mathbf{0}_{1\times3} & 0 & \mathbf{0}_{1\times3} \\ \mathbf{0}_{3\times3} & \mathbf{0}_{3\times1} & \mathbf{0}_{3\times3} \end{bmatrix}$, $\mathbf{C}(t) = [\mathbf{I}_3 \quad \mathbf{0}_{3\times1} \quad \mathbf{0}_{3\times3}]$. To guarantee the

nonlinear system described in Eq. (4.24) was observable, one should check the observability of the resulting linear time-varying system described in Eq. (4.28) on time interval $[t_0, t_f]$ by calculating the observability matrix defined in Eq. (2.19). Note that

the transition matrix $\boldsymbol{\Phi}(t, t_0) = \mathbf{I} + \int_{t_0}^{t_f} \mathbf{A}(\sigma_1)\, d\sigma_1 + \int_{t_0}^{t_f} \mathbf{A}(\sigma_1) \int_{\sigma_2}^{\sigma_1} \mathbf{A}(\sigma_2)\, d\sigma_2 d\sigma_1 +$

$\int_{t_0}^{t_f} \mathbf{A}(\sigma_1) \int_{\sigma_2}^{\sigma_1} \mathbf{A}(\sigma_2) \int_{\sigma_3}^{\sigma_2} \mathbf{A}(\sigma_3)\, d\sigma_3 d\sigma_2 d\sigma_1 + \cdots$, Then

$$\Phi(t, t_0) = \mathbf{I} + \int_{t_0}^{t_f} \mathbf{A}(\sigma) \, d\sigma = \begin{bmatrix} \mathbf{I_3} & -\int_{t_0}^{t_f} {}^B\mathbf{T} \, d\sigma & \int_{t_0}^{t_f} {}^E_B\mathbf{R}^T \, d\sigma \\ \mathbf{0_{1\times3}} & 1 & \mathbf{0_{1\times3}} \\ \mathbf{0_{3\times3}} & \mathbf{0_{3\times1}} & \mathbf{I_3} \end{bmatrix} \tag{4.29}$$

$$\mathbf{M}(t_0, t_f) = \int_{t_0}^{t_f} \Phi^T(t, t_0) \mathbf{C}^T(t) \mathbf{C}(t) \Phi(t, t_0) dt \tag{4.30}$$

$$\mathbf{M}(t_0, t_f) = \int_{t_0}^{t_f} \begin{bmatrix} \mathbf{I_3} \\ \mathbf{K}^T{}_{4\times3} \end{bmatrix} [\mathbf{I_3} \ \mathbf{K_{3\times4}}] dt \tag{4.31}$$

where $\mathbf{K_{3\times4}} = \left[-\int_{t_0}^{t_f} {}^B\mathbf{T} \, d\sigma \quad \int_{t_0}^{t_f} {}^E_B\mathbf{R}^T \, d\sigma \right]$, and one can get

$$\mathbf{M}(t_0, t_f) = \int_{t_0}^{t_f} \begin{bmatrix} \mathbf{I_3} & \mathbf{K_{3\times4}} \\ \mathbf{K}^T{}_{4\times3} & \mathbf{K}^T{}_{4\times3}\mathbf{K_{3\times4}} \end{bmatrix} dt \tag{4.32}$$

which satisfied $\mathbf{M}^T(t_0, t_f) = \mathbf{M}(t_0, t_f)$, now introduce a unit vector $\hat{\mathbf{q}} \in \mathbf{R}^{7\times1}$, and consider the quadratic form

$$Q = \hat{\mathbf{q}}^T \mathbf{M}(t_0, t_f) \hat{\mathbf{q}} \tag{4.33}$$

Q was positive definite if and only if all the principal minors were non-singular. Thus, if Q was positive definite, then $\mathbf{M}(t_0, t_f)$ was invertible. Expand the expression (4.9)

$$Q = \hat{\mathbf{q}}^T \int_{t_0}^{t_f} \begin{bmatrix} \mathbf{I_3} \\ \mathbf{K}^T{}_{4\times3} \end{bmatrix} [\mathbf{I_3} \ \mathbf{K_{3\times4}}] dt \, \hat{\mathbf{q}} \tag{4.34}$$

$$Q = \int_{t_0}^{t_f} \hat{\mathbf{q}}^T \begin{bmatrix} \mathbf{I_3} \\ \mathbf{K}^T{}_{4\times3} \end{bmatrix} [\mathbf{I_3} \ \mathbf{K_{3\times4}}] \hat{\mathbf{q}} dt \tag{4.35}$$

The induced norm of the matrix $\mathbf{K} \in \mathbf{R}^{m\times n}$ was defined as

$$\|\mathbf{K}\| \triangleq max\|\mathbf{Kq}\| \quad \exists \mathbf{q} \in \mathbf{R}^{n\times1}, \|\mathbf{q}\| = 1 \tag{4.36}$$

Hence, let the $\hat{\mathbf{q}}$ be such that the induced norm of a matrix is defined. Then the quadratic form can be written as

$$Q = \int_{t_0}^{t_f} \|[\mathbf{I_3} \ \mathbf{K_{3\times4}}]\|^2 dt \tag{4.37}$$

$$Q = \int_{t_0}^{t_f} \|[\mathbf{I_3} \ \mathbf{K_{3\times4}}]\hat{\mathbf{q}}\|^2 dt \tag{4.38}$$

If $\mathbf{M}(t_0, t_f)$ was not invertible, then $Q = 0$, and

$$\int_{t_0}^{t_f} \|[\mathbf{I_3} \ \mathbf{K_{3\times4}}]\hat{\mathbf{q}}\|^2 dt = 0 \tag{4.39}$$

$$\|[\mathbf{I_3} \ \mathbf{K_{3\times4}}]\hat{\mathbf{q}}\| = 0 \tag{4.40}$$

Let $\hat{\mathbf{q}} = \begin{bmatrix} \mathbf{q_1} \\ \mathbf{q_2} \end{bmatrix}$, where $\mathbf{q_1} \in \mathbf{R}^{3\times1}$ and $\mathbf{q_2} \in \mathbf{R}^{4\times1}$ then

$$\mathbf{q_1} + \mathbf{K_{3\times4}}\mathbf{q_2} = \mathbf{0} \tag{4.41}$$

$$\mathbf{q_1} + \left[-\int_{t_0}^{t_f} {}^B\mathbf{T} \, d\sigma \quad \int_{t_0}^{t_f} {}^E_B\mathbf{R}^T \, d\sigma \right] \mathbf{q_2} = \mathbf{0} \tag{4.42}$$

Setting $t_f = t_0$, then $\mathbf{q_1} = \mathbf{0}$. Hence

$$\left[-\int_{t_0}^{t_f} {}^B\mathbf{T}\,d\sigma \quad \int_{t_0}^{t_f} {}_B^E\mathbf{R}^T\,d\sigma\right]\mathbf{q_2} = \mathbf{0} \tag{4.43}$$

Let $\quad \mathbf{q_2} = \begin{bmatrix} q_{21} \\ q_{22} \\ q_{23} \\ q_{24} \end{bmatrix}$, $\quad {}^B\mathbf{T} = \begin{bmatrix} 0 \\ 0 \\ {}^BT \end{bmatrix}$, $\quad$ and $\quad {}_B^E\mathbf{R} = \mathbf{R}_Z(\alpha)\mathbf{R}_Y(\beta)\mathbf{R}_X(\gamma) =$

$\begin{bmatrix} c\alpha s\beta & c\alpha s\beta s\gamma - s\alpha c\gamma & c\alpha s\beta c\gamma + s\alpha s\gamma \\ s\alpha c\beta & s\alpha s\beta s\gamma + c\alpha c\gamma & s\alpha s\beta c\gamma - c\alpha s\gamma \\ -s\beta & c\beta s\gamma & c\beta c\gamma \end{bmatrix}$, where α, β, γ denoted roll, pitch, and

yaw angles, respectively. $c(\cdot)$ denoted the cosine of an angle, while $s(\cdot)$ denoted the sine of an angle. Rewriting Eq. (4.43), one can get

$$\int_{t_0}^{t_f}\begin{bmatrix} 0 & c\alpha s\beta & s\alpha c\beta & -s\beta \\ 0 & c\alpha s\beta s\gamma - s\alpha c\gamma & s\alpha s\beta s\gamma + c\alpha c\gamma & c\beta s\gamma \\ -{}^BT & c\alpha s\beta c\gamma + s\alpha s\gamma & s\alpha s\beta c\gamma - c\alpha s\gamma & c\beta c\gamma \end{bmatrix}\begin{bmatrix} q_{21} \\ q_{22} \\ q_{23} \\ q_{24} \end{bmatrix}d\sigma = \mathbf{0} \tag{4.44}$$

Taking time derivative of both sides of Eq. (4.44), one can get

$$\begin{cases} q_{22}c\alpha s\beta + q_{23}s\alpha c\beta + q_{24}(-s\beta) = 0 \\ q_{22}(c\alpha s\beta s\gamma - s\alpha c\gamma) + q_{23}(s\alpha s\beta s\gamma + c\alpha c\gamma) + q_{24}c\beta s\gamma = 0 \\ -q_{21}{}^BT + q_{22}(c\alpha s\beta c\gamma + s\alpha s\gamma) + q_{23}(s\alpha s\beta c\gamma - c\alpha s\gamma) + q_{24}c\beta c\gamma = 0 \end{cases} \tag{4.45}$$

Thus, if no $\mathbf{q_2} \in \mathbf{R}^4\backslash\{\mathbf{0}\}$ can be found that satisfies the condition in Eq. (4.45), the observability matrix $\mathbf{M}(t_0, t_f)$ was invertible. This implied that $\mathbf{M}(t_0, t_f)$ was invertible if and only if the following three sets of functions were linearly independent on $[t_0, t_f]$:

$$\{c\alpha s\beta, s\alpha c\beta, -s\beta\} \tag{4.46a}$$

$$\{c\alpha s\beta s\gamma - s\alpha c\gamma, s\alpha s\beta s\gamma + c\alpha c\gamma, c\beta s\gamma\} \tag{4.46b}$$

$$\{-{}^BT, c\alpha s\beta c\gamma + s\alpha s\gamma, s\alpha s\beta c\gamma - c\alpha s\gamma, c\beta c\gamma\} \tag{4.46c}$$

Using the same conditions as those of last section for ${}^B\mathbf{T}$, ${}^B\boldsymbol{\tau}$, ${}_E^B\mathbf{R}(t_0)$, and ${}^E\mathbf{b} = \begin{bmatrix} 0.3 \\ 0.2 \\ 0.1 \end{bmatrix}$ Newton. Initial guesses of the initial linear velocity was using the same as that of

last section for ${}^B\widehat{\mathbf{V}}(t_0)$, $\widehat{m}(t_0) = 0.14$ kg, and ${}^E\widehat{\mathbf{b}}(t_0) = \begin{bmatrix} 0 \\ 0 \\ 0 \end{bmatrix}$ Newton. The Kalman

filter parameters were set as $\mathbf{Q} = 0.01\mathbf{I}_7$, $\mathbf{R} = 0.01\mathbf{I}_3$, and the initial covariance matrix $\mathbf{P}(t_0) = \mathbf{I}_7$. The simulation results gave
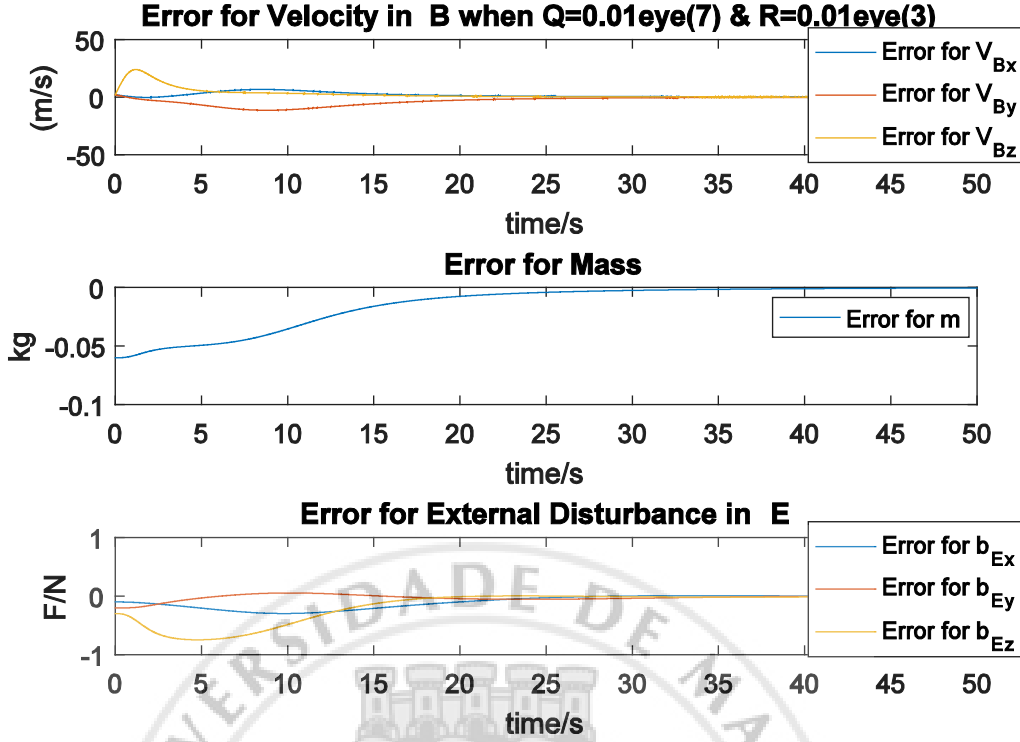
Figure 8. Simulation result of open loop system with observer

Thus, as long as the actuations ${}^{B}T$ and ${}^{B}\tau$ were not constant on $[t_0, t_f]$ and they were sufficiently rich, then the linear time-varying system was observable and the unknown system parameters like ${}^{E}\mathbf{b}$ and m could be recovered.

Apart from the above simulation, a special case involving the above three sets of equations was explored to explore the linear independence requirements specified in Eq. (4.46).

EXAMPLE 1 — Effects of a constant rotational matrix on the performance of the observer

The setting was equivalent to the limitation that $\dot{\alpha} = 0, \dot{\beta} = 0, \dot{\gamma} = 0$, and $\alpha \neq \frac{\pi}{2}, \beta \neq \frac{\pi}{2}, \gamma \neq \frac{\pi}{2}$. Then, a constant unit vector associated with the three sets of Eq. (4.46) could be easily found to be

$$\mathbf{q}_2 = \begin{bmatrix} 0 \\ 0 \\ -c\beta c\gamma \\ s\alpha s\beta c\gamma - c\alpha s\gamma \end{bmatrix} \in \mathbf{R}^4 \backslash \{\mathbf{0}\} \qquad (4.47)$$

Although no conclusion could be made theoretically to prove the observability of the nonlinear system described in Eq. (4.24), the stability of the estimator system was still ensured. Moreover, the estimated values of the states converged to constants, though are not guaranteed to converge to the correct parameters. The corresponding simulation results were shown in the following figure:
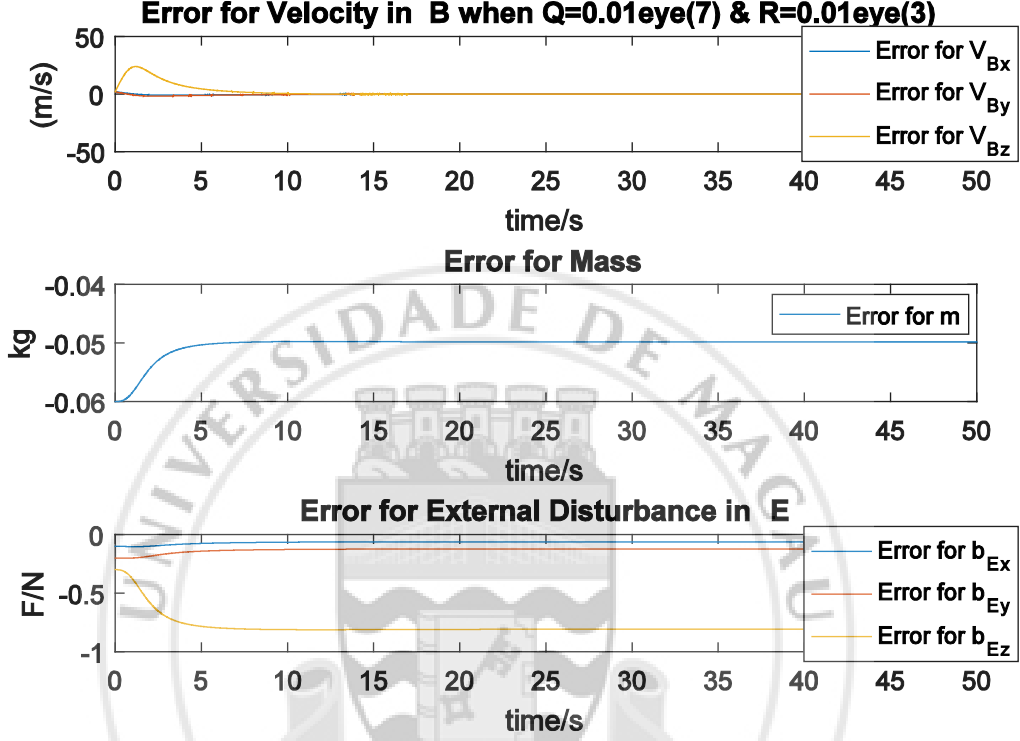
Figure 9. Simulation result of open loop system with observer and constant $_E^B\mathbf{R}$

Note that the conditions for the system should be set as $^B\mathbf{T} = \begin{bmatrix} 0 \\ 0 \\ 2 \end{bmatrix}$ Newton, $^B\boldsymbol{\tau} = \begin{bmatrix} 0 \\ 0 \\ 0 \end{bmatrix}$ rad/s², $^B\boldsymbol{\omega}(t_0) = \begin{bmatrix} 0 \\ 0 \\ 0 \end{bmatrix}$ rad/s. Initial guesses of the unknown parameters $^B\hat{\mathbf{V}}(t_0) = \begin{bmatrix} 2 \\ 2 \\ 2 \end{bmatrix}$ m/s, $\hat{m} = 0.02$ kg, $^E\hat{\mathbf{b}} = \begin{bmatrix} 0 \\ 0 \\ 0 \end{bmatrix}$ Newton.

As shown in figure 9, the estimation of both the mass of the quadrotor and the external force disturbance it experienced did not converge to the correct values. However, the convergence property still held for the observer system.

Chapter 5 CONTROLLER DESIGN

So far, full information about the states was known at the output of the designed observer in the last chapter. Controlling algorithm design and analysis were addressed in this chapter. Specifically, the controller should guarantee the convergence of positional error while enabling the quadrotor to follow certain predefined trajectories.

5.1 NONLINEAR BACKSTEPPING

Standard backstepping technique was adopted in developing a tunable controlling algorithm. The new dynamics was described in the following equation, equivalent to Eq. (4.24):

$$\begin{cases} {}_{B}^{E}\dot{\mathbf{R}} = {}_{B}^{E}\mathbf{R}\mathbf{S}({}^{B}\boldsymbol{\omega}) \\ {}^{E}\dot{\mathbf{P}} = {}_{B}^{E}\mathbf{R}\,{}^{B}\mathbf{V} \\ {}^{B}\dot{\mathbf{V}} = -\mathbf{S}({}^{B}\boldsymbol{\omega})\,{}^{B}\mathbf{V} - \frac{1}{m}{}^{B}\mathbf{T} + g\,{}_{E}^{B}\mathbf{R}\mathbf{e}_{3} + \frac{1}{m}{}_{E}^{B}\mathbf{R}\,{}^{E}\mathbf{b} \\ {}^{B}\dot{\boldsymbol{\omega}} = {}^{B}\boldsymbol{\tau} \end{cases} \tag{5.1}$$

Let ${}^{E}\mathbf{P}_{d}(t)$ be a bounded desired trajectory whose time derivatives were also bounded. The trajectory tracking problem now became the problem of designing the controlling

inputs ${}^{B}\mathbf{T}(t) = \begin{bmatrix} 0 \\ 0 \\ {}^{B}T(t) \end{bmatrix}$ and ${}^{B}\boldsymbol{\tau}(t) = \begin{bmatrix} {}^{B}\tau_{x}(t) \\ {}^{B}\tau_{y}(t) \\ {}^{B}\tau_{z}(t) \end{bmatrix}$ such that made the error dynamics

of the position error $\mathbf{z}_{1}(t) := {}^{E}\mathbf{P}(t) - {}^{E}\mathbf{P}_{d}(t)$ converge to zero as time t went from 0 to ∞. The backstepping procedures were stated as followed (time dependence and reference frames attached to each variable was omitted to suppress expressions).

Define the positional error

$$\mathbf{z}_{1} := \mathbf{P} - \mathbf{P}_{d} \tag{5.2}$$

and a corresponding Lyapunov function can be chosen as

$$V_{1} := \frac{1}{2}\mathbf{z}_{1}^{\mathrm{T}}\mathbf{z}_{1} \tag{5.3}$$

Referring to section 2.3, this particular kind of Lyapunov function had some preferred properties if no constraints were exerted on $\mathbf{z}_{1}$. Firstly, V_{1} had continuous partial derivatives with respect to $\mathbf{z}_{1}$, *i.e.* $\frac{\partial V_{1}}{\partial \mathbf{z}_{1}} = \frac{1}{2}\frac{(\partial \mathbf{z}_{1})^{\mathrm{T}}}{\partial \mathbf{z}_{1}}\mathbf{z}_{1} + \frac{1}{2}\mathbf{z}_{1}^{\mathrm{T}}\frac{\partial \mathbf{z}_{1}}{\partial \mathbf{z}_{1}} = \mathbf{z}_{1}^{\mathrm{T}}$, where $\mathbf{z}_{1}^{\mathrm{T}}$ was continuous as long as both ${}^{E}\mathbf{P}$ and ${}^{E}\mathbf{P}_{d}$ were continuous. Secondly, V_{1} was positive definite, *i.e.* $V_{1} := \frac{1}{2}\mathbf{z}_{1}^{\mathrm{T}}\mathbf{z}_{1} = \frac{1}{2}|\mathbf{z}_{1}|^{2} \geq 0$. Thirdly, V_{1} was radially unbounded provided

that no constraints like bounded conditions were exerted on $\mathbf{z}_1$. Now, it was desired that the Lyapunov function V_1 had negative time derivative, so that certain kind of stability could be concluded with respect to the positional error $\mathbf{z}_1$. The time derivative of V_1 was calculated to be:

$$\dot{V}_1 = \frac{1}{2}\dot{\mathbf{z}}_1^{\mathrm{T}}\mathbf{z}_1 + \frac{1}{2}\mathbf{z}_1^{\mathrm{T}}\dot{\mathbf{z}}_1 = \mathbf{z}_1^{\mathrm{T}}\dot{\mathbf{z}}_1 \qquad (5.4)$$

where $\dot{\mathbf{z}}_1 = \mathbf{R}\mathbf{V} - \dot{\mathbf{P}}_{\mathrm{d}}$, thus:

$$\dot{V}_1 = \mathbf{z}_1^{\mathrm{T}}(\mathbf{R}\mathbf{V} - \dot{\mathbf{P}}_{\mathrm{d}}) = -k_1\mathbf{z}_1^{\mathrm{T}}\mathbf{z}_1 + \mathbf{z}_1^{\mathrm{T}}\mathbf{R}[\mathbf{V} + \mathbf{R}^{\mathrm{T}}(-\dot{\mathbf{P}}_{\mathrm{d}} + k_1\mathbf{z}_1)] \qquad (5.5)$$

where k_1 was a positive real constant. The initiative now was to make $\dot{V}_1$ negative with respect to time so that certain kind of stability can be concluded. Note that the quadrotor in discussion was an underactuated one in the sense that the number of degrees of freedom (which was 6) was larger than the number of actuation (which was 4). Thus, it was impossible for the quadrotor to follow exactly the predefined trajectory and the dynamics that went along with the trajectory. According the reasoning in [16], instead of driving the quantity $\mathbf{V} + \mathbf{R}^{\mathrm{T}}(-\dot{\mathbf{P}}_{\mathrm{d}} + k_1\mathbf{z}_1)$ to zero, let:

$$\mathbf{z}_2 := \mathbf{V} + \mathbf{R}^{\mathrm{T}}(-\dot{\mathbf{P}}_{\mathrm{d}} + k_1\mathbf{z}_1) - \boldsymbol{\delta} \qquad (5.6)$$

where $\boldsymbol{\delta} = \begin{bmatrix} \delta_{\mathrm{x}} \\ \delta_{\mathrm{y}} \\ \delta_{\mathrm{z}} \end{bmatrix}$ was a constant vector with real number coordinates. Backstepping for

the error $\mathbf{z}_2$ gave:

$$V_2 := V_1 + \frac{1}{2}\mathbf{z}_2^{\mathrm{T}}\mathbf{z}_2 \qquad (5.7)$$

$$\dot{V}_2 = \dot{V}_1 + \mathbf{z}_2^{\mathrm{T}}\dot{\mathbf{z}}_2 \qquad (5.8)$$

where $\dot{\mathbf{z}}_2 = \dot{\mathbf{V}} + \dot{\mathbf{R}}^{\mathrm{T}}(-\dot{\mathbf{P}}_{\mathrm{d}} + k_1\mathbf{z}_1) + \mathbf{R}^{\mathrm{T}}(-\ddot{\mathbf{P}}_{\mathrm{d}} + k_1\dot{\mathbf{z}}_1) = -\mathbf{S}\mathbf{V} + g\mathbf{R}^{\mathrm{T}}\mathbf{e}_3 + \frac{1}{m}\mathbf{R}^{\mathrm{T}}\mathbf{b} - \frac{1}{m}\mathbf{T} - \mathbf{S}\mathbf{R}^{\mathrm{T}}(-\dot{\mathbf{P}}_{\mathrm{d}} + k_1\mathbf{z}_1) + \mathbf{R}^{\mathrm{T}}(-\ddot{\mathbf{P}}_{\mathrm{d}} + k_1\dot{\mathbf{z}}_1) = -\mathbf{S}\mathbf{V} + g\mathbf{R}^{\mathrm{T}}\mathbf{e}_3 + \frac{1}{m}\mathbf{R}^{\mathrm{T}}\mathbf{b} - \frac{1}{m}\mathbf{T} - \mathbf{S}(\mathbf{z}_2 + \boldsymbol{\delta} - \mathbf{V}) + \mathbf{R}^{\mathrm{T}}(-\ddot{\mathbf{P}}_{\mathrm{d}} + k_1\dot{\mathbf{z}}_1) = -\mathbf{S}(\mathbf{z}_2 + \boldsymbol{\delta}) + g\mathbf{R}^{\mathrm{T}}\mathbf{e}_3 + \frac{1}{m}\mathbf{R}^{\mathrm{T}}\mathbf{b} - \frac{1}{m}\mathbf{T} + \mathbf{R}^{\mathrm{T}}(-\ddot{\mathbf{P}}_{\mathrm{d}} + k_1\dot{\mathbf{z}}_1)$, as derived from Eq. (5.1) and Eq. (5.6). Thus:

$$
\begin{aligned}
\dot{V}_2 &= -k_1\mathbf{z}_1^{\mathrm{T}}\mathbf{z}_1 + \mathbf{z}_1^{\mathrm{T}}\mathbf{R}[\mathbf{V} + \mathbf{R}^{\mathrm{T}}(-\dot{\mathbf{P}}_{\mathrm{d}} + k_1\mathbf{z}_1)] + \mathbf{z}_2^{\mathrm{T}}\dot{\mathbf{z}}_2 \qquad (5.9)\\
&= -k_1\mathbf{z}_1^{\mathrm{T}}\mathbf{z}_1 + \mathbf{z}_1^{\mathrm{T}}\mathbf{R}(\mathbf{z}_2 + \boldsymbol{\delta}) + \mathbf{z}_2^{\mathrm{T}}\dot{\mathbf{z}}_2\\
&= -k_1\mathbf{z}_1^{\mathrm{T}}\mathbf{z}_1 - k_2\mathbf{z}_2^{\mathrm{T}}\mathbf{z}_2 + \mathbf{z}_1^{\mathrm{T}}\mathbf{R}(\mathbf{z}_2 + \boldsymbol{\delta}) + \mathbf{z}_2^{\mathrm{T}}\dot{\mathbf{z}}_2 + k_2\mathbf{z}_2^{\mathrm{T}}\mathbf{z}_2\\
&= -\sum_{i=1}^{2}k_i\mathbf{z}_i^{\mathrm{T}}\mathbf{z}_i + \mathbf{z}_1^{\mathrm{T}}\mathbf{R}(\mathbf{z}_2 + \boldsymbol{\delta}) + \mathbf{z}_2^{\mathrm{T}}(\dot{\mathbf{z}}_2 + k_2\mathbf{z}_2)\\
&= -\sum_{i=1}^{2}k_i\mathbf{z}_i^{\mathrm{T}}\mathbf{z}_i + \mathbf{z}_1^{\mathrm{T}}\mathbf{R}(\mathbf{z}_2 + \boldsymbol{\delta}) + \mathbf{z}_2^{\mathrm{T}}[-\mathbf{S}(\mathbf{z}_2 + \boldsymbol{\delta}) + g\mathbf{R}^{\mathrm{T}}\mathbf{e}_3 +\\
&\qquad \frac{1}{m}\mathbf{R}^{\mathrm{T}}\mathbf{b} - \frac{1}{m}\mathbf{T} + \mathbf{R}^{\mathrm{T}}(-\ddot{\mathbf{P}}_{\mathrm{d}} + k_1\dot{\mathbf{z}}_1) + k_2\mathbf{z}_2]
\end{aligned}
$$

$$= -\sum_{i=1}^{2} k_i \mathbf{z}_i^{\mathrm{T}} \mathbf{z}_i + \mathbf{z}_1^{\mathrm{T}} \mathbf{R}(\mathbf{z}_2 + \boldsymbol{\delta}) + \mathbf{z}_2^{\mathrm{T}} [-\mathbf{S}\boldsymbol{\delta} + g\mathbf{R}^{\mathrm{T}}\mathbf{e}_3 +$$

$$\frac{1}{m}\mathbf{R}^{\mathrm{T}}\mathbf{b} - \frac{1}{m}\mathbf{T} + \mathbf{R}^{\mathrm{T}}(-\ddot{\mathbf{P}}_{\mathrm{d}} + k_1\dot{\mathbf{z}}_1) + k_2\mathbf{z}_2]$$

where k_2 was a positive real constant. With the fact that for any skew-symmetric matrix $\mathbf{S}$, $\mathbf{z}_2^{\mathrm{T}}\mathbf{S}\mathbf{z}_2 \equiv 0$. According the reasoning in [16], one of the control inputs $\mathbf{T}$ can be determined at this stage if forcing the term $[-\mathbf{S}\boldsymbol{\delta} + g\mathbf{R}^{\mathrm{T}}\mathbf{e}_3 + \frac{1}{m}\mathbf{R}^{\mathrm{T}}\mathbf{b} - \frac{1}{m}\mathbf{T} +$ $\mathbf{R}^{\mathrm{T}}(-\ddot{\mathbf{P}}_{\mathrm{d}} + k_1\dot{\mathbf{z}}_1) + k_2\mathbf{z}_2]$ to zero. Let:

$$\mathbf{h} := g\mathbf{R}^{\mathrm{T}}\mathbf{e}_3 + \frac{1}{m}\mathbf{R}^{\mathrm{T}}\mathbf{b} + \mathbf{R}^{\mathrm{T}}(-\ddot{\mathbf{P}}_{\mathrm{d}} + k_1\dot{\mathbf{z}}_1) + k_2\mathbf{z}_2 \qquad (5.10)$$

then:

$$T = m\mathbf{e}_3^{\mathrm{T}}(-\mathbf{S}\boldsymbol{\delta} + \mathbf{h}) \qquad (5.11)$$

$$\mathbf{T} = T\mathbf{e}_3 = \begin{bmatrix} 0 \\ 0 \\ m\mathbf{e}_3^{\mathrm{T}}(-\mathbf{S}\boldsymbol{\delta} + \mathbf{h}) \end{bmatrix} \qquad (5.12)$$

To figure out the remaining three control inputs ${}^{B}\boldsymbol{\tau}(t) = \begin{bmatrix} {}^{B}\tau_{\mathrm{x}}(t) \\ {}^{B}\tau_{\mathrm{y}}(t) \\ {}^{B}\tau_{\mathrm{z}}(t) \end{bmatrix}$, backstepping

continued after some necessary transformation of the above equation:

$$\dot{V}_2 = -\sum_{i=1}^{2} k_i \mathbf{z}_i^{\mathrm{T}} \mathbf{z}_i + \mathbf{z}_1^{\mathrm{T}} \mathbf{R}(\mathbf{z}_2 + \boldsymbol{\delta}) + \mathbf{z}_2^{\mathrm{T}}(-\mathbf{S}\boldsymbol{\delta} - \frac{T}{m}\mathbf{e}_3 + \mathbf{h}) \qquad (5.13)$$

denote $\mathbf{z}_2 = \begin{bmatrix} z_{21} \\ z_{22} \\ z_{23} \end{bmatrix}$, $\mathbf{S} = \begin{bmatrix} 0 & -\omega_{\mathrm{z}} & \omega_{\mathrm{y}} \\ \omega_{\mathrm{z}} & 0 & -\omega_{\mathrm{x}} \\ -\omega_{\mathrm{y}} & \omega_{\mathrm{x}} & 0 \end{bmatrix}$, $\mathbf{h} = \begin{bmatrix} h_{\mathrm{x}} \\ h_{\mathrm{y}} \\ h_{\mathrm{z}} \end{bmatrix}$, then the part in Eq. (5.13):

$$\mathbf{z}_2^{\mathrm{T}}\left(-\mathbf{S}\boldsymbol{\delta} - \frac{T}{m}\mathbf{e}_3 + \mathbf{h}\right) = \begin{bmatrix} z_{21} & z_{22} & z_{23} \end{bmatrix} \left\{ -\begin{bmatrix} 0 & -\omega_{\mathrm{z}} & \omega_{\mathrm{y}} \\ \omega_{\mathrm{z}} & 0 & -\omega_{\mathrm{x}} \\ -\omega_{\mathrm{y}} & \omega_{\mathrm{x}} & 0 \end{bmatrix}\begin{bmatrix} \delta_{\mathrm{x}} \\ \delta_{\mathrm{y}} \\ \delta_{\mathrm{z}} \end{bmatrix} \right. \qquad (5.14)$$

$$-\begin{bmatrix} 0 & 0 & 1 \end{bmatrix}\left(\begin{bmatrix} h_{\mathrm{x}} \\ h_{\mathrm{y}} \\ h_{\mathrm{z}} \end{bmatrix} - \begin{bmatrix} 0 & -\omega_{\mathrm{z}} & \omega_{\mathrm{y}} \\ \omega_{\mathrm{z}} & 0 & -\omega_{\mathrm{x}} \\ -\omega_{\mathrm{y}} & \omega_{\mathrm{x}} & 0 \end{bmatrix}\begin{bmatrix} \delta_{\mathrm{x}} \\ \delta_{\mathrm{y}} \\ \delta_{\mathrm{z}} \end{bmatrix}\right)\begin{bmatrix} 0 \\ 0 \\ 1 \end{bmatrix}$$

$$+\begin{bmatrix} h_{\mathrm{x}} \\ h_{\mathrm{y}} \\ h_{\mathrm{z}} \end{bmatrix}\right\}$$

$$= \begin{bmatrix} z_{21} & z_{22} & z_{23} \end{bmatrix}\left(-\begin{bmatrix} -\omega_{\mathrm{z}}\delta_{\mathrm{y}} + \omega_{\mathrm{y}}\delta_{\mathrm{z}} \\ \omega_{\mathrm{z}}\delta_{\mathrm{x}} - \omega_{\mathrm{x}}\delta_{\mathrm{z}} \\ -\omega_{\mathrm{y}}\delta_{\mathrm{x}} + \omega_{\mathrm{x}}\delta_{\mathrm{y}} \end{bmatrix} + \begin{bmatrix} h_{\mathrm{x}} \\ h_{\mathrm{y}} \\ h_{\mathrm{z}} \end{bmatrix} +$$

$$+\begin{bmatrix} 0 \\ 0 \\ -\omega_{\mathrm{y}}\delta_{\mathrm{x}} + \omega_{\mathrm{x}}\delta_{\mathrm{y}} - h_{\mathrm{z}} \end{bmatrix}\right)$$

$$= \begin{bmatrix} z_{21} & z_{22} & z_{23} \end{bmatrix} \begin{bmatrix} h_x + \omega_z \delta_y - \omega_y \delta_z \\ h_y - \omega_z \delta_x + \omega_x \delta_z \\ 0 \end{bmatrix}$$

$$= \begin{bmatrix} z_{21} & z_{22} \end{bmatrix} \left(\begin{bmatrix} \omega_z \delta_y - \omega_y \delta_z \\ -\omega_z \delta_x + \omega_x \delta_z \end{bmatrix} + \begin{bmatrix} h_x \\ h_y \end{bmatrix} \right)$$

Meanwhile, $\ddot{\mathbf{z}}_1 = \dot{\mathbf{R}} \mathbf{V} + \mathbf{R} \dot{\mathbf{V}} - \ddot{\mathbf{P}}_d = \mathbf{RSV} + \mathbf{R} \left(-\mathbf{SV} + g \mathbf{R}^T \mathbf{e}_3 + \frac{1}{m} \mathbf{R}^T \mathbf{b} - \frac{1}{m} \mathbf{T} \right) -$

$\ddot{\mathbf{P}}_d = g \mathbf{e}_3 + \frac{1}{m} \mathbf{b} - \frac{\mathbf{R}}{m} \mathbf{T} - \ddot{\mathbf{P}}_d$, $\dot{\mathbf{z}}_2 = -\mathbf{S}(\mathbf{z}_2 + \boldsymbol{\delta}) - \frac{T}{m} \mathbf{e}_3 + \mathbf{h} - k_2 \mathbf{z}_2$. Let $\mathbf{M} =$

$\begin{bmatrix} 1 & 0 & 0 \\ 0 & 1 & 0 \end{bmatrix}$, $\boldsymbol{\delta}_n = \begin{bmatrix} 0 & -\delta_z & \delta_y \\ \delta_z & 0 & -\delta_x \end{bmatrix}$, $\boldsymbol{\omega} = \begin{bmatrix} \omega_x \\ \omega_y \\ \omega_z \end{bmatrix}$, then Eq. (5.14) became:

$$\mathbf{z}_2^T \left(-\mathbf{S}\boldsymbol{\delta} - \frac{T}{m} \mathbf{e}_3 + \mathbf{h} \right) = (\mathbf{M}\mathbf{z}_2)^T (\boldsymbol{\delta}_n \boldsymbol{\omega} + \mathbf{Mh}) \tag{5.15}$$

Let $\mathbf{z}_{2n} = \mathbf{M}\mathbf{z}_2$, $\mathbf{h}_n = \mathbf{Mh}$, then Eq. (5.13) became:

$$\dot{V}_2 = -\sum_{i=1}^{2} k_i \mathbf{z}_i^T \mathbf{z}_i + \mathbf{z}_1^T \mathbf{R}(\mathbf{z}_2 + \boldsymbol{\delta}) + \mathbf{z}_{2n}^T (\boldsymbol{\delta}_n \boldsymbol{\omega} + \mathbf{h}_n) \tag{5.16}$$

Continuing the backstepping process, let:

$$\mathbf{z}_3 := \boldsymbol{\delta}_n \boldsymbol{\omega} + \mathbf{h}_n \tag{5.17}$$

$$V_3 := V_2 + \frac{1}{2} \mathbf{z}_3^T \mathbf{z}_3 \tag{5.18}$$

$$\dot{V}_3 = \dot{V}_2 + \mathbf{z}_3^T \dot{\mathbf{z}}_3 \tag{5.19}$$

where $\dot{\mathbf{z}}_3 = \boldsymbol{\delta}_n \dot{\boldsymbol{\omega}} + \dot{\mathbf{h}}_n = \boldsymbol{\delta}_n \boldsymbol{\tau} + \mathbf{M}\dot{\mathbf{h}} = \boldsymbol{\delta}_n \boldsymbol{\tau} + \mathbf{M} \left[g \dot{\mathbf{R}}^T \mathbf{e}_3 + \frac{1}{m} \dot{\mathbf{R}}^T \mathbf{b} + \dot{\mathbf{R}}^T (-\ddot{\mathbf{P}}_d + $

$k_1 \dot{\mathbf{z}}_1) + \mathbf{R}^T (-\dddot{\mathbf{P}}_d + k_1 \ddot{\mathbf{z}}_1) + k_2 \dot{\mathbf{z}}_2 \right] = \boldsymbol{\delta}_n \boldsymbol{\tau} + \mathbf{M} \left[-g \mathbf{SR}^T \mathbf{e}_3 - \frac{1}{m} \mathbf{SR}^T \mathbf{b} - \mathbf{SR}^T (-\ddot{\mathbf{P}}_d + $

$k_1 \dot{\mathbf{z}}_1) + \mathbf{R}^T (-\dddot{\mathbf{P}}_d + k_1 \ddot{\mathbf{z}}_1) + k_2 \dot{\mathbf{z}}_2 \right]$. Then:

$$\dot{V}_3 = -\sum_{i=1}^{3} k_i \mathbf{z}_i^T \mathbf{z}_i + \mathbf{z}_1^T \mathbf{R}(\mathbf{z}_2 + \boldsymbol{\delta}) + \mathbf{z}_{2n}^T \mathbf{z}_3 + \mathbf{z}_3^T \dot{\mathbf{z}}_3 + k_3 \mathbf{z}_3^T \mathbf{z}_3 \tag{5.20}$$

$$= -\sum_{i=1}^{3} k_i \mathbf{z}_i^T \mathbf{z}_i + \mathbf{z}_1^T \mathbf{R}(\mathbf{z}_2 + \boldsymbol{\delta}) + \mathbf{z}_3^T (\dot{\mathbf{z}}_3 + k_3 \mathbf{z}_3 + \mathbf{z}_{2n})$$

$$= -\sum_{i=1}^{3} k_i \mathbf{z}_i^T \mathbf{z}_i + \mathbf{z}_1^T \mathbf{R}(\mathbf{z}_2 + \boldsymbol{\delta}) + \mathbf{z}_3^T (\boldsymbol{\delta}_n \boldsymbol{\tau} + \dot{\mathbf{h}}_n + k_3 \mathbf{z}_3 + \mathbf{z}_{2n})$$

According the reasoning in [16], the torque control can be set such that the term $(\boldsymbol{\delta}_n \boldsymbol{\tau} + \dot{\mathbf{h}}_n + k_3 \mathbf{z}_3 + \mathbf{z}_{2n})$ was zero:

$$\boldsymbol{\delta}_n \boldsymbol{\tau} + \dot{\mathbf{h}}_n + k_3 \mathbf{z}_3 + \mathbf{z}_{2n} = 0 \tag{5.21}$$

$$\boldsymbol{\delta}_n \boldsymbol{\tau} = -\dot{\mathbf{h}}_n - k_3 \mathbf{z}_3 - \mathbf{z}_{2n} \tag{5.22}$$

Note that the size of $\boldsymbol{\delta}_n$ was 2 by 3, which was not a square matrix. Thus, pseudoinverse of $\boldsymbol{\delta}_n$ was used to calculate $\boldsymbol{\tau}$ in the Eq. (5.22). Due to the fact that $(\boldsymbol{\delta}_n \boldsymbol{\delta}_n^T)(\boldsymbol{\delta}_n \boldsymbol{\delta}_n^T)^{-1} = \mathbf{I}$:

$$(\boldsymbol{\delta}_n \boldsymbol{\delta}_n^T)(\boldsymbol{\delta}_n \boldsymbol{\delta}_n^T)^{-1} (-\dot{\mathbf{h}}_n - k_3 \mathbf{z}_3 - \mathbf{z}_{2n}) = -\dot{\mathbf{h}}_n - k_3 \mathbf{z}_3 - \mathbf{z}_{2n} \tag{5.23}$$

Then, $\boldsymbol{\tau}$ can be calculated as:

$$\boldsymbol{\tau} = -\boldsymbol{\delta}_n^T(\boldsymbol{\delta}_n\boldsymbol{\delta}_n^T)^{-1}(\dot{\mathbf{h}}_n + k_3\mathbf{z}_3 + \mathbf{z}_{2n}) \tag{5.24}$$

Note that the inverse of the matrix $\boldsymbol{\delta}_n\boldsymbol{\delta}_n^T$ existed if and only if $det(\boldsymbol{\delta}_n\boldsymbol{\delta}_n^T) \neq 0$, which

indicated that $\begin{vmatrix} \delta_y^2 + \delta_z^2 & -\delta_x\delta_y \\ -\delta_x\delta_y & \delta_x^2 + \delta_z^2 \end{vmatrix} = (\delta_y^2 + \delta_z^2)(\delta_x^2 + \delta_z^2) - \delta_x^2\delta_y^2 = \delta_z^2(\delta_x^2 + \delta_y^2 +$

$\delta_z^2) \neq 0$. Obviously, as long as $\delta_z \neq 0$, then the inverse of the matrix $\boldsymbol{\delta}_n\boldsymbol{\delta}_n^T$ existed,

and a $\boldsymbol{\tau}$ can be correspondingly calculated. Thus, selection of the constant vector $\boldsymbol{\delta} =$

$\begin{bmatrix} \delta_x \\ \delta_y \\ \delta_z \end{bmatrix}$ would have a restriction that $\delta_z \neq 0$.

5.2 EQUILIBRIUM POINTS

For the nonlinear system described in Eq. (5.1), the primary goal was to follow a pre-defined trajectory $^E\mathbf{P}_d \in \mathbf{R}^{3\times1}$ parametrized in time. With the analysis throughout section 5.1, the trajectory tracking problem became one with three error states defined in section 5.1. Summing up, one can get:

$$\begin{cases} \dot{\mathbf{z}}_1 = \mathbf{RV} - \dot{\mathbf{P}}_d \\ \dot{\mathbf{z}}_2 = -\mathbf{S}(\mathbf{z}_2^* + \boldsymbol{\delta}) - \dfrac{1}{m}\mathbf{T} + \mathbf{h} - k_2\mathbf{z}_2 \\ \dot{\mathbf{z}}_3 = \boldsymbol{\delta}_n\boldsymbol{\tau} + \dot{\mathbf{h}}_n \end{cases} \tag{5.25}$$

With $\mathbf{T}(\mathbf{z}, t)$ and $\boldsymbol{\tau}(\mathbf{z}, t)$, define $\dot{\mathbf{z}} := \begin{bmatrix} \dot{\mathbf{z}}_1 \\ \dot{\mathbf{z}}_2 \\ \dot{\mathbf{z}}_3 \end{bmatrix} = g(\mathbf{z}, t)$. It was observed that the overall

dynamic system of tracking errors was non-autonomous. Using the definition of equilibrium points defined in Eq. (2.2), one assumed there was/were some equilibrium

points, denoted as $\mathbf{z}^* = \begin{bmatrix} \mathbf{z}_1^* \\ \mathbf{z}_2^* \\ \mathbf{z}_3^* \end{bmatrix}$, associated with the above error dynamics. Then:

$$g(\mathbf{z}^*, t) \equiv \mathbf{0} \qquad \forall t \geq t_0 \tag{5.26}$$

Substituting the expression of $\mathbf{z}$ with $\mathbf{z}^*$ in Eq. (5.25), one can get:

$$\begin{cases} \mathbf{RV} - \dot{\mathbf{P}}_d = \mathbf{0} \\ -\mathbf{S}(\mathbf{z}_2^* + \boldsymbol{\delta}) - \dfrac{1}{m}\mathbf{T} + \mathbf{h} - k_2\mathbf{z}_2^* = \mathbf{0} \\ \boldsymbol{\delta}_n\boldsymbol{\tau} + \dot{\mathbf{h}}_n = \mathbf{0} \end{cases} \tag{5.27}$$

With the control input $\mathbf{T} = m\mathbf{e}_3^T(-\mathbf{S}\boldsymbol{\delta} + \mathbf{h})\mathbf{e}_3$ and $\boldsymbol{\tau} = -\boldsymbol{\delta}_n^T(\boldsymbol{\delta}_n\boldsymbol{\delta}_n^T)^{-1}(\dot{\mathbf{h}}_n + k_3\mathbf{z}_3 +$

$\mathbf{z}_{2n})$ available, equation (5.27) became

$$\begin{cases} \mathbf{RV} - \dot{\mathbf{P}}_d = 0 \\ -\mathbf{Sz}_2^* - k_2\mathbf{z}_2^* + k_2\mathbf{Dz}_2^* + \mathbf{D}(-\mathbf{S\delta} + g\mathbf{R}^T\mathbf{e}_3 + \mathbf{R}^T\frac{\mathbf{b}}{m} - \mathbf{R}^T\ddot{\mathbf{P}}_d) = 0 \quad (5.28) \\ -k_2\mathbf{z}_3^* - \mathbf{Mz}_2^* = 0 \end{cases}$$

where $\mathbf{D} = \begin{bmatrix} 1 & 0 & 0 \\ 0 & 1 & 0 \\ 0 & 0 & 0 \end{bmatrix}$. Thus, the trivial equilibrium point was $\mathbf{z}^* = \begin{bmatrix} \mathbf{z}_1^* \\ \mathbf{z}_2^* \\ \mathbf{z}_3^* \end{bmatrix}$, which

indicated that the quadrotor may not follow exactly the same dynamics of the predefined trajectory $\mathbf{P}_d$ and its derivatives $\dot{\mathbf{P}}_d$, $\ddot{\mathbf{P}}_d$. On the other hand, the only state variable of interest was the position tracking error $\mathbf{z}_1$. At $\mathbf{z}_1^*$, $\ddot{\mathbf{z}}_1^* = \frac{\mathbf{RT}}{m} + g\mathbf{e}_3 + \frac{\mathbf{b}}{m} - \ddot{\mathbf{P}}_d = 0$, thus

$\mathbf{R}T\mathbf{e}_3 = mg\mathbf{e}_3 + \mathbf{b} - m\ddot{\mathbf{P}}_d$. Hence, at equilibrium points $\ddot{\mathbf{z}}^*$, $_B^E\mathbf{R}\,^BT\mathbf{e}_3 = {}_B^E\mathbf{RR}_z(\varphi)\,^BT\mathbf{e}_3$, which indicated that the control quantity $^B\boldsymbol{\tau}$ had one element, $^B\tau_z$, that contributed nothing to the trajectory tracking. And this extra degree of freedom could be exploited within controller design to control the orientation and heading of the quadrotor.

5.3 STABILITY OF THE CONTROLLER WITH CORRECT PARAMETERS

Following the proof from [17], the stability of the controlling algorithm was proved to be exponentially stable under the condition that the desired trajectory $\mathbf{P}_d$ was sufficiently smooth and its time-derivatives were bounded by an upper bound. The Lyapunov function

$$V_3 = \sum_{i=1}^{3} \frac{1}{2}\mathbf{z}_i^T\mathbf{z}_i \tag{5.29}$$

was always positive definite. With the feedback control law, its derivative became

$$\dot{V}_3 = -\sum_{i=1}^{3} k_i\mathbf{z}_i^T\mathbf{z}_i + \mathbf{z}_1^T\mathbf{R}(\mathbf{z}_2 + \boldsymbol{\delta}) \tag{5.30}$$

$$= -\sum_{i=1}^{3} k_i\mathbf{z}_i^T\mathbf{z}_i + \mathbf{z}_1^T\mathbf{Rz}_2 + \mathbf{z}_1^T\mathbf{R\delta}$$

Using Young's inequality in Eq. (2.21), for any $\gamma > 0$,

$$\dot{V}_3 \leq -\sum_{i=1}^{3} k_i\mathbf{z}_i^T\mathbf{z}_i + \mathbf{z}_1^T\mathbf{Rz}_2 + \frac{\gamma}{2}\mathbf{z}_1^T\mathbf{z}_1 + \frac{1}{2\gamma}(\mathbf{R\delta})^T\mathbf{R\delta} \tag{5.31}$$

$$\leq -(k_1\mathbf{z}_1^T\mathbf{z}_1 - \mathbf{z}_1^T\mathbf{Rz}_2 + k_2\mathbf{z}_2^T\mathbf{z}_2) - k_3\mathbf{z}_3^T\mathbf{z}_3 + \frac{\gamma}{2}\mathbf{z}_1^T\mathbf{z}_1 + \frac{1}{2\gamma}(\mathbf{R\delta})^T\mathbf{R\delta}$$

$$\leq -\left[(k_1 - \frac{\gamma}{2})\mathbf{z}_1^T\mathbf{z}_1 - \|\mathbf{z}_1\|\|\mathbf{z}_2\| + k_2\mathbf{z}_2^T\mathbf{z}_2\right] - k_3\mathbf{z}_3^T\mathbf{z}_3 + \frac{1}{2\gamma}\|\boldsymbol{\delta}\|^2$$

$$\leq -\left\|\sqrt{k_1 - \frac{\gamma}{2}}\mathbf{z}_1 - \sqrt{k_2}\mathbf{z}_2\right\|^2 - k_3\mathbf{z}_3^T\mathbf{z}_3 + \frac{1}{2\gamma}\|\boldsymbol{\delta}\|^2 -$$

$$2\sqrt{k_2\left(k_1 - \frac{\gamma}{2}\right)}\|\mathbf{z}_1\|\|\mathbf{z}_2\|$$

Here, choose $k_1 k_2 \geq \frac{1}{4}$ and $k_1 > \frac{\gamma}{2}$ would be enough to make the term

$2\sqrt{k_2\left(k_1 - \frac{\gamma}{2}\right)} \|\mathbf{z}_1\|\|\mathbf{z}_2\| > 0$. And there existed a constant $\lambda > 0$, such that

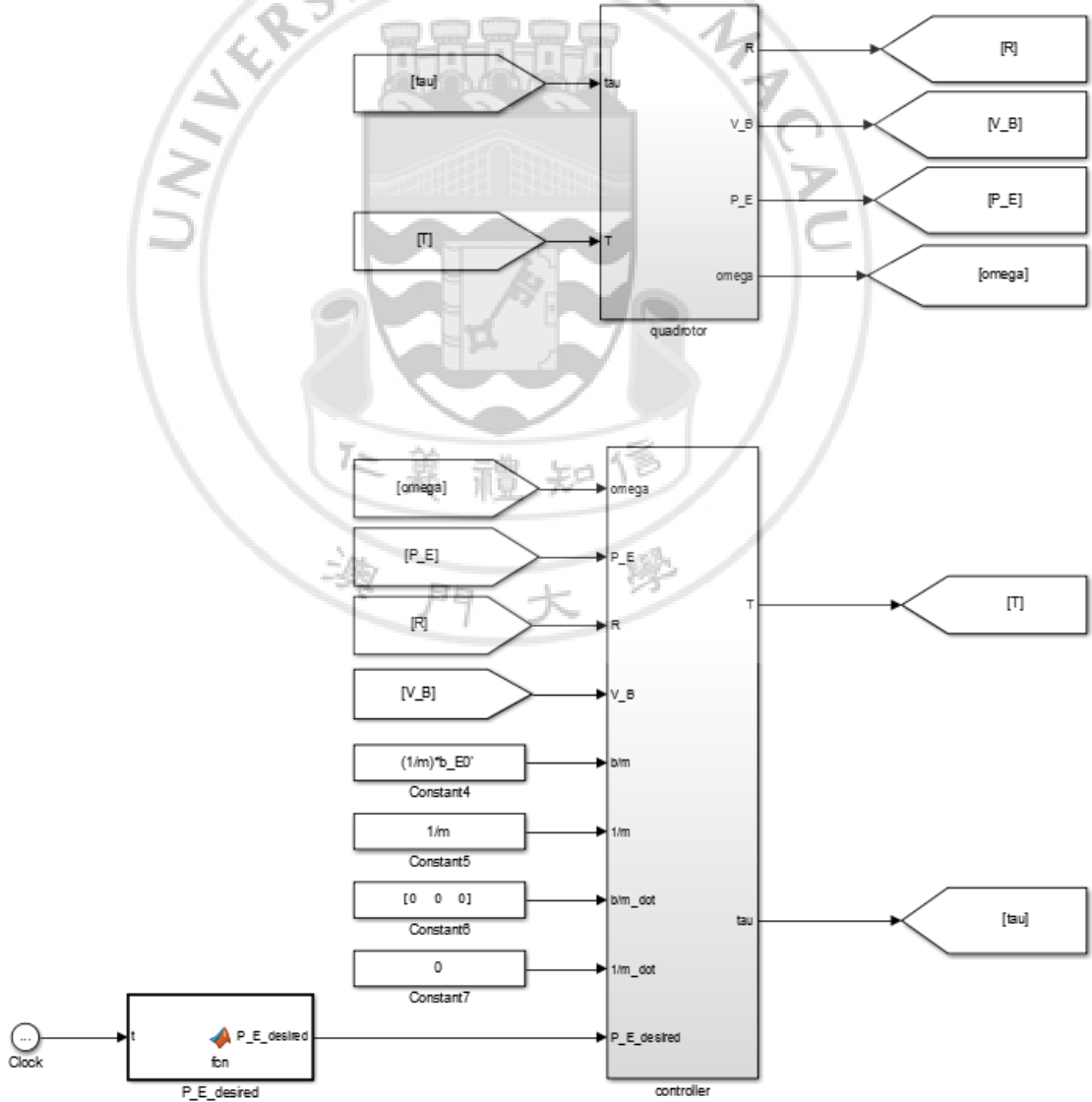$$\dot{V}_3 \leq -\lambda V_3 + \frac{1}{2\gamma}\|\boldsymbol{\delta}\|^2 \tag{5.32}$$

From Eq. (2.22) and Eq. (2.23),

$$V_3(t) \leq e^{-\lambda t}V_3(0) + \frac{1}{2\lambda\gamma}\|\boldsymbol{\delta}\|^2 \qquad t \geq 0 \tag{5.33}$$

Thus, $\|\mathbf{z}_1(t)\|^2 \leq 2V_3(t)$, and after infinite time

$$\|\mathbf{z}_1(t)\| \leq \frac{\|\boldsymbol{\delta}\|}{\sqrt{2\lambda\gamma}} \qquad t \rightarrow \infty \tag{5.34}$$

And the radius $\frac{\|\boldsymbol{\delta}\|}{\sqrt{2\lambda\gamma}}$ could be made as small as possible by appropriately choosing the controller parameters.


Figure 10. Quadrotor and controller model

The interconnected system of quadrotor and the proposed controller was implemented in SIMULINK environment. The controller was fed with correct values of the unknown parameters. Controller alone with correct parameters can be simulated by setting the noise level in the Kalman-Bucy filter to zero and setting the parameters of interest to their correct values, respectively. Specifically, the mass of the quadrotor $m = 0.206$ kg, the gravity $g = 9.7877$ m/s^2, and external force disturbance $^E\mathbf{b} = \begin{bmatrix} 0.3 \\ 0.2 \\ 0.1 \end{bmatrix}$ Newton.

Initial position $\mathbf{P}(t_0) = \begin{bmatrix} 0 \\ 0 \\ -1 \end{bmatrix}$ m, initial linear and angular velocities were zero. By assumption, the desired trajectory was a smooth and bounded function parametrized in time. Here, it was assumed to be a simple circle with radius of $1.2 \, m$ defined as

$$\begin{cases} x(t) = 1.2 \cos t \\ y(t) = 1.2 \sin t \qquad t \geq 0 \\ \quad z(t) = -1 \end{cases} \tag{5.35}$$

Set control parameters $k_1 = 4.5$, $k_2 = 4$, $k_3 = 3$, and $\boldsymbol{\delta} = \begin{bmatrix} 0 \\ 0 \\ 0.15 \end{bmatrix}$ m/s.
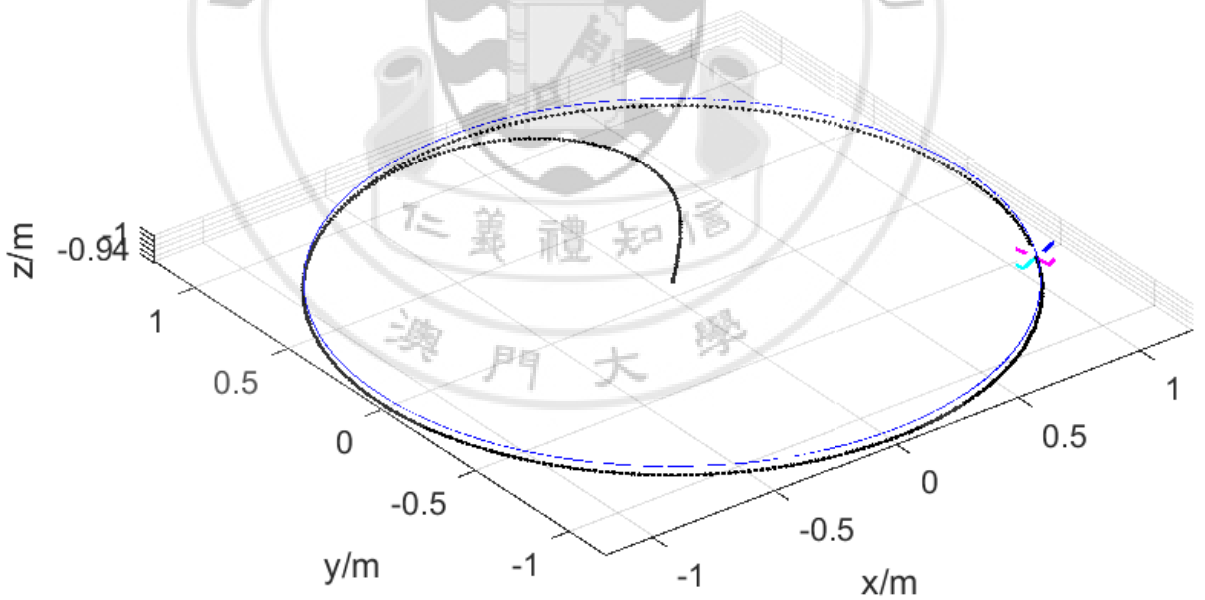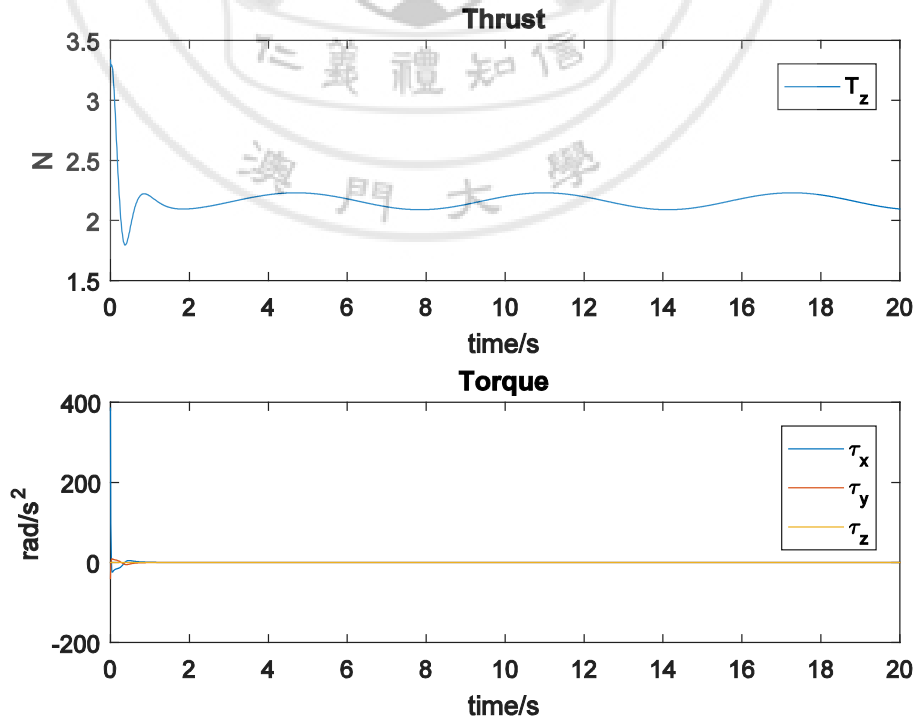

Figure 11. Simulation result of trajectory tracking with correct parameters

As indicated from the figure above, the quadrotor followed the desired trajectory (painted in blue) regardless of its initial deviation. Note also that the quadrotor tilted itself in order to resist the external force disturbance. The following figure showed error propagation of this configuration.
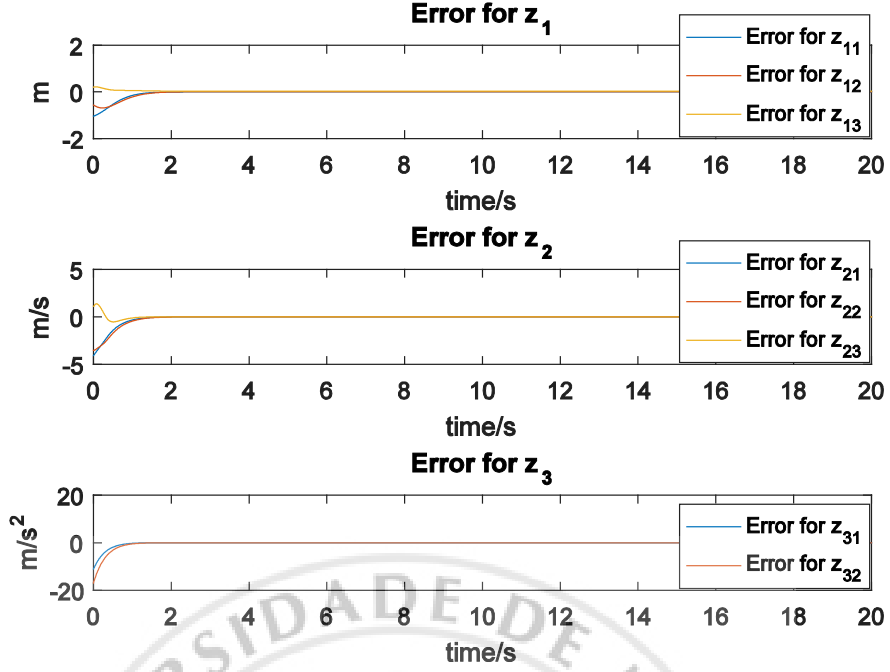
Figure 12. Error propagation of trajectory tracking with correct parameters

As indicated in the figure above, $\mathbf{z}_1$, $\mathbf{z}_2$, $\mathbf{z}_3$ converged to zero in less than seconds. Other than the fact that the quadrotor approached to the desired trajectory, it can be also inferred that the quadrotor approached both the linear velocities and angular velocities that was inexplicitly defined in Eq. (5.35). Propagation of actuation variables $\mathbf{T}$ and $\boldsymbol{\tau}$ was shown in the following figure.

Figure 13. Actuation propagation of trajectory tracking with correct parameters

As indicated from the figure above, the actuation remained bounded for all time. During the transition period, the quadrotor tended to lift itself to approach the desired trajectory, thus $\mathbf{T}$ surged to a peak. At the same time, the torque $\boldsymbol{\tau}$ also changed vibrated to regulate the quadrotor to balance the external force disturbance. What's more, it was interesting to see that the result met the expectation that the third element in torque $\boldsymbol{\tau}$, namely τ_z, played no role in trajectory tracking, as explained in section 5.2.

To prove that the actuation variables $\mathbf{T}$ and $\boldsymbol{\tau}$ indeed remain bounded for all time, zero dynamics of the nonlinear system should be analyzed.

5.4 ZERO DYNAMICS ANALYSIS

From the definition of linear velocity in Eq. (5.6),

$$\mathbf{V} = \mathbf{z}_2 - \mathbf{R}^{\mathrm{T}}\left(-\dot{\mathbf{P}}_{\mathrm{d}} + k_1\mathbf{z}_1\right) + \boldsymbol{\delta} \tag{5.35}$$

there would be a time after which $\mathbf{V}$ remains bounded. Because $\dot{\mathbf{z}}_1 = \mathbf{R}\mathbf{V} - \dot{\mathbf{P}}_{\mathrm{d}}$, $\dot{\mathbf{z}}_1$ will remain bounded as well. From the definition of angular velocity in Eq. (5.17),

$$\boldsymbol{\omega} = -\boldsymbol{\delta}_{\mathrm{n}}^{\mathrm{T}}(\boldsymbol{\delta}_{\mathrm{n}}\boldsymbol{\delta}_{\mathrm{n}}^{\mathrm{T}})^{-1}\left[\mathbf{z}_3 - g\mathbf{M}\mathbf{R}^{\mathrm{T}}\mathbf{e}_3 - \mathbf{M}\mathbf{R}^{\mathrm{T}}\frac{\mathbf{b}}{m} - \mathbf{M}\mathbf{R}^{\mathrm{T}}\left(-\ddot{\mathbf{P}}_{\mathrm{d}} + k_1\dot{\mathbf{z}}_1\right) - k_2\mathbf{M}\mathbf{z}_2\right] \tag{5.36}$$

$\boldsymbol{\omega}$ will remain bounded since $\mathbf{z}_1, \mathbf{z}_2, \mathbf{z}_3$ converge to zero exponentially. Thus, inner states would not escape to infinity.

Chapter 6 INTERCONNECTION SYSTEM ANALYSIS

Stability of the interconnected system of the proposed observer and the controller was addressed and analyzed in this chapter, followed by experiments for a real quadrotor. The Kalman-Bucy filter used for estimating the unknown parameters is exponentially stable if the linear time-varying system specified in Eq. (2.18) is uniformly complete observable. This requires that the linear dependence of the functions in (4.46a), (4.46b), and (4.46c) must happen uniformly throughout all time and that each individual function must not degenerate into another. Thus, given sufficiently rich control signals, the parameter errors converge exponentially, and are independently of the convergence of the trajectory tracking errors.

For the proposed controller introduced in chapter 5, it was assumed that the controller design procedure used the correct parameters. However, if a connection of the observer and controller was considered, the estimated parameters $\left(\widehat{\dfrac{1}{m}}\right)$ and $\left(\widehat{\dfrac{b}{m}}\right)$ would replace the correct parameters $\dfrac{1}{m}$ and $\dfrac{b}{m}$. To this effect, it was triggered to analyze the altered controlling algorithm in the same fashion in chapter 5. In this chapter onwards, define $\zeta_1 = \dfrac{1}{m}$, $\zeta_2 = \dfrac{b}{m}$, $\widehat{\zeta}_1 = \left(\widehat{\dfrac{1}{m}}\right)$, $\widehat{\zeta}_2 = \left(\widehat{\dfrac{b}{m}}\right)$ for calculation convenience. When correct parameters were used, Eq. (5.20) became

$$\dot{V}_3 = -\sum_{i=1}^{3} k_i z_i^T z_i + z_1^T R(z_2 + \delta) \tag{6.1}$$

with control variables $\mathbf{T} = \begin{bmatrix} 0 \\ 0 \\ m e_3^T(-S\delta + h) \end{bmatrix}$ and $\tau = -\delta_n^T(\delta_n \delta_n^T)^{-1}\left(\dot{h}_n + k_3 z_3 + z_{2n}\right)$.

Now, using estimated parameters that came out of the observer, all of the original terms that contained $\widehat{\zeta}_1$ and $\widehat{\zeta}_2$ were placed with an overbar in Eq. (5.20):

$$\widehat{\mathbf{T}} = \begin{bmatrix} 0 \\ 0 \\ \dfrac{1}{\widehat{\zeta}_1} e_3^T(-S\delta + \hat{h}) \end{bmatrix} \tag{6.2}$$

and

$$\hat{\tau} = -\delta_n^T(\delta_n \delta_n^T)^{-1}\left(\widehat{\dot{h}}_n + k_3 \widehat{z}_3 + z_{2n}\right) \tag{6.3}$$

$$= -\boldsymbol{\delta}_n^T(\boldsymbol{\delta}_n\boldsymbol{\delta}_n^T)^{-1}\Big\{\mathbf{M}\mathbf{z}_2$$

$$+ \mathbf{M}\Big[-g\mathbf{S}\mathbf{R}^T\mathbf{e}_3 - \mathbf{S}\mathbf{R}^T\widehat{\boldsymbol{\zeta}}_2 + \mathbf{R}^T\widehat{\dot{\boldsymbol{\zeta}}}_2 - \mathbf{S}\mathbf{R}^T(-\ddot{\mathbf{P}}_d + k_1\dot{\mathbf{z}}_1)$$

$$+ \mathbf{R}^T(-\dddot{\mathbf{P}}_d + k_1\widehat{\ddot{\mathbf{z}}}_1) + k_2\widehat{\ddot{\mathbf{z}}}_2\Big] + k_3(\boldsymbol{\delta}_n\boldsymbol{\omega} + \widehat{\mathbf{h}_n})\Big\}$$

Let $\mathbf{P}_1 = \mathbf{M}\mathbf{z}_2 + k_3\boldsymbol{\delta}_n\boldsymbol{\omega} - g\mathbf{M}\mathbf{S}\mathbf{R}^T\mathbf{e}_3 - \mathbf{M}\mathbf{S}\mathbf{R}^T(-\ddot{\mathbf{P}}_d + k_1\dot{\mathbf{z}}_1) - \mathbf{M}\mathbf{R}^T\dddot{\mathbf{P}}_d$, so that all of the remaining terms include estimated terms $\widehat{\boldsymbol{\zeta}}_1$ and $\widehat{\boldsymbol{\zeta}}_2$, then

$$\hat{\boldsymbol{\tau}} = -\boldsymbol{\delta}_n^T(\boldsymbol{\delta}_n\boldsymbol{\delta}_n^T)^{-1}\Big[\mathbf{P}_1 - \mathbf{M}\mathbf{S}\mathbf{R}^T\widehat{\boldsymbol{\zeta}}_2 + k_1\mathbf{M}\mathbf{R}^T\widehat{\dot{\mathbf{z}}}_1 + k_2\mathbf{M}\widehat{\dot{\mathbf{z}}}_2 + k_3\mathbf{M}\hat{\mathbf{h}}\Big]$$

$$= -\boldsymbol{\delta}_n^T(\boldsymbol{\delta}_n\boldsymbol{\delta}_n^T)^{-1}\Big\{\mathbf{P}_1 - \mathbf{M}\mathbf{S}\mathbf{R}^T\widehat{\boldsymbol{\zeta}}_2 + k_1\mathbf{M}\mathbf{R}^T\big(g\mathbf{e}_3 + \widehat{\boldsymbol{\zeta}}_2 - \widehat{\boldsymbol{\zeta}}_1\mathbf{R}\mathbf{T} -$$

$$\dddot{\mathbf{P}}_d\big) + k_2\mathbf{M}\big[-\mathbf{S}(\mathbf{z}_2 + \boldsymbol{\delta}) - \widehat{\boldsymbol{\zeta}}_1\hat{\mathbf{T}} + \hat{\mathbf{h}} - k_2\mathbf{z}_2\big] + k_3\mathbf{M}\hat{\mathbf{h}} + \mathbf{M}\mathbf{R}^T\widehat{\boldsymbol{\zeta}}_2\Big\}$$

Let $\mathbf{P}_2 = \mathbf{P}_1 + k_1 g\mathbf{M}\mathbf{R}^T\mathbf{e}_3 - k_1\mathbf{M}\mathbf{R}^T\dddot{\mathbf{P}}_d - k_2\mathbf{S}(\mathbf{z}_2 + \boldsymbol{\delta}) - k_2^2\mathbf{M}\mathbf{z}_2$, so that all of the remaining terms include estimated terms $\widehat{\boldsymbol{\zeta}}_1$ and $\widehat{\boldsymbol{\zeta}}_2$, then

$$\hat{\boldsymbol{\tau}} = -\boldsymbol{\delta}_n^T(\boldsymbol{\delta}_n\boldsymbol{\delta}_n^T)^{-1}\Big[\mathbf{P}_2 - \mathbf{M}\mathbf{S}\mathbf{R}^T\widehat{\boldsymbol{\zeta}}_2 + k_1\mathbf{M}\mathbf{R}^T\widehat{\boldsymbol{\zeta}}_2 - k_1\mathbf{M}\mathbf{R}^T\widehat{\boldsymbol{\zeta}}_1\mathbf{R}\hat{\mathbf{T}} -$$

$$k_2\mathbf{M}\widehat{\boldsymbol{\zeta}}_1\hat{\mathbf{T}} + (k_2 + k_3)\mathbf{M}\hat{\mathbf{h}} + \mathbf{M}\mathbf{R}^T\widehat{\boldsymbol{\zeta}}_2\Big]$$

$$= -\boldsymbol{\delta}_n^T(\boldsymbol{\delta}_n\boldsymbol{\delta}_n^T)^{-1}\Big[\mathbf{P}_2 + \mathbf{M}(k_1\mathbf{I}_3 - \mathbf{S})\mathbf{R}^T\widehat{\boldsymbol{\zeta}}_2 - (k_1 +$$

$$k_2)\mathbf{M}\widehat{\boldsymbol{\zeta}}_1\frac{1}{\widehat{\boldsymbol{\zeta}}_1}\mathbf{e}_3^T(-\mathbf{S}\boldsymbol{\delta} + \hat{\mathbf{h}})\mathbf{e}_3 + (k_2 + k_3)\mathbf{M}\hat{\mathbf{h}} + \mathbf{M}\mathbf{R}^T\widehat{\boldsymbol{\zeta}}_2\Big]$$

$$= -\boldsymbol{\delta}_n^T(\boldsymbol{\delta}_n\boldsymbol{\delta}_n^T)^{-1}\Big[\mathbf{P}_2 + \mathbf{M}(k_1\mathbf{I}_3 - \mathbf{S})\mathbf{R}^T\widehat{\boldsymbol{\zeta}}_2 + (k_1 + k_2)\mathbf{M}\mathbf{e}_3^T\mathbf{S}\boldsymbol{\delta}\mathbf{e}_3 -$$

$$(k_1 + k_2)\mathbf{M}\mathbf{e}_3^T\hat{\mathbf{h}}\mathbf{e}_3 + (k_2 + k_3)\mathbf{M}\hat{\mathbf{h}} + \mathbf{M}\mathbf{R}^T\widehat{\boldsymbol{\zeta}}_2\Big]$$

$$= -\boldsymbol{\delta}_n^T(\boldsymbol{\delta}_n\boldsymbol{\delta}_n^T)^{-1}\Big\{\mathbf{P}_2 + \mathbf{M}(k_1\mathbf{I}_3 - \mathbf{S})\mathbf{R}^T\widehat{\boldsymbol{\zeta}}_2 + (k_1 + k_2)\mathbf{M}\mathbf{e}_3^T\mathbf{S}\boldsymbol{\delta}\mathbf{e}_3 -$$

$$(k_1 + k_2)\mathbf{M}\mathbf{e}_3^T\big[g\mathbf{R}^T\mathbf{e}_3 + \mathbf{R}^T\widehat{\boldsymbol{\zeta}}_2 + \mathbf{R}^T(-\ddot{\mathbf{P}}_d + k_1\dot{\mathbf{z}}_1) + k_2\mathbf{z}_2\big]\mathbf{e}_3 +$$

$$(k_2 + k_3)\mathbf{M}\big[g\mathbf{R}^T\mathbf{e}_3 + \mathbf{R}^T\widehat{\boldsymbol{\zeta}}_2 + \mathbf{R}^T(-\ddot{\mathbf{P}}_d + k_1\dot{\mathbf{z}}_1) + k_2\mathbf{z}_2\big] +$$

$$\mathbf{M}\mathbf{R}^T\widehat{\boldsymbol{\zeta}}_2\Big\}$$

Let $\mathbf{P}_3 = \mathbf{P}_2 + (k_1 + k_2)\mathbf{M}\mathbf{e}_3^T\mathbf{S}\boldsymbol{\delta}\mathbf{e}_3 - (k_1 + k_2)\mathbf{M}\mathbf{e}_3^T\big[g\mathbf{R}^T\mathbf{e}_3 + \mathbf{R}^T(-\ddot{\mathbf{P}}_d + k_1\dot{\mathbf{z}}_1) + k_2\mathbf{z}_2\big]\mathbf{e}_3 + (k_2 + k_3)\mathbf{M}\big[g\mathbf{R}^T\mathbf{e}_3 + \mathbf{R}^T(-\ddot{\mathbf{P}}_d + k_1\dot{\mathbf{z}}_1) + k_2\mathbf{z}_2\big]$, so that all of the remaining terms include estimated terms $\widehat{\boldsymbol{\zeta}}_1$ and $\widehat{\boldsymbol{\zeta}}_2$, then

$$\hat{\boldsymbol{\tau}} = -\boldsymbol{\delta}_n^T(\boldsymbol{\delta}_n\boldsymbol{\delta}_n^T)^{-1}\Big[\mathbf{P}_3 + \mathbf{M}(k_1\mathbf{I}_3 - \mathbf{S})\mathbf{R}^T\widehat{\boldsymbol{\zeta}}_2 - (k_1 +$$

$$k_2)\mathbf{M}\mathbf{e}_3^T\mathbf{R}^T\widehat{\boldsymbol{\zeta}}_2\mathbf{e}_3 + (k_2 + k_3)\mathbf{M}\mathbf{R}^T\widehat{\boldsymbol{\zeta}}_2 + \mathbf{M}\mathbf{R}^T\widehat{\boldsymbol{\zeta}}_2\Big]$$

$$= -\boldsymbol{\delta}_n^T(\boldsymbol{\delta}_n\boldsymbol{\delta}_n^T)^{-1}\Big[\mathbf{P}_3 + (k_1 + k_2 + k_3)\mathbf{MR}^T\widehat{\boldsymbol{\zeta}}_2 - \mathbf{MSR}^T\widehat{\boldsymbol{\zeta}}_2 - (k_1 +$$

$$k_2)\mathbf{Me}_3^T\mathbf{R}^T\widehat{\boldsymbol{\zeta}}_2\mathbf{e}_3 + \mathbf{MR}^T\dot{\widehat{\boldsymbol{\zeta}}}_2\Big]$$

Define $\widetilde{\zeta}_1 = \zeta_1 - \widehat{\zeta}_1$ and $\widetilde{\boldsymbol{\zeta}}_2 = \boldsymbol{\zeta}_2 - \widehat{\boldsymbol{\zeta}}_2$, Eq. (5.20) became

$$\dot{V}_3 = -\sum_{i=1}^{3} k_i \mathbf{z}_i^T \mathbf{z}_i + \mathbf{z}_1^T \mathbf{R}(\mathbf{z}_2 + \boldsymbol{\delta}) + \tag{6.4}$$

$$\mathbf{z}_3^T\Big[(k_1 + k_2 + k_3)\mathbf{MR}^T\widetilde{\boldsymbol{\zeta}}_2 - \mathbf{MSR}^T\widetilde{\boldsymbol{\zeta}}_2 - (k_1 + k_2)\mathbf{Me}_3^T\mathbf{R}^T\widetilde{\boldsymbol{\zeta}}_2\mathbf{e}_3 + \mathbf{MR}^T\dot{\widetilde{\boldsymbol{\zeta}}}_2\Big]$$

The closed-loop system can be regarded as a perturbed system with state $\mathbf{z}_1$, $\mathbf{z}_2$, $\mathbf{z}_3$ and perturbations $\widetilde{\boldsymbol{\zeta}}_2$, $\dot{\widetilde{\boldsymbol{\zeta}}}_2$. Since the velocities $\mathbf{V}$ and $\boldsymbol{\omega}$ remain bounded for all time, the matrix $\mathbf{S}$ remain bounded. Thus, the perturbed system is locally Lipschitz in the state and perturbations. To simplify the result, consider $\|\widetilde{\boldsymbol{\zeta}}\| = \max(\|\widetilde{\boldsymbol{\zeta}}_2\|, \|\dot{\widetilde{\boldsymbol{\zeta}}}_2\|)$, $\mathbf{z} = \begin{bmatrix}\mathbf{z}_1\\\mathbf{z}_2\\\mathbf{z}_3\end{bmatrix}$. And notice that from Eq. (5.31), when large γ is chosen, an upper bound on the derivative of the Lyapunov function can be expressed as

$$\dot{V}_3 \le -k\|\mathbf{z}\|\big(\|\mathbf{z}\| - B\widetilde{\boldsymbol{\zeta}}\big) \tag{6.5}$$

where $k > 0$ and it depends on k_1, k_2, γ. B is a positive constant. For sufficiently large tracking errors, $\dot{V}_3$ is negative definite. According to the theorem in section 2.2.5, the closed-loop system is locally input-to-state stable to perturbations $\widetilde{\boldsymbol{\zeta}}_2$ and $\dot{\widetilde{\boldsymbol{\zeta}}}_2$. Because the external perturbations arising from the estimation errors are exponential stable, the interconnection of the proposed observer and the controller is locally asymptotically stable.

The interconnected system of quadrotor, the proposed observer and the proposed controller was implemented in SIMULINK environment, as shown in figure 14. The controller was fed with estimated values of the unknown parameters that came from the observer, namely $\widehat{\zeta}_1 = \left(\frac{1}{m}\right)$, $\widehat{\boldsymbol{\zeta}}_2 = \left(\frac{\mathbf{b}}{m}\right)$. Note that one of the control variable $\boldsymbol{\tau}$ was calculated inside the observer due to the problem of algebraic loops.

The overall interconnected system can be simulated by setting the noise level in the Kalman-Bucy filter to zero. Specifically, the mass of the quadrotor $m = 0.206$ kg, the gravity $g = 9.7877$ m/s^2, and external force disturbance $^E\mathbf{b} = \begin{bmatrix}0.3\\0.2\\0.1\end{bmatrix}$ Newton. Initial

position $\mathbf{P}(t_0) = \begin{bmatrix} 0 \\ 0 \\ -1 \end{bmatrix}$ m, initial linear and angular velocities were zero. For the observer, set initial guess of the mass $\hat{m}(t_0) = 0.1$ kg, and initial external force $^E\hat{\mathbf{b}}(t_0) = \begin{bmatrix} 0 \\ 0 \\ 0 \end{bmatrix}$ Newton. By assumption, the desired trajectory was a smooth and bounded function parametrized in time. Here, it was assumed to be a simple circle with radius of $1.2\,m$ defined as

$$\begin{cases} x(t) = 1.2 \cos t \\ y(t) = 1.2 \sin t \qquad t \geq 0 \\ \quad z(t) = -1 \end{cases} \qquad (6.6)$$

Set control parameters $k_1 = 4.5,\ k_2 = 4,\ k_3 = 3$, and $\boldsymbol{\delta} = \begin{bmatrix} 0 \\ 0 \\ 0.15 \end{bmatrix}$ m/s.
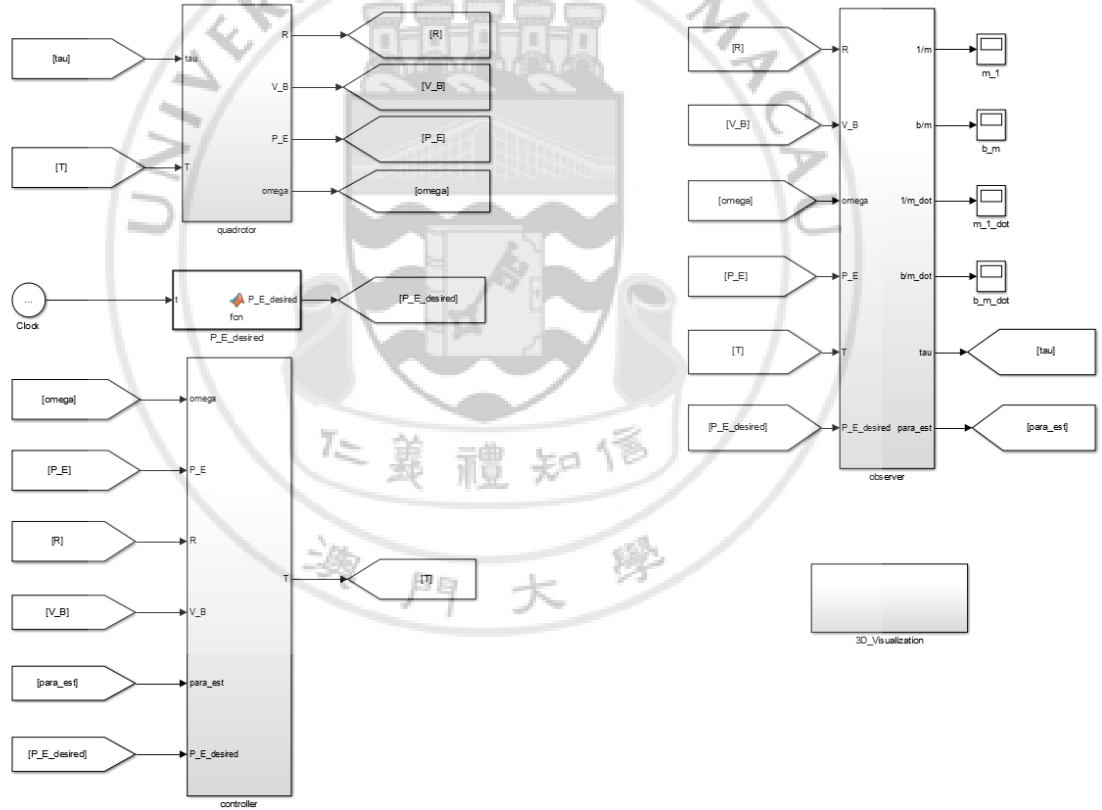
Figure 14. Quadrotor, observer and controller model

After simulation, errors of unknown parameters and backstepping errors were checked, shown in the following figures. As indicated from figures below, the unknown parameters $\frac{1}{m}$ and $\frac{\mathbf{b}}{m}$ converged to a small neighborhood around zero after a while. Notice that the error for the external force along z-axis was larger than those along x-

axis and y-axis. This was due to the fact that the initial estimation of the mass was smaller than the actual mass of $0.2\ kg$, which led to a bigger control value for the thrust to keep the quadrotor from falling down. In such a way, the initial estimation of the external force along z-axis was larger than the actual value of $0.3\ Newton$ to "compensate" the gravity downwards in the presence of a bigger thrust upwards.
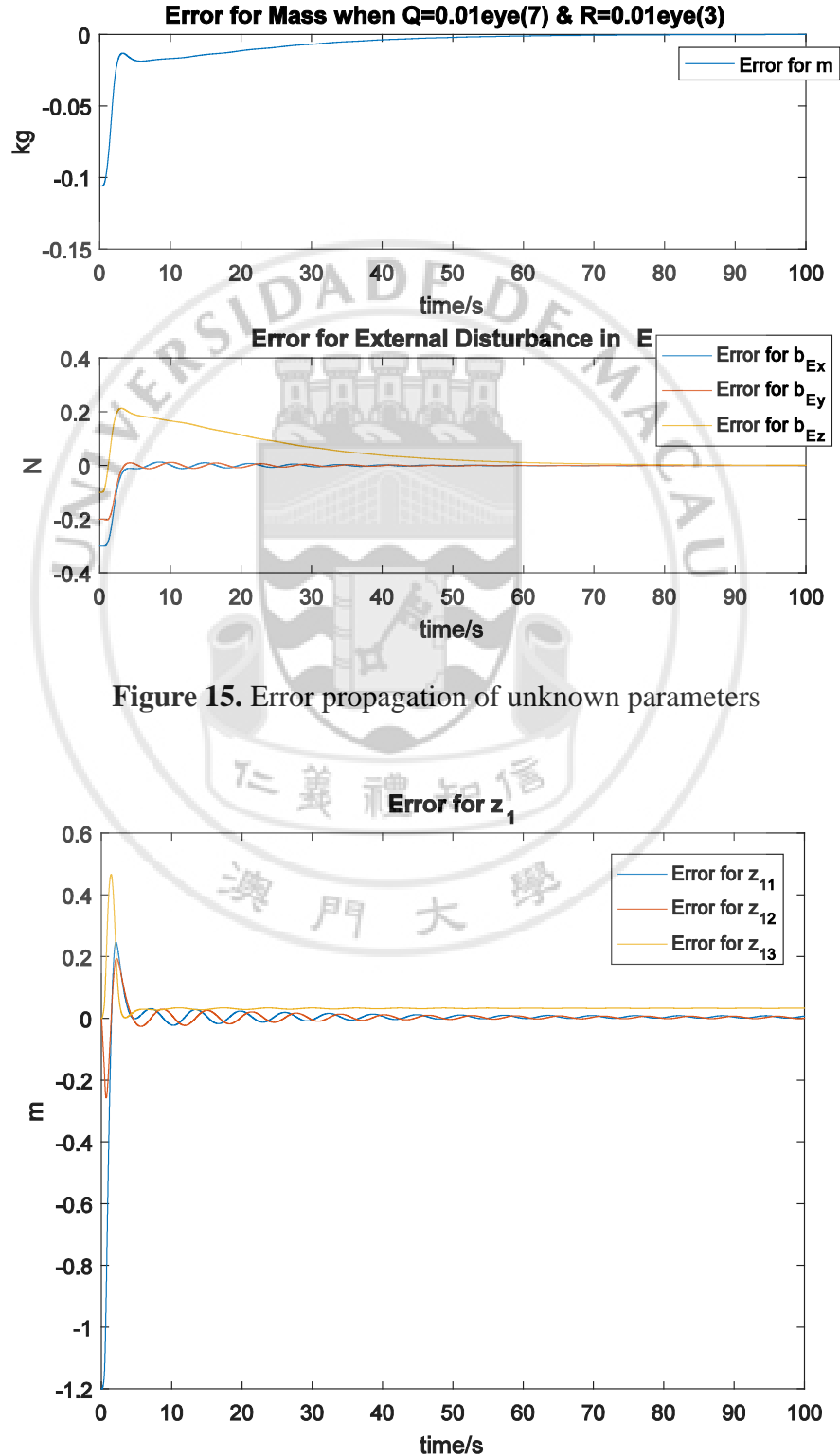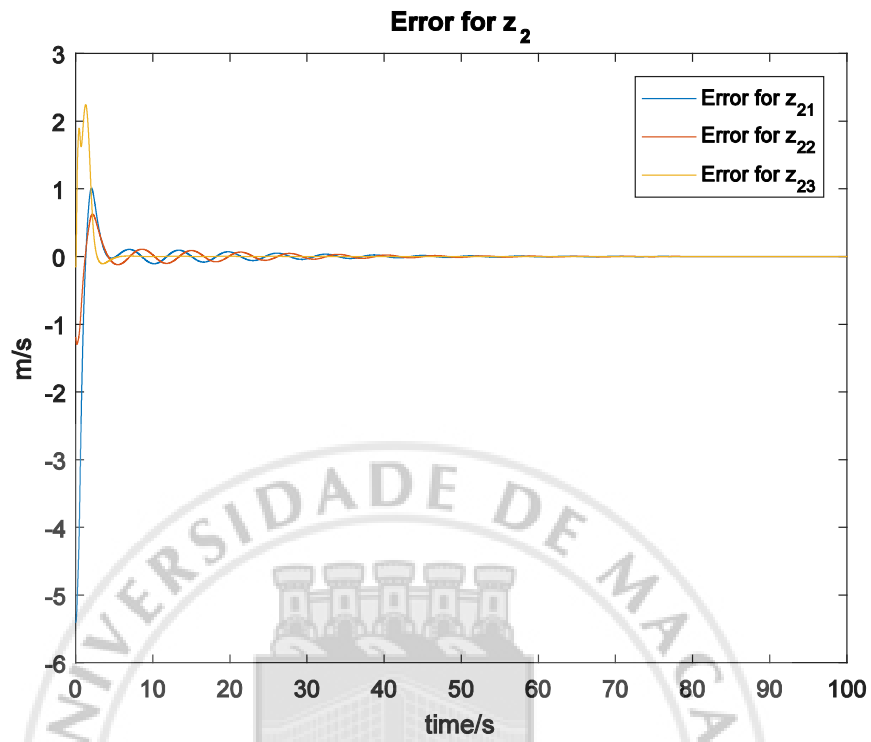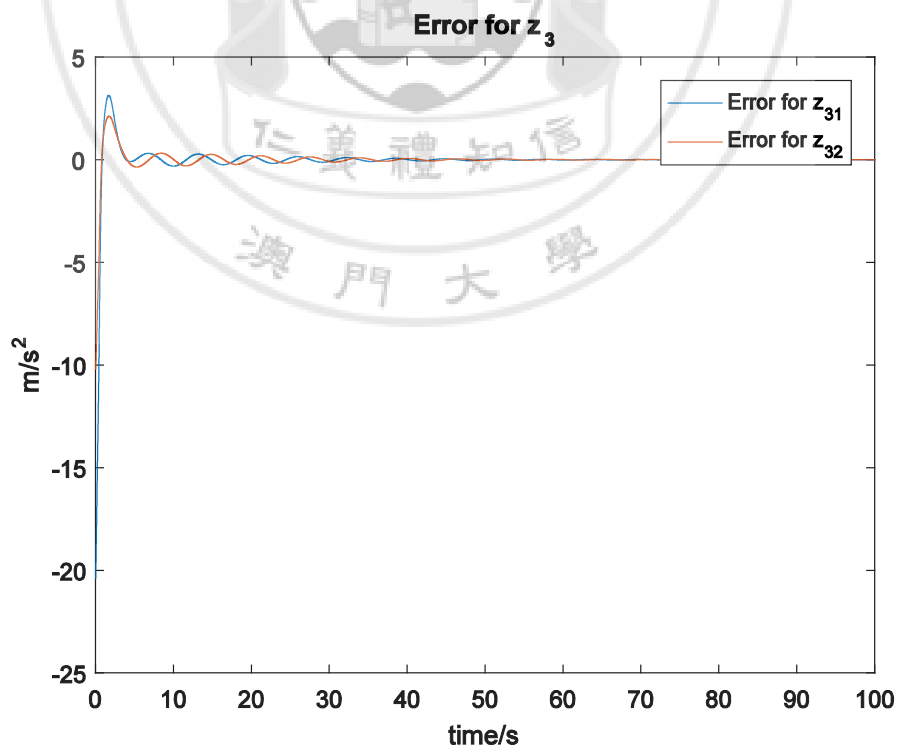

Figure 15. Error propagation of unknown parameters

Error for z$_2$

Figure 17. Error propagation of backstepping error $\mathbf{z}_2$

Error for z$_3$

Figure 18. Error propagation of backstepping error $\mathbf{z}_3$

As indicated in the figures above, $\mathbf{z}_1$, $\mathbf{z}_2$, $\mathbf{z}_3$ converged to desired tracking dynamics in a while. When the estimated parameters approached their real values at around $55\ s$, the tracking errors approached equilibrium points near zero. As derived before, the position error $\mathbf{z}_1$ converged to a constant in a small neighborhood around zero of a radius of $3\ cm$, which was favorable in practical cases. Signal propagation for the thrust and the torque were shown in the figure below:
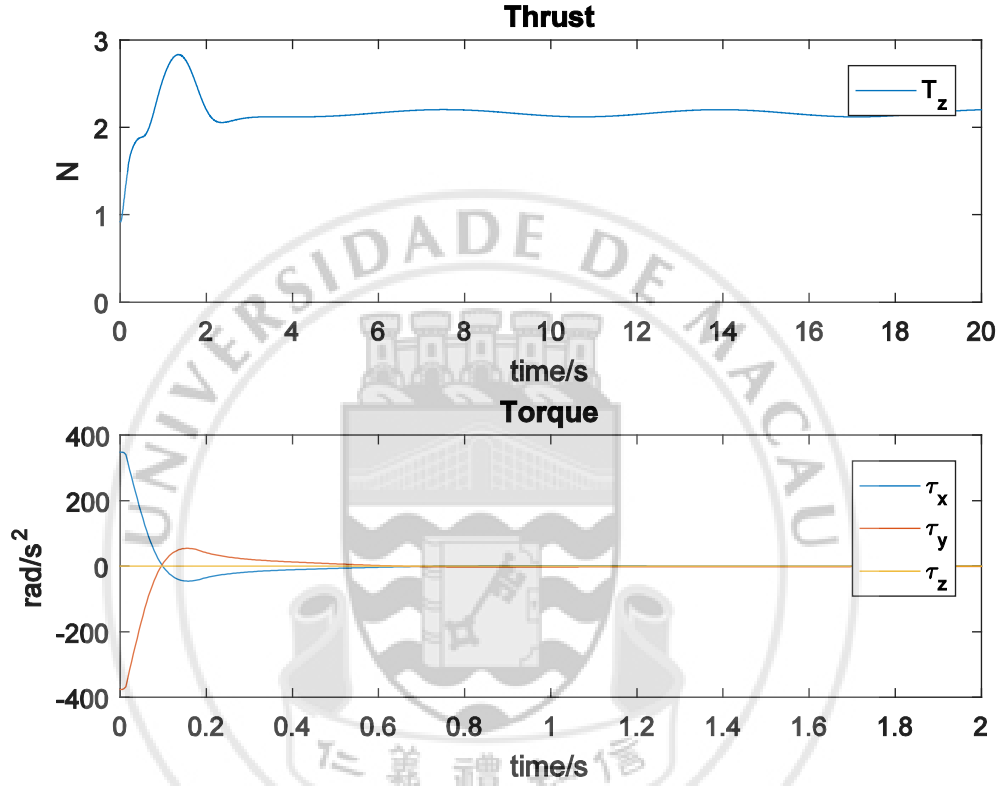

Figure 19. Propagation of actuation variables

As indicated from the figure above, the thrust and the torque tended to stay still around the equilibrium points. And the third element of torque, ${}^B\tau_z$, remained zero for all time with no contribution to the task of trajectory tracking, as proved in section 5.2. The fact that the thrust showed a slowly varying sinusoidal wave around $2\ Newton$ could be explained with the equation in section 5.2, specifically $\mathbf{R}T\mathbf{e}_3 = mg\mathbf{e}_3 + \mathbf{b} - m\ddot{\mathbf{P}}_d$. As the time-varying term $\ddot{\mathbf{P}}_d$ was related to the predefined trajectory, the quadrotor would have to tilt itself to accelerate in any directions in xy-plane. So that the term $\mathbf{R}T$ would also follow the dynamics of $\ddot{\mathbf{P}}_d$. The rotational matrix $\mathbf{R}$ would lead the quadrotor to orient to the direction of linear velocity in xy-plane. Thus, T would also vary with respect to time.

Chapter 7 EXPERIMENTAL RESULTS

The section presented the experimental results using the proposed observer and controller on a real quadrotor. Experiments were conducted in MATLAB/SIMULINK environment that integrated an optical motion capture system, VICON, and radio communication with the quadrotor. VICON Bonita motion capture system played the role of external sensors for the quadrotor due to the lack of on-board sensors. The quadrotor's position, orientation, linear velocity and angular velocity can be estimated with relatively low noise. A graphical representation of the overall architecture was shown in the figure below.
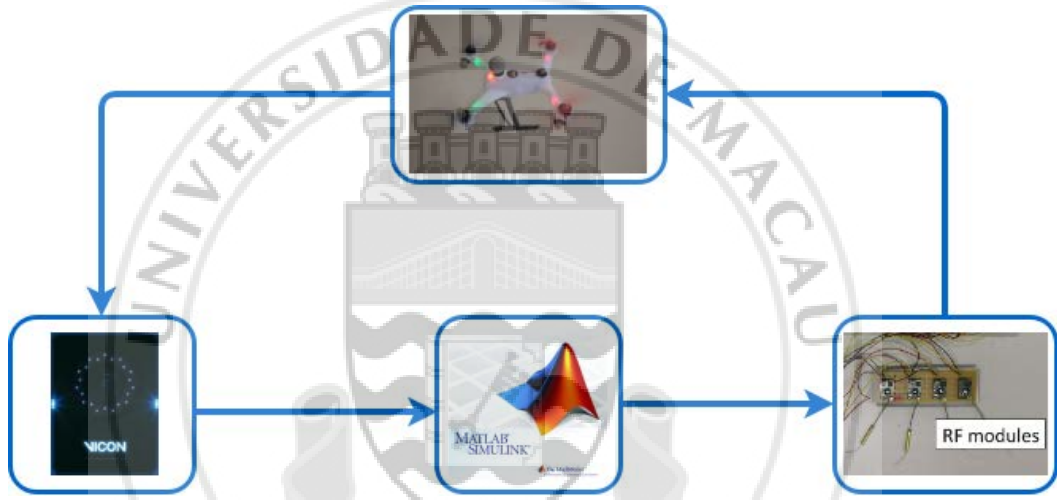
Figure 20. Quadrotor measurement and communication architecture [18]

The controller gains for the experiments were adjusted to $k_1 = 4.5$, $k_2 = 3$, $k_3 = 2$, and $\boldsymbol{\delta} = \begin{bmatrix} 0 \\ 0 \\ 0.1 \end{bmatrix}$ m/s. The Kalman filter parameters of the observer were $\mathbf{Q} = 0.01\mathbf{I}_7$, $\mathbf{R} = 0.01\mathbf{I}_3$, and the initial covariance matrix $\mathbf{P}(t_0) = \mathbf{I}_7$. Actual mass of the quadrotor was 0.206 kg. Initial guess of the mass $\hat{m}(t_0) = 0.1$ kg, and initial external force $^E\hat{\mathbf{b}}(t_0) = \begin{bmatrix} 0 \\ 0 \\ 0 \end{bmatrix}$ Newton. The initial guess of the linear velocity was ignored here because the estimated linear velocity coming from the observer was not used for the proposed controller. The quadrotor was initially placed at Initial position $\mathbf{P}(t_0) =$

$$\begin{bmatrix} -0.06 \\ 0.83 \\ -0.24 \end{bmatrix}$$ m, with initial orientation $\mathbf{R}(t_0) = \mathbf{I}_3$, and zero initial linear and angular velocities. The observer was active right from the start of the experiments.

Two experiments were conducted with different desired trajectories. Next two sections discussed experimental results, separately.
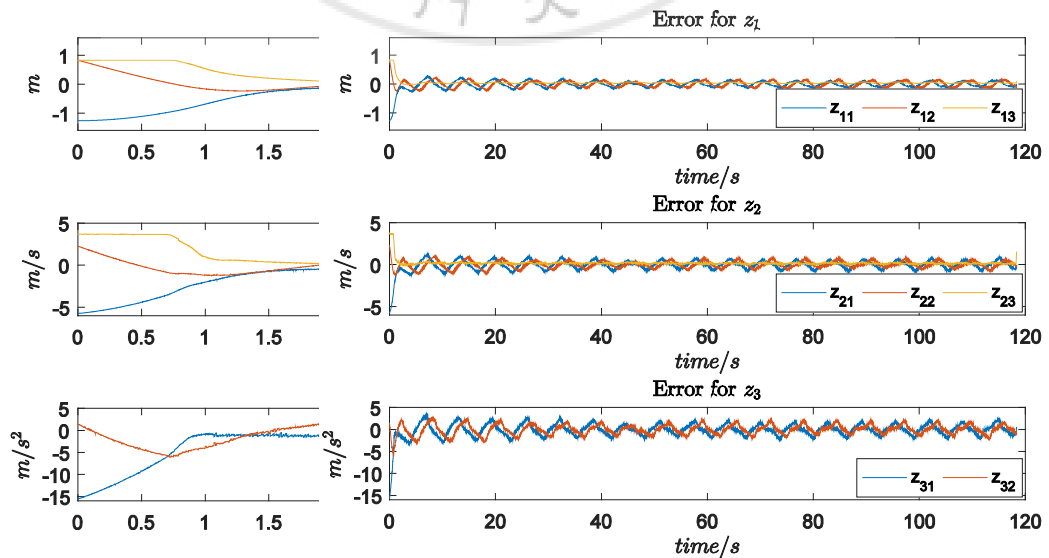
7.1 EXPERIMENT RESULTS OF FOLLOWING A CIRCLE IN 2D SPACE

The first experiment evaluated the performance of the proposed controller with an oval trajectory, namely a circle in two-dimensional plane described by:

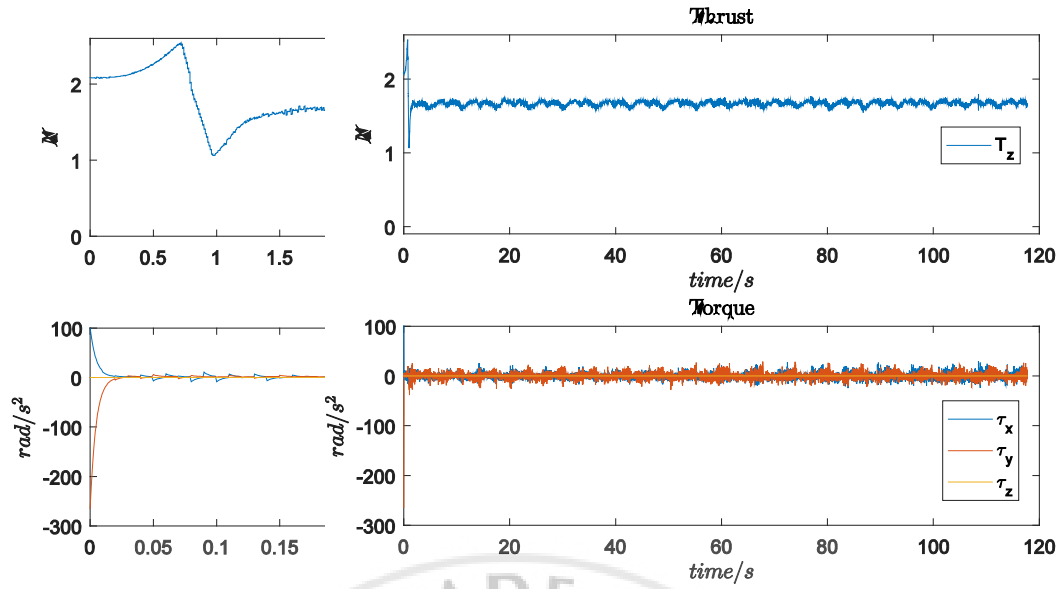$$\mathbf{P}_d(t) = \begin{bmatrix} 1.2\cos t \\ 1.2\sin t \\ -1 \end{bmatrix} \qquad t \geq 0 \qquad (7.1)$$
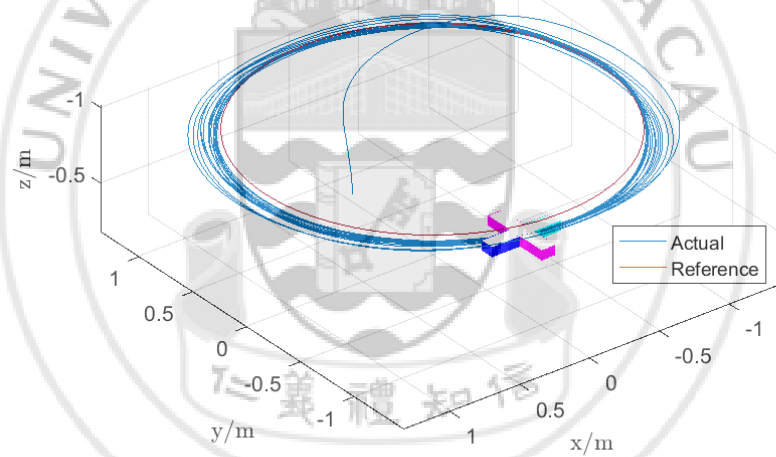
Figure 21. Comparison of the desired reference trajectory and the actual trajectory

Figure 22. Time evolution of errors

44

Figure 23. Time evolution of actuation
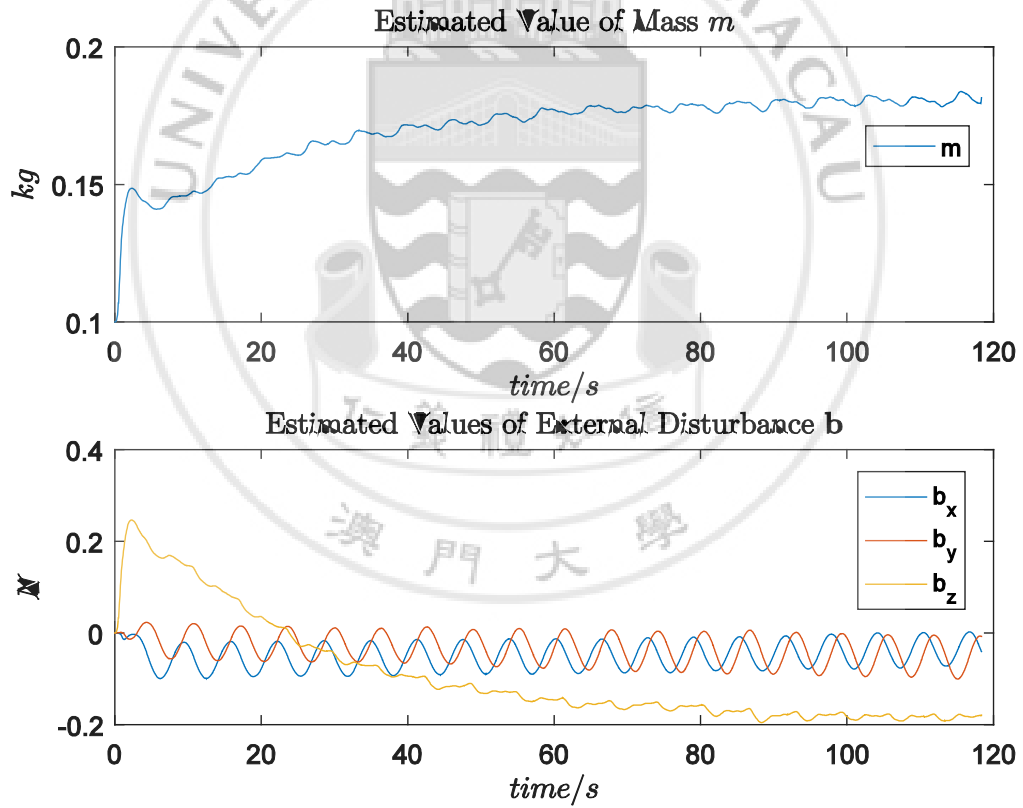
Figure 24. Time evolution of estimated parameters

A comparison between the desired trajectory and the actual one was shown in figure 21. In spite of initial errors in position, linear velocity and angular velocity, the quadrotor gradually approached the oval trajectory, shown by the curve in blue.

Figure 22 showed the evolution of errors. Quantitively, after initial transient for about 2 seconds, the position error had not gone beyond 0.1 meters. Meanwhile, the other two errors converged also within seconds. In steady state, the position error was bounded by 0.05 meters in magnitude. The steady state errors were due to:

- theoretical upper bounds of the errors, specified in Eq. (5.34) and Eq. (6.5);
- imperfect modeling of the quadrotor. There existed aerodynamic forces that depended on the states of the quadrotor;
- a non-constant external force disturbance in the surrounding. The quadrotor could suffer varying external disturbance like the wind disturbance, uneven mass distribution;
- varying power output from the on-board battery.

In figure 24, the estimated parameters slowly converged to a neighborhood around their actual values. Estimated values of the external forces along x-axis and y-axis in earth frame were better estimated than that along z-axis. This was due to the fact that the dynamics of the estimated mass and the estimated external force disturbance was closely related to the thrust. And the thrust always pointed nearly upwards in earth frame, making the estimated value of the estimated external force disturbance along z-axis varying in order to stabilize the quadrotor. Within 80 seconds, the estimated parameters entered steady states. Reasons that the estimated parameters, especially the estimated mass and the estimated external force disturbance along z-axis, did not converge to their correct parameters were:

- almost constant rotational matrix after seconds, leading to a similar result of that simulated in Example 1, section 4.2;
- the quadrotor was indeed stabilized to follow the desired trajectory, and it could work with a smaller estimated value of its mass and its external force disturbance along z-axis.

7.2 EXPERIMENT RESULTS OF FOLLOWING A LEMNISCATE IN 3D SPACE

The second experiment evaluated the performance of the proposed controller with a lemniscate trajectory in three-dimensional space described by:

$$\mathbf{P}_d(t) = 1.3\mathbf{R}_x(-\frac{\pi}{18})\mathbf{R}_y(0)\mathbf{R}_z(0)\begin{bmatrix} \frac{\sin\phi(t)\cos\phi(t)}{(\cos\phi(t))^2+1} \\ \frac{\sin\phi(t)}{(\sin\phi(t))^2+1} \\ -1 \end{bmatrix} \qquad t \geq 0 \qquad (7.2)$$

where $\mathbf{R}_x$, $\mathbf{R}_y$, and $\mathbf{R}_z$ were rotation matrices defined by **Z-Y-X fixed angles**. That was, the original trajectory rotated first about z-axis defined in earth frame, then rotated about y-axis, finally about z-axis. $\phi(t)$ followed $\dot{\phi}(t) = V\sqrt{\sin^2 t + 1}$, where V was the desired speed. In the experiment, $V = 1$ m/s.
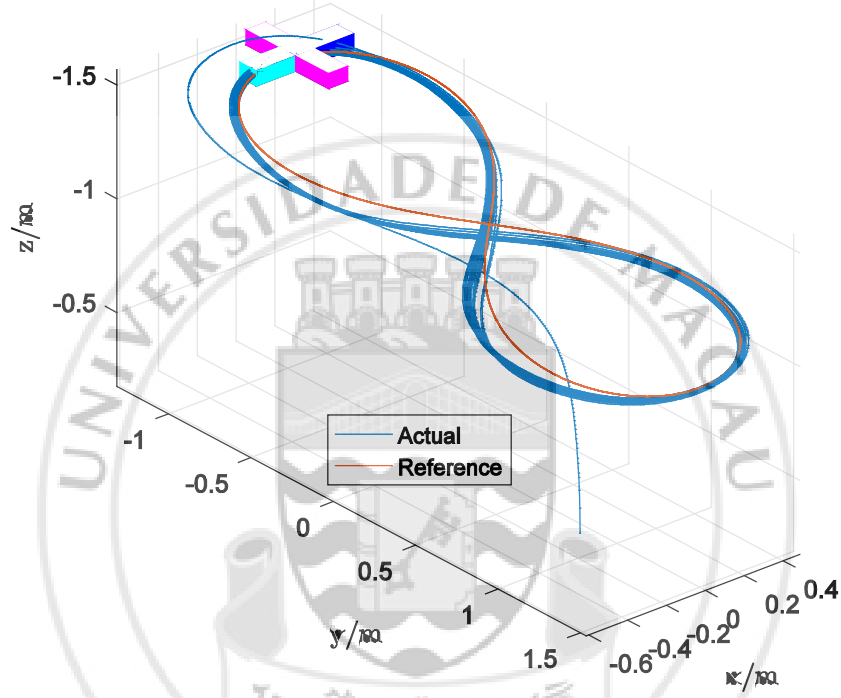
Figure 25. Comparison of the desired reference trajectory and the actual trajectory
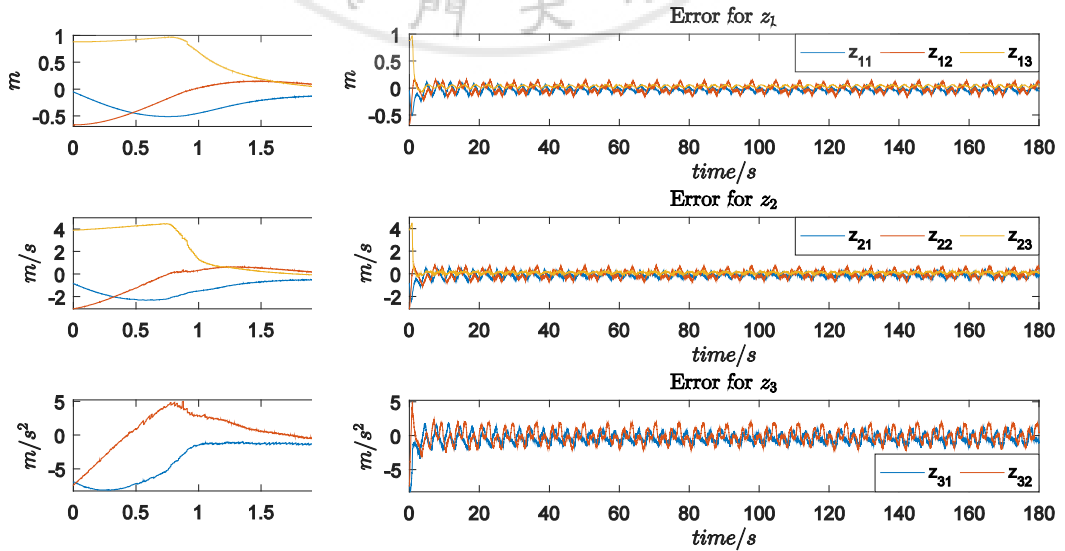
Figure 26. Time evolution of errors
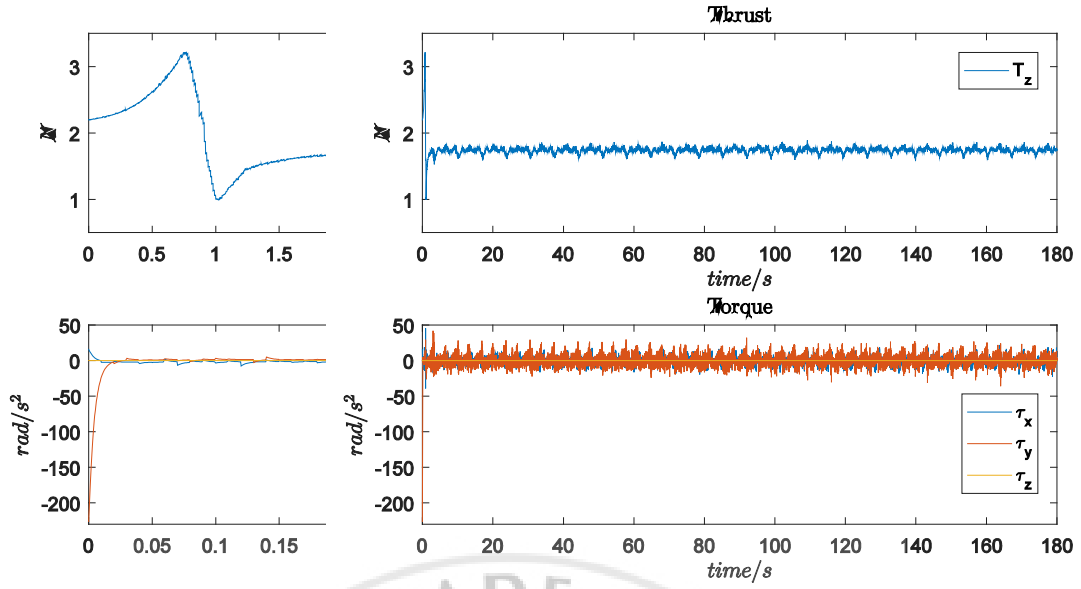
Figure 27. Time evolution of actuation
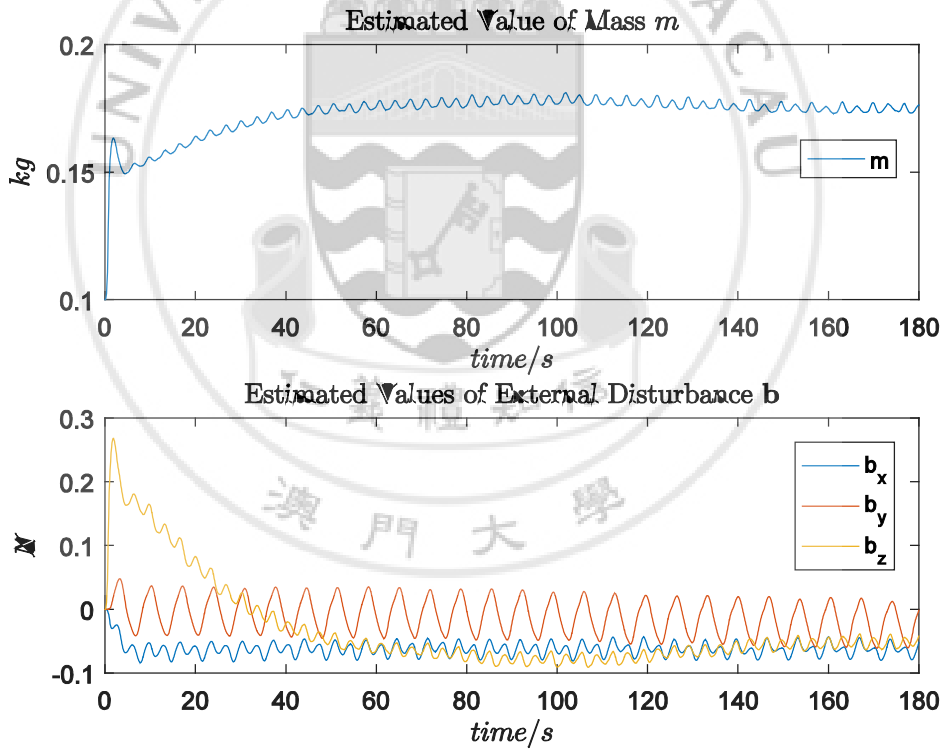
Figure 28. Time evolution of estimated parameters

As shown in the figures above, similar patterns of all signals could be seen when the quadrotor was following the lenmiscate trajectory in three-dimensional space. The estimated parameters became smaller from 120 seconds onwards, which may due to less output power from battery.

Chapter 8 PROBLEMS ENCOUNTERED

5.1 NOISE GENERATION FOR SIMULATION

Practically, the noise came from the uncertainty in modeling, disturbance in the surroundings, etc. The noise was modeled only in chapter 4 for evaluation of the performance of the observer. Here, white noise was generated by randomly distributed discrete sampling points. However, the Kalman-Bucy filter worked only in continuous time case. Thus, the parameters for Kalman-Bucy filter may not guarantee optimal convergence rate for the generated noise. For chapter 6 where the proposed controller was involved, there were no noised added in the dynamics of the overall system. On one hand, the modeling of the quadrotor itself did include the state noise. On the other hand, the estimated parameters came from the observer, which depended on the dynamics of linear velocity. However, the linear velocity was in fact accurate enough. Moreover, algebraic loop errors would occur if manually generated white noise was added into the system, which was not desirable.

5.2 ALGEBRAIC LOOPS IN SIMULINK

Algebraic loops occurred in simulation of the interconnected system, specified in chapter 6. Normally, an algebraic loops occurred when there were feedforward or feedback loops inside a system such that MATLAB itself was unable to solve for the initial values inside the loops. In such a way, an algebraic variable would go around within the problematic loop. Some common ways to fix the problem were to specify manually the initial values by adding a delay block or initial condition block inside SIMULINK. However, these ways would change the proposed control law, which was not desirable. Thus, each algebraic loop was checked and solved separately by changing the block design in SIMULINK. In this specific case, when the thrust and the torque signals were put together inside the same block for controller, the update control law for the torque depended on estimated values of derivatives of unknown parameters. However, those values were inputs for the observer block and could not deliver out to other blocks at the very start of the simulation. Thus, the control law for the torque was calculated inside the observer rather than inside the controller. And the new configuration solved the occurrence of algebraic loops.

Chapter 9 CONCLUSIONS

The dynamics of the quadrotor was derived through basic physics and was simplified within reasonable level. Firstly, the model for an open loop model of the quadrotor in Simulink was created for observation and control purposes. The open loop model was tested with inputs defined arbitrarily to verify its reliability. Secondly, in the case that some system parameters were unknown, the dynamics equation was transformed into a linear time-varying one that can mimic exactly the behavior of the nonlinear system dynamics. Observability of the linear system was checked and with the use of Kalman-Bucy filter, the error dynamics of all of the states converged to zero in short time interval. The effects of the self-tuned noise levels in the design of Kalman-Bucy filter were exploited. Thirdly, a nonlinear control algorithm was proposed. Using correct values of unknown parameters, the controller guaranteed global exponential stability of the tracking error. Lastly, the interconnected system of the model, the observer, and the controller was proved and assessed to have local asymptotically stability. Adaptive control of the quadrotor using the designed feedback system was achieved by reacting to uncertainties in modeling and the surroundings of the quadrotor.
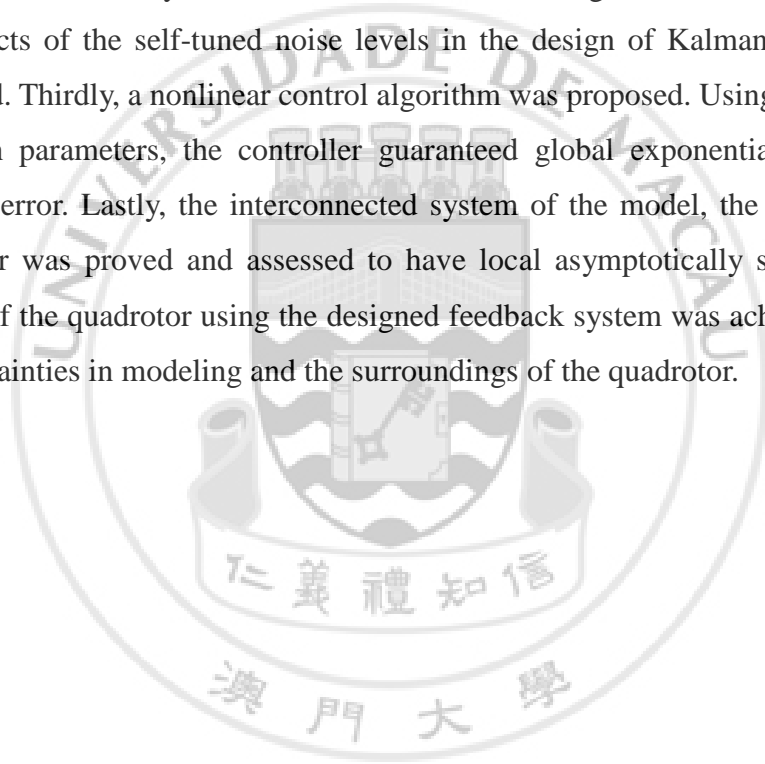
Chapter 10 RECOMMENDATIONS FOR FUTURE RESEARCH

7.1 DIFFERENT KALMAN FILTER PARAMETERS FOR THE OBSERVER

For above all simulation and experiments, the parameters for the Kalman-Bucy filter, namely, $\mathbf{Q}$ and $\mathbf{R}$, were unchanged. In fact, these two parameters influenced the convergence rate of the estimated states. Given low noise level in the linear velocity, these two parameters would have to be a lot smaller to guarantee optimal convergence rate. It is expected that smaller $\mathbf{Q}$ and $\mathbf{R}$ will lead a shorter time for estimated m and $\mathbf{b}$ to converge to their real values. However, the primary concern in this article was to implement trajectory tracking for the quadrotor rather than estimating parameters, as long as the estimate error dynamics was stable.

7.2 EXPERIMENTS IN VARIOUS SETTINGS

Although the mass and external force disturbance were assumed to be constant for all time, they can be varying with time in the presence of an observer that guarantees their convergence to their actual values. For this reason, further experiments can be conducted within some common scenarios when:

- the quadrotor experiences wind disturbance in its flying zone;
- sudden mass change in the quadrotor such as caching or releasing loads;
- unpredictable output from the onboard motors such as sudden change in thrust. It can be made deliberately by changing the control law at some time.

7.3 RESEARCH INTO THE INERTIAL MATRIX

Although the inertia matrix of the quadrotor was assumed a scalar matrix in the dynamics equations of the quadrotor, it would be useful either when one wanted to estimate it or when the control algorithm involved the inertia matrix. When attempting to estimate the inertia matrix through the state and output transformation, problems occur due to the nonlinear nature in the dynamics. Assume that the inertia matrix is a

diagonal one ${}^{B}\mathbf{I} = \begin{bmatrix} I_{xx} & 0 & 0 \\ 0 & I_{yy} & 0 \\ 0 & 0 & I_{zz} \end{bmatrix}$, ${}^{B}\boldsymbol{\omega} = \begin{bmatrix} {}^{B}\boldsymbol{\omega}_x \\ {}^{B}\boldsymbol{\omega}_y \\ {}^{B}\boldsymbol{\omega}_z \end{bmatrix}$ and ${}^{B}\boldsymbol{\tau} = \begin{bmatrix} {}^{B}\boldsymbol{\tau}_x \\ {}^{B}\boldsymbol{\tau}_y \\ {}^{B}\boldsymbol{\tau}_z \end{bmatrix}$. Then through

the computation with Eq. (3.18), one could get:

$$B\dot{\boldsymbol{\omega}} = \begin{bmatrix} \frac{I_{zz}-I_{yy}}{I_{xx}} {}^B\boldsymbol{\omega}_y {}^B\boldsymbol{\omega}_z - \frac{1}{I_{xx}} {}^B\boldsymbol{\tau}_x \\ \frac{I_{xx}-I_{zz}}{I_{yy}} {}^B\boldsymbol{\omega}_x {}^B\boldsymbol{\omega}_z - \frac{1}{I_{yy}} {}^B\boldsymbol{\tau}_y \\ \frac{I_{yy}-I_{xx}}{I_{zz}} {}^B\boldsymbol{\omega}_x {}^B\boldsymbol{\omega}_y - \frac{1}{I_{zz}} {}^B\boldsymbol{\tau}_z \end{bmatrix} \tag{10.1}$$

where the elements of the inertia matrix were not linear with state and thus cannot follow the building methods of LTV mimicking system as in this work. Attempts could be made in finding a proper transformation in the form of $\mathbf{T}_x(\mathbf{x}(t)) = \begin{bmatrix} \mathbf{x} \\ \mathbf{T}_a(\mathbf{x}(t)) \end{bmatrix}$, and the observability of the resulting mimicking system should be checked afterwards to guarantee the observability of the nonlinear system described in Eq. (5.1).

$$B\dot{\boldsymbol{\omega}} = \begin{bmatrix} \frac{I_{zz}-I_{yy}}{I_{xx}} {}^B\boldsymbol{\omega}_y {}^B\boldsymbol{\omega}_z - \frac{1}{I_{xx}} {}^B\boldsymbol{\tau}_x \\ \frac{I_{xx}-I_{zz}}{I_{yy}} {}^B\boldsymbol{\omega}_x {}^B\boldsymbol{\omega}_z - \frac{1}{I_{yy}} {}^B\boldsymbol{\tau}_y \\ \frac{I_{yy}-I_{xx}}{I_{zz}} {}^B\boldsymbol{\omega}_x {}^B\boldsymbol{\omega}_y - \frac{1}{I_{zz}} {}^B\boldsymbol{\tau}_z \end{bmatrix}$$

REFERENCES

[1] Slotine, J. E., & Li, W., 1991. Applied nonlinear control. Englewood Cliffs, NJ: Prentice Hall, pp. 45-47.

[2] Guenard, N., Hamel, T., & Mahony, R., 2008. A practical visual servo control for an unmanned aerial vehicle. IEEE Transactions on Robotics, 24,331–340.

[3] Hoffmann, G. M., Huang, H., Waslander, S. L., & Tomlin, C. J., 2011. Precision flight control for a multi-vehicle quadrotor helicopter testbed. Control Engineering Practice, 19, 1023–1036.

[4] T. J. Koo and S. Sastry, "Output tracking control design of a helicopter model based on approximate linearization," in Proc. IEEE Conference on Decision and Control, 1998, pp. 3635–3640.

[5] Guenard, N., Hamel, T., & Mahony, R., 2008. A practical visual servo control for an unmanned aerial vehicle. IEEE Transactions on Robotics, 24, 331–340.

[6] R. Cunha, D. Cabecinhas and C. Silvestre, "Nonlinear trajectory tracking control of a quadrotor vehicle," 2009 European Control Conference (ECC), Budapest, 2009, pp. 2763-2768.

[7] W. Janusz and M. Niezabitowski, "Joint state and parameter estimation of quadrotor based on extended Kalman filter and complementary filter," 2016 17th International Carpathian Control Conference (ICCC), Tatranska Lomnica, 2016, pp. 274-279.

[8] VICON. (2012). Motion capture systems from vicon. URL: http://www.vicon.com.

[9] Slotine, J. E., & Li, W., 1991. Applied nonlinear control. Englewood Cliffs, NJ: Prentice Hall, pp. 41-47, 102-109.

[10] Khalil, H. K., 2014. Nonlinear systems (2nd ed.). Upper Saddle River, NJ: Prentice Hall, pp. 217-219.

[11] D. Viegas, P. Batista, P. Oliveira and C. Silvestre, "Nonlinear observability and observer design through state augmentation," 53rd IEEE Conference on Decision and Control, Los Angeles, CA, 2014, pp. 133-138.

[12] Rugh, W. J., 1996. Linear system theory. Upper Saddle River, NJ: Prentice Hall, p. 148.

[13] S. Sastry and C. Desoer, "The robustness of controllability and observability of linear time-varying systems," in IEEE Transactions on Automatic Control, vol. 27, no. 4, pp. 933-939, Aug 1982.

[14] A. Jazwinski, Stochastic Processes and Filtering Theory, ser. Mathematics in Science and Engineering. Elsevier Science, 1970.

[15] RESULTADOS DAS OBSERVAÇÕES METEOROLÓGICAS. (2012, April). Retrieved December 12, 2016, from http://www.smg.gov.mo/smg/database/pdf/CLI_M/CLI_201204.tmp.pdf

[16] Wei Xie, Robot motion control of underactuated autonomous surface craft. Master's thesis, Unversity of Macau, 2016.

[17] A. P. Aguiar and J. P. Hespanha, "Trajectory-Tracking and Path-Following of Underactuated Autonomous Vehicles With Parametric Modeling Uncertainty," in IEEE Transactions on Automatic Control, vol. 52, no. 8, pp. 1362-1379, Aug. 2007. doi: 10.1109/TAC.2007.902731

[18] URL: https://www.vicon.com/products/camera-systems/vantage.